^{222}Rn as a tracer for air mass transport

Characterization at a 100-m-high tower on the Southwest Spanish coast

Claudia Grossi

Doctoral Dissertation

Supervisor:
Dr. Arturo Vargas Drechsler

Institut de Tecniques Energetique (INTE)
Technical University of Catalonia (UPC)

Solo chi fortemente vuole identifica gli elementi necessari
alla realizzazione della propria volontá. (A. Gramsci)

Ad Anna, a Bruno ed a Luca

Oficina de Doctorat
UNIVERSITAT POLITÈCNICA DE CATALUNYA

Acta de qualificació de tesi doctoral

Curs acadèmic:

Nom i cognoms

DNI / NIE / Passaport

Programa de doctorat

Unitat estructural responsable del programa

Resolució del Tribunal

Reunit el Tribunal designat a l'efecte, el doctorand / la doctoranda exposa el tema de la seva tesi doctoral titulada

_____

_____.

Acabada la lectura i després de donar resposta a les qüestions formulades pels membres titulars del tribunal, aquest atorga la qualificació:

☐ APTA/E ☐ NO APTA/E

(Nom, cognoms i signatura) President/a	(Nom, cognoms i signatura) Secretari/ària	
(Nom, cognoms i signatura) Vocal	(Nom, cognoms i signatura) Vocal	(Nom, cognoms i signatura) Vocal

_____, _____ d'/de _____ de _____

El resultat de l'escrutini dels vots emesos pels membres titulars del tribunal, efectuat per l'Oficina de Doctorat, a instància de la Comissió de Doctorat de la UPC, atorga la MENCIÓ CUM LAUDE:

☐ SI ☐ NO

(Nom, cognoms i signatura) Vicerectora de Recerca Presidenta de la Comissió de Doctorat	(Nom, cognoms i signatura) Cap de l'Oficina de Doctorat Secretària de la Comissió de Doctorat	(Nom, cognoms i signatura) Secretari/ària del tribunal (o membre del tribunal de la UPC)

Barcelona, _____ d'/de _____ de _____

Diligència "Internacional del títol de doctor o doctora"

Com a secretari/ària del tribunal faig constar que la tesi s'ha defensat en part, i com a mínim pel que fa al resum i les conclusions, en una de les llengües habituals per a la comunicació científica en el seu camp de coneixement i diferent de les que són oficials a Espanya. Aquesta norma no s'aplica si l'estada, els informes i els experts externs provenen d'un país de parla hispana.

(Nom, cognoms i signatura) Secretari/ària del tribunal

Acknowledgments

During these years of my doctoral research at the INTE Institute of Barcelona, I have met different people who have helped me to grow both scientifically and personally. People who were by my side each day and helped me to go on with my work. I would like to thank all of them because they have aided me in so many different ways and each one has been an important part of my PhD team.

First of all, I would like to thank the Institute of Energy and Technology of the Technical University of Catalonia which offered me the possibility to carry on with my research during these years and for providing me with the scientific and technical tools to complete it. I would particularly like to thank the previous Institute Director Dr. Merce Guillarme, who trusted me and offered me this PhD position four years ago.

Thanks to the National Institute of Aerospace Technology where the instrumentation of this work has been located within a MICINN (Spanish Ministry of Science and Innovation) founded project (Reference CGL2008-00473). Thanks to the Dr. Israel Lopéz-Coto for his collaboration in my work.

Thanks to Dr. Arturo Vargas for sharing part of his scientific knowledge with me, for teaching me how to be a good scientist, planning experiments in order to answer scientific questions, analyzing results and writing papers to present to the scientific community. I would like to thank him for coping with my Napolitan temperament. I am grateful for his rigour at each phase of this work, in spite of my complaints I really understand and appreciate it.

Thanks to Dr. Delia Arnold. She was the first person to welcome me to the INTE Institute. Thank you for introducing an experimental physicist to the world of the modelling. I found it to be full of interest and charm. Thanks to her for the really interesting discussion on MM5, Flexpart and all issues related with inverse modelling, I learnt a lot from you. Furthermore, I am really greatful to you for showing me the PhD Comics.

A mi amigo y futuro Doctor, Miguel Ángel González de Perosanz, por la amistad que ha hecho muy agradables los largos días en el INTE. Por introducirme en el mundo de la escalada, gracias a lo cual he podido descubrir la maravillosa naturaleza existente en Cataluña.

A Vicente Blasco, por su humanidad. Por su increible capacidad de escuchar y de illuminar con la luz de la ironía incluso las cosas negativas. Gracias por estar siempre a mi lado tanto en el laboratorio como en la vida privada. Gracias por involucrarme en la exposición de fotos y texto de La Estacion del Alma. Esto me ha recordado que mi alma necesita expresarse tanto como que mi cerebro necesita investigar.

A la Dr Belén Goméz Hornillos, por su aguda ironía y su reservada amistad, por las charlas de la comida en el parque de mate y a las risas hablando de nuestro presente y de nuestro futuro.

A Isabel Serrano y a Silvia Pérez, dos mujeres encantadoras, fuertes y sensibles, que he tenido el gusto de conocer, por todos los preciosos momentos que he podido compartir con ellas.

A la Dra. Isabel Valles, a Juan Antonio Romero, a Laura Prats y a Mari Carmen Riverola porque siempre me han acogido con una sonrisa y han puesto su experiencia humana y profesional a mi alcance.

A tots els estudiants de doctorat de l'INTE, en particular a la Marta, al Vitaly, a la Montse i al Roger. A las xarrades rapides en els passadissos de l'Institut o a l'hora de dinar, a les calçotades al Vendrell, al cigarret a la porta.

A tutti i miei amici napoletani che vivono a Barcellona, a Mario Napolitano, ad Alexander Albore e ad Annalisa Arcella, che sono stati i miei punti fermi durante l'inizio in una cittá nuova e continuano ad essere la mia famiglia napoletana.

A Borja, que me ha llevado de la mano y me ha enseñado los rincones mas escondidos de Cataluña, a menudo dando color mediante pinceladas de la cultura andaluza. Por enseñarme una manera distinta de vivir la vida y hacerme sentir cada día mas amada.

Scientific Production

The scientific production carried out during my PhD thesis is resumed in the following list, where there is a list of the papers published in indexed scientific journals and the scientific contributions to conferences and workshops by oral presentations and/or posters.

1. Indexed Papers

   - **Grossi**, C. Vargas, A. Camacho, A. et al, 2011. Inter-comparison of different direct and indirect methods to determine ^{222}Rn flux from soil, Rad. Meas. Vol 46, Issue 1, p. 112-118.
   - **Grossi**, C. Arnold, D. Adame, J. A. et al., 2011. ^{222}Rn characterization by atmospheric concentration observations and source term at El Arenosillo tall tower of 100 meter in south-west Spain. Rad. Meas. Article In Press. doi: 10.1016/j.radmeas.2011.11.006.
   - Baeza, A., Corbacho, J.A. Rodríguez, A. Galvin, J. García-Tenorio, R. Manjn, G. Mantero, J. Vioque, I. Arnold, D. **Grossi**, C. Serrano, I. Vallés, I. Vargas, A. 2011. Increased levels of environmental radioactive fallout in Spain due to Fukushima. Submitted to J. Env. Rad.

2. Conferences and workshops contributions

   - Moreno, V. Baixeras, C. Amgarou, K. Font, Ll. **Grossi**, C. Vargas, A. 2011. Study of radon detector response under extreme environmental conditions. II Congres SEFM-SEPR. 10-13 may, Sevilla (Spain).
   - **Grossi**, C. Vargas, A. Arnold, D. et al, 2010. Set-up of a radon monitoring station in a 100 m height tower in the southern coast of Spain, 6th Conference on Protection against Radon at Home and at Work. 13-17 September, Prague (Czech Republic). Poster.
   - **Grossi**, C. Vargas, A. and Arnold, A., 2009. Quality study of electret radon flux monitors by in situ inter-comparison in Spain. IAEA/WMO Technical Meeting on Sources and measurements of radon and radon progeny applied to climate and air quality studies. 22-24 June, Vienna (Austria). Oral presentation.
   - Arnold, D. Vargas, A. **Grossi**, C. et al, 2009. Influence of heterogeneous and distant radon sources on local and regional radon transport. IAEA/WMO Technical Meeting on Sources and measurements of radon and radon progeny applied to climate and air quality studies. 22-24 June, Vienna (Austria).
   - Vargas, A. Arnold, D. **Grossi** C., 2009. Continuous Radon Measurement Campaign Applied to Model Validation at the 100 Meters Tower of El Arenosillo Station on the Huelva Coast (Spain). IAEA/WMO Technical Meeting on Sources and measurements of radon and radon progeny applied to climate and air quality studies. 22-24 June, Vienna (Austria).

- **Grossi**, C. Vargas, A. Lopéz-Coto, I., 2008. Comparison campaign of radon exhalation rate in some stations of the Spanish Automatic surveillance Network (REA). II Reunion Anual de la Red de Radiacion Natural (RadNa). 18-21 November, Huelva (Spain). Poster.
- Vargas, A. Arnold, D. Gonzalez, M.A. **Grossi**, C. et al, 2008. Temporal variation analysis of radon progeny ratio behavior in outdoor air at two radio meteorological stations in Barcelona and Madrid. EGU General Assembly, 13-18 April, Vienna (Austria).

3. Attendance at Congresses and Workshops

- Mediterranean School on Mesoscale Metereology 3rd edition - Fundamentals and applications of probabilistic forecasts and Ensemble Prediction Systems, 26-30 Maggio 2008, ARPA Sardegna, Alghero, Italy.
- Introductory course on MM5-MPP, FLEXPART and their applications, 27-30 Novembre 2007, INTE-UPC, Barcelona.

4. Seminars

- ^{222}Rn gas as tracer for air mass transport. Characterization of a 100 m high tower on the southwest Spanish coast. 8th December, 2011. Institut of Agricultural Science, ETH Zurich.
- Characterization of ^{222}Rn exhalation source in the Huelva phosphogypsum pile and statistical analysis of ^{222}Rn and ^{220}Rn gases concentration in air. III Meeting PRIMA, INTE-UPC. Barcelona 16th July, 2010.
- Radon gas concentration measurements to the INTA metereological station of *El Arenosillo*. II Meeting PRIMA, INTE-UPC. Barcelona, 11st Dicember, 2009.
- Comparison campaign of radon exhalation rate in some stations of the Spanish Automatic Surveillance Network (REA). I Meeting PRIMA, INTE-UPC. Barcelona, 17th Dicember, 2008.

Index

List of figures

List of tables

Part I

Introduction and Objectives

Chapter 1

Introduction and Background

1.1 Introduction

Natural radionuclides are widely used to examine a large variety of relevant atmospheric processes and to validate comprehensive global transport models (WMO,2004). Particularly,natural radioactive radon (^{222}Rn), thoron (^{220}Rn) and their progenies are the main contributors to environmental radioactivity present in the atmosphere (Nazaroff and Nero, 1988). Because these source/sink distributions are reasonably well constrained, these radionuclides can be used to assess the characteristics of the large and global scale transport of gases and aerosols as depicted in General Circulation Models (GCMs) (GAW, 2004).

^{222}Rn gas has proven to be very useful as a tracer to validate the Atmospheric Transport Models (ADM) and has been studied in the past as well as nowadays by several researchers such as Chevillard et al., 2002; Considine et al., 2005; Tagushi et al., 2002 and the PhD thesis of Arnold, 2009. Intensive research has been carried out on a global scale using ^{222}Rn for global atmospheric transport model evaluation as well as for estimating fluxes of atmospheric constituents or pollution such as by Vinuesa and Galmarini, 2007. Furthermore, a new application in recent years has been the use of radon for estimating regional scale greenhouse gas emission such as by Biraud et al, 2000 and by Hawkins et al., 2010. In addition, the determination of the vertical profile of ^{222}Rn concentration at a high tower is also being studied because it is really useful in order to understand atmospheric processes such as nocturnal inversion (Galmarini, 2006; Cohen et al, 1972) and for validation of transport models with different spatial resolutions (Seibert, et al, 1998).

^{222}Rn is a naturally occurring gas generating from ^{226}Ra decay as is illustrated in the decay chain of ^{238}U in Figure 1.1, the radon can be detected in the atmosphere and its exhalation from soil can be directly evaluated on a local scale (Morawska, 1989; Grossi et al, 2011) or indirectly extrapolated on regional/global scales related to radium content in

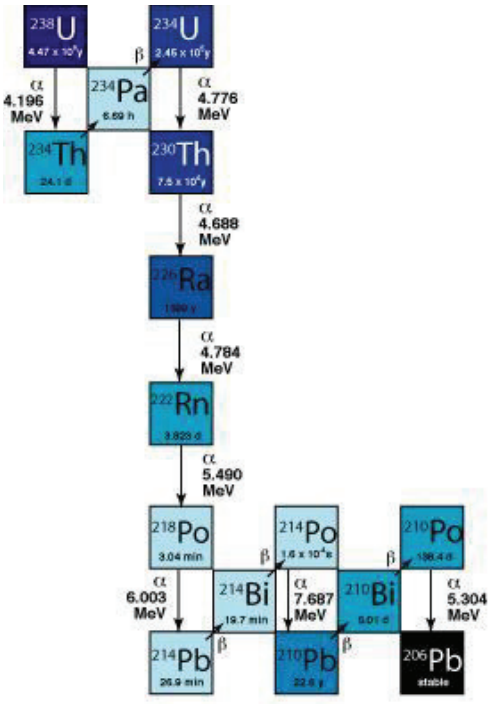

Figure 1.1: Decay chain of ^{238}U

the soil (Nazaroff and Nero, 1988), to the soil parameters (PhD thesis López-Coto, 2011) or to the terrestrial gamma dose rate (Szagvary et al, 2007). However, the efficient use of radon in atmospheric modelling studies is limited by the accuracy of the spatial and the temporal variation of the radon source function, which is used by models (WMO, 2009). Furthermore, there is still an uncoordinated global approach for radon flux andatmospheric radon concentration measurements, data archiving and data quality which does not provide the scientific community with both a complete and harmonized data base (WMO, 2009).

Indeed, the use of radon for validation of atmospheric transport models relies in part on accurate estimates of the ^{222}Rn source term (PhD thesis Arnold, 2009). Radon exhalation from the soil depends on several factors which are related to soil material characteristics and environmental conditions. All these facts make the exact measurement of radon flux quite complex (Nazaroff and Nero, 1998) and the creation of radon flux inventories taking into account the spatial and temporal variation of radon flux is a really important task for the scientific community (WMO, 2009). On the other hand using the ^{222}Rn as a tracer for atmospheric studies is related to the availability of high quality data of atmospheric radon concentrations, measured with a good spatial distribution both on the horizontal

as well as on the vertical scale (WMO, 2009).

Nowadays, some European projects and data bases, such as the TTtorch (www.ttorch.lsce.ipsl.fr) and the InGOS (www.ingos-infrastructure.eu), are carrying out continous measurements of atmospheric ^{222}Rn gas concentrations together with others greenhouse gases measurements at high towers because there is a great need to support and integrate atmospheric monitoring (GAW, 2004). However, these atmospheric high towers are still quite geographically sparse and there is a need for a data harmony (GAW, 2004). Furthermore, many studies have been done and are still improving the ^{222}Rn source function estimation with regard to its spatial and temporal variations by both direct and indirect methods (WMO, 2009). Indeed, several suitable global datasets for predicting the ^{222}Rn emissions are nowadays becoming available to modellers (Schery and Huang, 2004; Szagvary et al, 2007). Particularly, a model built by Lopéz-Coto, 2011 during his doctoral research to try to take into account the temporal variations of radon flux due to metereological conditions and the spatial variations of radon flux due to the geological soil characteristics.

Within this framework, and within a MICINN (Spanish Ministry of Science and Innovation) founded project (Reference CGL2008-00473), the present thesis aims to build and characterize a new atmospheric radon station at the *El Arenosillo* station, on the south-western coast of Spain to performe atmospheric radon concentration measurements at different height due to the presence of a 100-m-high tower at this station. Furthermore, the study aims to properly characterize radon flux background in this area. Therefore, the present study includes analysis of atmospheric radon gas concentration by the electrostatic chamber method under seasonal metereological parameters at two different heights together with characterization of the radon flux of the *El Arenosillo* station area by direct methods on local scale and by indirect radon flux inventories on regional scale.

The *El Arenosillo* station, which belongs to the National Institute of Aerospace Technology of Spain (www.inta.es), was selected for devoloping this work because it can be potentially used for atmospheric tranport models evaluations with atmospheric radon observations. Indeed, several air masses reach the *El Arenosillo* station as pointed out by Hernández-Ceballo et al, 2011 and its surroundings have a quite low radon flux background. Furthermore, the *El Arenosillo* station is equipped with a 100-m-high meteorological tower.

The direct method used for radon flux measurement was performed by the Electret Ionization Chamber (EIC) monitors of E-Perm (Kotrappa, 2009 and Grossi et al, 2011). Beforestarting the radon flux study at the *El Arenosillo* station, the EIC E-Perm monitor response was analyzed by laboratory and *in situ* comparison with other direct and indirect methods. In addition,a potential high radon source was identified in the phosphogypsum pile of the city of Huelva, which is only 25 km away from the *El Arenosillo* station and therefore the radon exhaled from its surface could be detected at the *El Arenosillo* tower. Two fields campaigns were carried out during wet and dry seasons to evaluate the radon

flux on the phosphogypsum pile surface both for its restored and unrestored areas by direct and indirect methods. In order to measure the atmospheric radon gas concentration at the *El Arenosillo* tall tower, two Atmospheric Radon MONitors (ARMON) were designed, built, calibrated and set up at *El Arenosillo* station at 10 m and at 100 m heights. Analysis of atmospheric radon time observations at 10 m and at 100 m during 2009-2011 and their influence arising from metereological parameters were studied in order to find out typical radon gas behaviour at this station. Finally, a preliminary analysis of the origin of air masses reaching the *El Arenosillo* station and related synoptic situations was done by back-trajectories with the HYSPLIT4 model and GDAS metereological files (Draxler et al, 2009).

1.2 Background

1.2.1 Overview

Radon (^{222}Rn) and thoron (^{220}Rn) gases are present in soil because they are produced in the decay chain of ^{238}Ra and ^{232}Th, respectively (Nazaroff and Nero, 1988). Indeed, the ^{222}Rn and the ^{220}Rn gases after having been exhaled from the soil, undergo dispersion and diffusion processes in the atmosphere and their only sink is by radioactive decay, with a half-life of 3.8 days for radon and 56 seconds for thoron.

In the early 1980s the first studies concerning ^{222}Rn and its decay products were mainly focused on their radiological risk (UNSCEAR, 2000). Later on, ^{222}Rn was proven to be a useful passive naturally occuring tracer in atmospheric transport studies and several interesting works appeared using radon as an atmospheric tracer at different scale magnitudes (Butterweck et al, 1994; Porstendorfer, 1994). As it is a noble gas, it is not removed from the atmosphere by dry or wet deposition processes, nor does it become attached to aerosols so it can be used as a good tracer for air mass movements. Particularly, radon with its long-range transport, due to its half-life of 3.8 days, can be provide a good test for the treatment of advection and diffusion in global and regional models (Lupu and Cuculeanu, 2001).

Another important characteristic of radon is that its half-life of 3.82 days makes it a valuable instrument to identify air masses which have passed over land within the previous few days or, on the other hand, those passing over the sea and are hence poor in ^{222}Rn (Whittlestone and Zahorowski, 1995). As it is emitted primarily from land surfaces, radon is especially useful for studying vertical dispersion in the atmosphere, and for distinguishing between continental and maritime air masses (Omori et al, 2009). Furthermore, the presence of this gas in the atmosphere is constant and does not require specific monitored release as in artificial radionuclides case studies (PhD thesis Arnold, 2009). All these characteristics described above make radon a really useful tracer (WMO, 2009).

Several studies have been done from very locale scales, in order to analyse vertical mixing within the PBL, up to regional and hemispheric scales, for validation studies of atmospheric transport models. Studies have even been done on the global scale (Zahorowski et al, 2004). For example, the classical treatment of the vertical dispersion of ^{222}Rn and its daughter products under steady-state atmospheric conditions is due to Jacobi (Jacobi and Andre, 1963). Based on an assumed vertical variation of eddy diffusivity for their typical stability classes ranging from unstable to stable cases, they evaluated concentration profiles in the troposphere up to 10 km. Subsequently, studies extended the treatment to include time variation of the eddy diffusivity profile (Butterweck et al., 1994).

As a consequence of natural radionuclides being used as atmospheric tracers, a first international expert meeting was held in 2003 on sources and measurements of natural radionuclides applied to climate and air quality studies,particularly for radon. This meeting was co-sponsored by the World Meteorological Organization (WMO), the International Atomic Energy Agency (IAEA) and the Centre National de la Recherche Scientifique (CNRS) (WMO, 2004). The meeting conclusions underlined how the effective use of radon gas is limited by the lack of an accurate estimation of its source and its spatial/temporal variation used in models and by the absence of a globally coordinated approach to measure atmospheric radon gas as well as radon flux. The main conclusion of the meeting pointed towards a future harmonization of these data. Furthermore, in the recent years the increased availability of relatively low cost high-precision detectors has made the gathering of radon datasets more affordable. An example of such data collection is the use of radon monitors as part of the World Meteorological Organization's Global Atmosphere Watch (GAW) network. Concentrations of this natural radionuclide are monitored at GAW Global stations because they can aid the interpretation of meteorological processes occurring at the stations and especially how these processes affect concentrations of other atmospheric pollutants measured at the same stations (GAW, 2007).

Along these lines, several new projects and programs were started in 2009-2011 years such as the InGOS (http://www.ingos-infrastructure.eu/) and the TTorch ESF RNP (http://ttorch.lsce.ipsl.fr/). The InGOS is a 5-year EU-funded infrastructure project targeted at improving and extending the European observation capacity for non-CO_2 greenhouse gases and related tracers such as ^{222}Rn. The InGOS involves 34 partners from 15 countries. The TTorch program aspires to create a network of observatories of long lived non-CO_2 greenhouse gases and related tracers because the combination of atmospheric observations and inverse atmospheric transport models enables us to detect trends in concentrations and emissions.

The great importance of ^{222}Rn gas as a tracer for atmospheric models validation led to the need to organise a second Expert Technical Meeting by the IAEA. This was held in 2009 with the specific focus on radon and its progeny used as tracers for atmospheric models validations (WMO, 2009). The main topics of this meeting were the debate of the problems related to the direct measurement of radon flux from the Earth's surface, set-up and use of models for radon flux estimation from the soil infunction of soil proprieties

and metereological conditions, the harmonization of measurements of atmospheric radon and radon progeny concentrations. Furthermore, the meeting conclusions pointed out the importance of improvements in the use of continuous PBL concentrations or of vertical gradients and the development and/or the use of high-resolution atmospheric transport models. Developments in these areas were considered to be needed to improve the usefulness and reliability of input data used for atmospheric transport models validation and to study atmospheric processes (WMO, 2009).

1.2.2 Atmospheric ^{222}Rn concentration

Historically, the first radon measurements in the outdoor atmosphere were done by integrated detectors with the aim of analyzing its vertical distribution. Several studies were done at high altitude (Wilkening, 1970) and for high towers (Moses et al, 1963; Cohen et al, 1972; Ussler et al, 1994), which offer the possibility of obtaining a radon concentration profile. In particular, high towers allow eddy diffusivity to be studied by measurement at two different tower heights (Cuculeanu and Lupu, 1996; Guedalia et al, 1974; Fontan et al, 1979). However, integrated detectors did not provide a good temporal variability analysis for this gas on an hourly scale and were not useful for studies of the atmospheric boundary layer.

It is clear that the position of radon as useful tracer has involved a great improvement in the research regarding detection techniques (Whittlestone and Zahoroski, 1970). The first continuous monitoring of radon concentration in air was carried out in the mid 1960s in inland areas (Taylor and Lucas, 1966). However, this monitoring was not efficient enough for measurements at coastal sites, where radon concentration values can even be lower than 1 Bq m^{-3} (Zahorowski et al, 2004). Atmospheric radon monitors able to measure radon gas concentrations of the order of a hundred of mBq m^{-3} using measurement of radon progeny concentrations have been used since the 1970s (Lambert et al, 1970). Indeed, in the beginning radon progeny monitors were commonly used and the radon gas concentration had to be extrapolated by a technique that required accompanyning assumptions regarding equilibrium of the progeny with respect to the ambient radon. However, these assumptions were not always true mainly under really unstable conditions of atmospheric layers (Kritz et al, 1990). Subsequently, the first instrument able to measure radon gas directly was built by Hopke, 1989. Nowadays the most common techniques used for atmospheric radon concentrations measurements are usually based on two filters (Zahorowski et al, 2004) and electrostatic detection methods (Hopke, 1989; Roca et al, 2004). In the two-filter method the sampled air is drawn into the detector through a first filter which removes aerosols as well as ambient ^{222}Rn and ^{220}Rn progeny. Once inside the detector delay chamber, ^{222}Rn is delayed for sufficient time to allow new progeny to be produced. The new progeny are then collected on a second filter. Since they have been produced in controlled conditions, their number is proportional to the ^{222}Rn gas concentration (and to ^{220}Rn, if present in the delay chamber) (Zahorowski et

al, 2004). The collected progeny are counted using an alpha particle detector. The second filter can be used as a filter tape or a wire mesh (Whittlestone and Zahorowski, 1995). Usually a zinc sulphide scintillator and a photo multiplier tube are used as an alpha particle detector. This means that this method does not allow alpha peak separation (WMO, 2004). In the electrostatic method the ^{222}Rn flows through a first filter which stops aerosols particles and radon/thoron progeny. The collection of ^{218}Po generated by radon decay in the detection volume is then done by a uniform electric potential of several kV between the detection volume walls and the surface of a solid state detector. A multichannel analyser is used for signal processing. This method allows a high resolution spectral analysis of alpha particles and it will be fully explained in the next chapter of this thesis (Iida et al, 1996).

The increase of the importance of radon as a tracer meant that it was included with other gases in international atmospheric research campaigns (Bates et al, 1998; Colle et al, 1995) and its applications as a tracer started for general circulation models (Iida et al, 1996). Most environmental radon studies were focused on temporal and spatial radon concentration variability in the atmosphere and its correlation with radon exhalation or with meteorological factors. The correlation between ground level radon concentrations and meteorological conditions in the lower atmosphere has been extensively studied by Pearson and Moses, 1966; Ikebe, 1970; Beck and Gogolak, 1979; Kataoka et al, 2001 and Galmarini, 2006. Such types of analysis need a consistent data base of radon concentration time series and of meteorological parameters such as temperature, humidity, pressure, wind speed and wind direction. Furthermore, knowing both wind speed and direction at a specific site is also useful for making a preliminary qualitative analysis about the origin of air masses that are rich/poor in radon (Crawford et al, 2009). These types of analysis can be done by relating wind speed and direction observations to measured local radon concentrations (Levin et al, 2002). This provides better knowledge of the ^{222}Rn source term, thus enabling a more accurate study of the local radon contribution in the lower atmosphere (WMO, 2004).

It is important to underline the fact that the variation of radon concentration measured at a particular site not only depends on the local radon exhalation rate from the soil, but also on the transported radon contribution (Zahorowski et al, 2004; Crawford et al, 2009; Arnold et al, 2010). This contribution from remote sources cannot be neglected and, obviously, it is strongly influenced by the transport pattern affecting regions (Arnold et al, 2010). Therefore, the installation of high towers became very useful in these studies in order to measure radon concentration both at low and high levels and to evaluate both the local and remote contribution (WMO, 2009). In the last 4 years great improvements have been made in Europe in atmospheric monitoring and particularly in observations and studies related with radon. Nevertheless, there is still a lack of available data of radon measurements at high towers well distributed over Europe. Indeed for example, there is not yet atmospheric monitoring for high towers in the South of Europe such as the South of Spain, Portugal, Italy and Greece. These monitoring areas could offer the possibility of not only studying the vertical radon concentration profile, but also of evaluating the

remote radon source contribution coming from the North of Africa.

1.2.3 ^{222}Rn flux

First studies on radon exhalation rate started at the beginning of the 80s by laboratory measurement on soil samples (Keller et al, 1982; Keller and Schutz, 1988; Morawska, 1989). All these studies supposed that the sample volume was smaller than the radon diffusion length in the material. This enables the radon emanated from soil grains to the pore space for diffusion to the soil/air interface (Morawska, 1989). The following studies focussed on the influence of material humidity content and other metereological parameters on the radon exhalation rate such as the studies by Stranden, 1984 and Bossus, 1984. Subsequently, studies on measurement of radon flux directly *in situ* in soil were performed in order to measure the radon diffusion coefficient in different soil types and to understand the influence of geological soils parameters of observed radon flux (Damkjaer and Korsbech, 1985).

Understanding of radon flux (Bq m^{-2} h^{-1}) and its distribution over the earth is still under question because of a lack of direct radon flux measurements in many regions (WMO, 2009). Indeed, direct measurements of radon flux could ideally be carried out using the accumulation method (Keller et al, 1982) which allows ^{222}Rn gas to accumulate and to be measured in a chamber placed over the soil. Nevertheless, direct radon flux measurements raise several open questions about the influence of environmental conditions on radon exhalation from the soil surface (WMO, 2009; Grossi et al, 2011) and the influence of the measurement method itself on radon flux (WMO, 2009). Furthermore, all intruments actually used for radon flux measurements are based on the accumulation method, which will be presented in the following chapter, but this approach is not practical on a worldwide scale and measuring radon flux does not seem to be so trivial (DeMartino and Sabbarese, 1997; WMO, 2009). Indeed, ^{222}Rn concentration in soil and its exhalation rate depend not only on soil properties such as the geology of an area, the porosity and permeability of the soil, the structure of the terrain and associated ^{238}U mineralization (Nazaroff and Nero, 1988).

This previous discussion explains how mapping the variation of ^{222}Rn flux over the Earth's surface also requires knowledge of many metereological factors such as atmospheric precipitation and atmospheric temperature which can strongly influence soil temperature and soil humidity and this leads to a different release of ^{222}Rn gas to the atmosphere (Nazaroff and Nero, 1988; PhD thesis López-Coto, 2011). In addition, the radon flux measurement method could influence the device response because it could reduce natural radon accumulation by diffusion in the volume as ideally happens in free soil. All these factors make radon flux measurement quite difficult and leads to the need forharmonising the whole measurement process.

Diffusion is the main process which allows ^{222}Rn to escape from soil pores to the atmosphere after formation by ^{226}Ra decay when the pressure gradient between the pore soil interstices is negligible (Nazaroff and Nero, 1988). In spite of sufficient understanding of the theoretical processes controlling release of ^{222}Rn from the soil to the atmosphere (Nazaroff and Nero, 1988; Porstendorfer, 1994), understanding of radon flux and its distribution over the earth is still under question because of the difficulties in obtaining direct radon flux measurements due to their dependence on all the above cited factors. Nowadays, researchers used different approaches to overcome the need for labour-intensive direct observations. Indirect mapping of radon flux has been carried out due to existing knowledge about parameters related to radon flux and for which more large-scale information is available than for radon flux itself. The different approaches have been applied in order to indirectly map radon flux. The simplest assumption is that of a radon flux value from the land surface of 1 atom cm^{-2} s^{-1} between 60 °S and 60 °N , of 0.5 atom cm^{-2} s^{-1} between 60 °N and 70 °N and of 0 atom cm^{-2} s^{-1} for the sea (Rash, 2000). A modification with a linear decrease from 1 atom cm^{-2} s^{-1} at 30 °N to 0.2 atom cm^{-2} s^{-1} at 70 °N was proposed by Conen and Robertson, 2002. These estimates are based on atmospheric ^{222}Rn inventories.

Another approach was developed within the Swiss project *European Radon Flux Map for atmospheric tracer applications* by Basel University in 2009. It is based on the determination of an empirical linear relation between radon flux and terrestrial gamma dose on a European scale. These last values were extracted during the project from routinely reported emergency monitoring data. These data are available in quasi real time at the Joint Research Centre of the European Commission of ISPRA (Italy) from each of the 3.600 stations of the national emergency monitoring network in Europe, EURDEP (Szagvary et al, 2007). Knowledge about the detectors used in each contributing country, detector elevation above sea level and the possible contribution from artificial radionuclides, mainly ^{137}Cs, enables the extraction and the spatial modelling of the terrestrial gamma dose (Szagvary et al, 2007). The dose-rate values for the EURDEP network regarding Spain are provided by the REA, the Spanish Automatic Surveillance Network of the Spanish Nuclear Safety Council (CSN). A different option to obtain the terrestrial gamma dose rates is by radiometric data generated through the Spanish National Uranium Exploration and Investigation Plan. This work has been developed within the Spanish MARNA project (Quindós et al, 2004; PhD thesis Arnold, 2009). Recently a new indirect method to get ^{222}Rn flux map on regional scale has been developed in the PhD work of Lopéz-Coto, 2011. This method aims to include in the indirect method metereological informations, gelogical parameters and ^{226}Ra activity in soil which have an extreme influence on radon exhalation from the soil surface (Grossi et al, 2011). The ^{226}Ra activity wasextrapolated for this study by uranium concentration conversion factors of the International Atomic Energy Agency (IAEA) and the uranium activity data were obtained by FOREGS as explained in the PhD thesis of López-Coto, 2011. The information on geophysical soil property is extracted by a HWSD data base which offers soil parameters with a spatial resolution of 1 km. Finally, metereological informations were obtained by ERA-40 global

re-analysis (PhD thesis López-Coto, 2011).

Actually, the most realistic alternative at the moment to obtain an optimal radon map on the local and global scale seems to require a modest number of high quality direct accumulator measurements at carefully chosen locations, representative of different geological regions and to extrapolate these measurements, by indirect methods, for similar regions including the metereological informations (WMO, 2009).

1.2.4 Atmospheric Modelling

Forecast simulations of possible atmospheric releases are performed to assess environmental consequences and to plan the appropriate protection strategy. The atmospheric dispersion modelling of radioactive plumes is then an important part of emergency programs that are established for each individual nuclear facility. These are thus needed to establish source-receptor relationships in order to estimate the atmospheric concentrations or interpret measurements. Backward models are computationally more efficient and are often preferred when there are more sources than receptors, or when the number of receptors is limited and the sources are unknown (PhD thesis Arnold, 2009).

The usefulness of radon as a tracer to atmospheric studies has been previously remarked. In environmental science such studies usually require the use of modelling tools, both in meteorological as well as in dispersion issues. With the improvement of computer capabilities, numerical models have rapidly spread among the scientific community and so modelling work and model improvements are a hot topic nowadays (Seibert and Frank, 2004; Stohl et al, 2003). Actually, one of the most used metereological models for mesoscale analysis by the scientific community is the Weather Research and Forecasting (WRF) model. The WRF is a next-generation mesoscale numerical weather prediction system designed to serve both operational forecasting and atmospheric research needs. It features multiple dynamical cores, a 3-dimensional variational (3DVAR) data assimilation system, and a software architecture allowing for computational parallelism and system extensibility. The WRF is suitable for a broad spectrum of applications across scales ranging from metres to thousands of kilometres (http://www.wrf-model.org/index.php). Others used models are the Integrated Forecast System (IFS) and the American Global Forecast System (GFS). The IFS is an operational global meteorological forecasting model. It is developed and maintained by the European Centre for Medium-Range Weather Forecasts (ECMWF) based in Reading, England. Because of its source, it is often known as the ECMWF or the "European model" in North America, to distinguish it from the American Global Forecast System (GFS). Furthermore, there is the Global Data Assimilation System (GDAS). This system consists of a complex system of data analysis. It has spectral statistical interpolation (SSI) routine related to a three-dimensional variational analysis (3DVAR) (Kalnay, 2003).

As regards Atmospheric Transport Models (ATM), they use mathematical algorithms to simulate how pollutants in the ambient atmosphere disperse and, in some cases, how they react in the environment. The dispersion models require input data such as meteorological conditions, emissions parameters and orography. The meteorological conditions include wind speed and direction, the amount of atmospheric turbulence, the ambient air temperature and the height to the bottom of any inversion aloft that may be present. The emissions parameters consist of source location and height, source vent stack diameter and exit velocity, exit temperature and mass flow rate. Finally, the orography provides informations about terrain elevation at the source location and at the receptor location, together with the location, height and width of any obstructions (such as buildings or other structures) in the path of the emitted gaseous plume (PhD thesis Arnold, 2009). The trajectory models define the paths of infinitesimally small particles of air traced both in backward or forward mode. While forward trajectories give information about where an air parcel will go, backward trajectories show where it comes from. The trajectory models are fast and not computationally expensive since they use a simple advection schem, and as they have a simple output, they are easy to represent on a map, this makes them very attractive to be used. Nevertheless, the computation of trajectories from meteorological data (ie. ECMWF) have certain inaccuracies and this becomes a limitation in their applicability since it should be pointed out that they do not account for dispersion.

Nowadays, one of the most used models by the scientific community are the FLEXPART model (http://transport.nilu.no/flexpart), a lagrangian particles model capable of simulating dispersion phenomena from the global to the local scale (Seibert et al, 1998; Seibert and Frank, 2004; Arnold et al, 2010) and the Hybrid Single Particle Lagrangian Integrated Trajectory model (HYSPLIT), version 4 (http://ready.arl.noaa.gov/HYSPLIT.php).
The HYSPLIT model was developed by the Laboratory of NOAA Air Resources (ARL) (Draxler and Hess, 1998; Draxler et al, 2009). The HYSPLIT4 usually works with GDAS meteorological files as input files, but it has been recently modified to work with WRF meteo files. The HYSPLIT4 was selected to perform the back trajectory analysis in this thesis because it is user friendly, it can be quickly downloaded online with information about past courses and it has an optimal visual package which is downloaded with program.

1.3 Thesis Aim and Milestones

The ^{222}Rn is a good tracer for atmospheric studies and for the validation of atmospheric transport models. Knowing the radon source term as an input for ATM models is required because this knowledge, together with meteorological input conditions, strongly influences reliability of the ATM model. Furthermore, having high quality atmospheric radon concentrations data at different heights can be really useful for comparison with transport model results, for understanding the atmospheric boundary layer phenomena on an hourly time scale and, lastly, the data can be assimilated into models. Therefore, radon was decided to be used as a tracer and the aim of this work is to set-up a new atmospheric radon station in the South of Europe which will offer high quality data of atmospheric radon concentration at different heights and at a coastal site. Furthermore, this thesis aims to study radon flux in this area in order to obtain precise knowledge of it.

This work contemplated some intermediate milestones that had to be achieved. Each of them was composed of several study and work steps:

a) The ^{222}Rn flux as an input for atmospheric transport models:

1. Bibliographic research on methods for measuring radon flux both directly and indirectly.
2. Study of the response of the Electret Ion Chamber (EIC) under controlled environmental conditions in the INTE-UPC radon chamber and on soil samples.
3. Validation of an inter-comparison campaign study with different direct and indirect ^{222}Rn flux methods to check the reliability of Electret Ion Chamber (EIC) monitors *in situ* in soils.
4. ^{222}Rn flux characterization of the *El Arenosillo* station; measurement at the *El Arenosillo* tower and near the Huelva phosphogypsum pile by direct and indirect methods.
5. Study of ^{222}Rn flux estimation for surrounding areas of the *El Arenosillo* station on a regional scale, in order to appreciate distant radon source contributions.

b) ^{222}Rn gas concentration measurements in the lower atmosphere

1. Bibliographic research on methods for measuring radon gas in air.
2. Development of an atmospheric radon monitor (ARMON) to measure atmospheric ^{222}Rn concentrations. Monitor calibration under controlled environmental conditions in the INTE-UPC radon chamber.

3. Set-up of two radon monitors at *El Arenosillo* station at 10 m and at 100 m heights.
4. Statistical analysis of acquired radon concentration data at 10 m and at 100 m heights at the *El Arenosillo* station during 2009-2010 and its influence by meteorological parameters.

c) Origin of air mass quality study on the synoptic scale

1. Selection of the most common synoptic scenarios at the *El Arenosillo* station.
2. Study by back-trajectory analysis of the origin of air masses reaching the *El Arenosillo* station during the selected synoptic scenarios.

The work is presented in the following Chapters:

CAP 2 Material and methods used in this study are presented and described in this chapter. The Electret Ionization Chamber (EIC) E-Perm is the chosen method for direct radon flux measurement. Two Atmospheric Radon MONitors (ARMON) were built and calibrated for atmospheric radon measurements at two heights. Finally, the HYSPLIT4 model was used to perform the back-trajectory analysis. The *El Arenosillo* station site and the Huelva phosphogypsum pile are described in this chapter.

CAP 3 A laboratory validation study was done in order to evaluate the response of EIC E-Perm and of the ARMON monitors for different radon concentration exposures and under different well-know environmental conditions, in the radon chamber of the INTE-UPC. Materials and methods used in this study are presented in this chapter together with discussion of the results.

CAP 4 EIC E-Perm monitors results were validated by a comparison campaign directly *in situ* in soil together with other direct and indirect radon flux methods at four sites of Eastern Spain. Methods and instruments used are presented in this chapter. Results of the study are reported and discussed.

CAP 5 A laboratory study was carried out to evaluate the reliability of the EIC E-Perm monitors for radon flux measurement from different volume of soil samples with different humidity contents. Materials and methods used in this study are presented in this chapter together with a discussion of the results.

CAP 6 Characterization of the radon flux area, on a local and on a regional scale, in the surroundings of the *El Arenosillo* station was performed by direct and indirect methods. Methods are presented together with the results.

CAP 7 Atmospheric radon concentrations were measured at *El Arenosillo* station at 10 m and at 100 m for two years and analyzed together with wind direction and wind speed parameters in order to study the diurnal and seasonal radon gas behaviour at this station. Materials and Methods used in this analysis are presented. Results of the whole analysis are reported and discussed in this chapter.

CAP 8 Observed scenarios of radon concentration measured at *El Arenosillo* station were selected for performing a set of back-trajectories. The study allows a qualitative analysis of the origin of different air masses reaching the *El Arenosillo* station. Methods and Results of this study are presented in this chapter.

CAP 9 A summary of conclusions for each work step and the general conclusions of the thesis are reported in this chapter.

Part II

Instruments, Methods and Validation studies

Chapter 2

Materials and Methods

2.1 Introduction

The instruments and methods to be used in this work will be described in detail in this chapter. The Electrostatic Ionization Chamber (EIC) from the Rad Elec Inc. Company (www.radelec.com) was used for the ^{222}Rn flux study. This device will be described together with the accumulation method, which is the theoretical basis of several integrated and continous radon flux instruments (Nazaroff and Nero, 1988). ^{222}Rn concentration in atmospheric layers was measured by the Atmospheric Radon MONitor (ARMON) developed at the INTE-UPC, which is based on the alpha spectrum analysis of the electrostatically collected ^{218}Po on a PIPS detector (Grossi et al, 2011a). Finally, the transport model HYSPLIT, version 4, was used to run a set of back-trajectories to analyze the presence of remote radon sources. Furthermore, the geographical location and the orography characteristics of the *El Arenosillo* station will be presented in order to explain its selection as an optimal radon station. Finally, the Huelva phosphogypsum pile will be described because it was chosen as a possible high radon source.

2.2 ^{222}Rn flux

2.2.1 The accumulation method

^{222}Rn flux can be measured by both integrated and continuous monitors which are based on the accumulation method (Morawska, 1989). ^{222}Rn exhaled from the soil surface is accumulated during a time period (T) in a monitor with a known volume, which was preliminarily located on the soil surface (De Martino and Sabbarese, 1997). The temporal

variation of the ^{222}Rn concentration in the chamber is expressed by the following equation 2.1.

$$\frac{dC(t)}{dt} = \frac{E_{Rn}}{V_u} + \lambda^0 C(t) \tag{2.1}$$

C(t=0)=0 is the initial concentration (Bq m^{-3}) of the radon in the closed volume, E_{Rn} is the exhalation velocity, which is defined as the ^{222}Rn gas quantity leaving the soil in the time unit (Bq h^{-1}), V_u is the available chamber volume (m^3) and the constant $\lambda^0=\lambda + \lambda^*$ (h^{-1}) is given by the sum of the ^{222}Rn decay (λ) and the ventilation constant (λ^*). λ^* quantifies the possible changes of ^{222}Rn with external air because of leaks in the chamber.

Another physical factor which may be taken into account in the ^{222}Rn accumulation is called back-diffusion and is the possibility of ^{222}Rn being adsorbed back from the soil surface. This last factor is insignificant for short-time measurements as applied in our analysis (Morawska and Phillips, 1980; De Martino et al, 1998). The solution of the Equation 2.1 is the Equation 2.2.

$$C(t) = \frac{E_{Rn}}{\lambda^0 V_u}(1 - e^{-\lambda^0 t}) \tag{2.2}$$

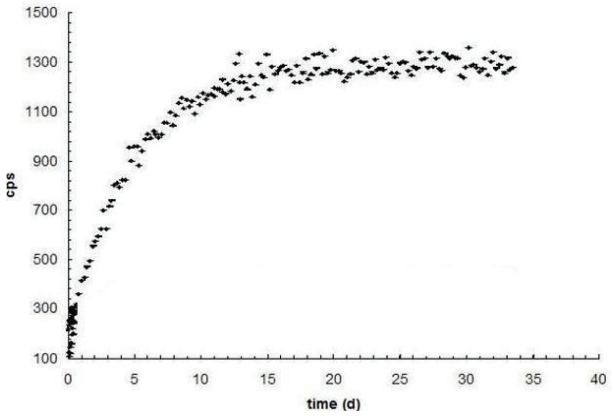

Figure 2.1: ^{222}Rn accumulation evolution in time inside a closed volume.

In Figure 2.1 the ^{222}Rn concentration accumulation in an closed volume is illustrated (MSc thesis Grossi, 2006). The value $E_{Rn}{\lambda^0}^{-1}{V_u}^{-1}$ (Bq m^{-3}) is the saturation concentration value exhaled in the air-tight chamber after almost 20 days. In the case of short-time measurements and negligible leakages in the chamber, $\lambda^0 t << 1$ can be assumed.The previous Equation 2.2 can be simplified by developing the exponential into Equation 2.3

which describes a linear relation between the ^{222}Rn concentration in the chamber and time.

$$C(t) = \frac{E_{Rn}}{V_u}t = \frac{FA}{V_u}t \tag{2.3}$$

F(Bq m^{-2} s^{-1}) is the ^{222}Rn flux and A is the surface area covered by the accumulation chamber. The linear method (Equation 2.3) is used for continuous methods (De Martino and Sabbarese, 1997).

$$C(Rn)Av = \frac{1}{T}\int_0^T C(t)dt = \frac{FxA}{\lambda^0 V_u}\left(1 - \left(\frac{1 - e^{-\lambda^0 t}}{\lambda^0 T}\right)\right) \tag{2.4}$$

The radon flux by integrated systems can be measured using the average ^{222}Rn concentration inside the chamber above a given time T calculated by Equation 2.4 (Kotrappa and Steck, 2009). From Equation 2.3 and Equation 2.4 the ^{222}Rn flux F can be derived, for both the continuous and the integrated methods, respectively.

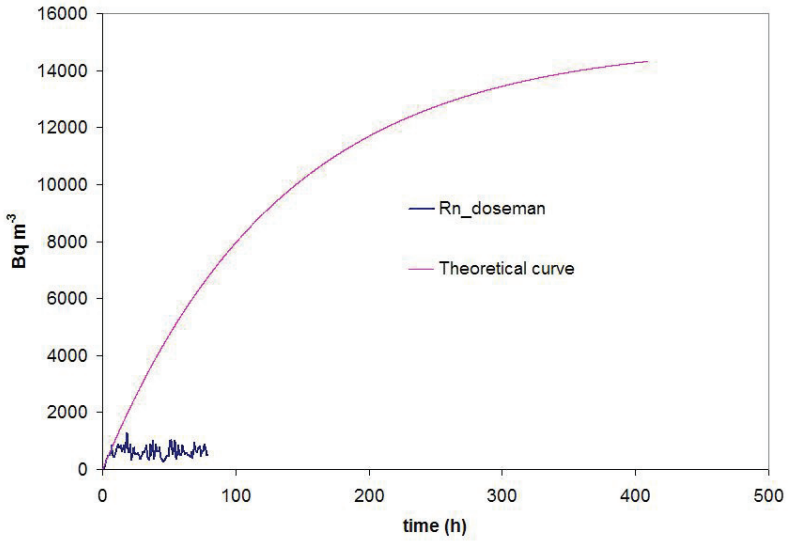

Figure 2.2: Comparison between ^{222}Rn concentration evolution expected by the accumulation method and that observed by the continuous monitor measurement

Equation 2.2 is based on the hypothesis that the radon diffusion inside the closed volume is only due to the concentration gradient between the pore material, which is located inside the sealed volume, and the air in the volume, while the advection factor due to the

pressure gradient between the air surface and the pore material is practically negligible. Nevertheless, when this equation is applied for measuring the ^{222}Rn flux directly in the soil special attention should be paid. Indeed, in the theoretical curve presented in Figure 2.1 the concentration of saturation takes approximately 30 days to be reached inside the volume, while continuous radon monitoring carried out directly in situ in soil by the research groups of the Technical University of Catalonia, Basel University and Huelva University, saturation was usually obtained in only several hours and with a concentration of saturation lower than as expected, as is shown in the example of Figure 2.2 and will be explained in greater depth in the following chapters of this thesis. This could mean that the radon in some way was not able to enter the volume and the radon exhalation process was practically modified. This effect could be due to a Darcy effect (Nazaroff and Nero, 1988) which takes into account the pressure difference between free external air and the air inside the radon flux monitor. However, Equation 2.3 is still true in this case and it can still be still used for t = 4-5 h. However, mistakes could happen in ^{222}Rn flux evaluation by integrated methods which use Equation 2.4 or for continuous methods where the first hours of measurement are carried out under environmental conditions which could have an influence on radon flux. All these prior observations will be investigated in the following chapters of this thesis.

2.2.2 EIC radon flux monitors

In order to perform the ^{222}Rn flux study in this thesis the Electrostatic Ionization Chamber (EIC) instruments developed by the Rad Elec Inc. Company were selected (Kotrappa and Steck, 2009). The EIC monitors are quite cheap and they do not need any expensive maintenance. Furthermore, they have both a small and light volume which makes them really easy to be transported.

Each EIC chamber works as an integrating ionization chamber with an internal electrically charged electret at the top. A Tyvek window allows the radon gas exhaled from the soil to enter the electret ion chamber over a time period T. The electret voltage drops in relation to the total ionized air due to radon decay inside the chamber.The electret voltage is measured directly in situ before starting measurements and 3 hours after measurements end, using a portable SPER-1E Electret Voltage from the Rad. Elec. Company. Two types of monitors are available (Kotrappa and Steck, 2009), both device types consist of a 960-ml chamber (H chamber) and an electret detector for short-term measurements, named ST. This configuration is denoted HST. The single device scheme for both monitors is illustrated in Figure 2.3. Together with these monitors a background monitor has to be used at each measurement site.

The first type of EIC radon flux monitor will be denoted as RT-EIC from now on, as it measures both radon exhalation and the contribution due to thoron exhalation from the soil. The second EIC modified monitor, denoted R-EIC, minimizes thoron response due to a buffer zone where air enters before reaching the detection chamber. It is rec-

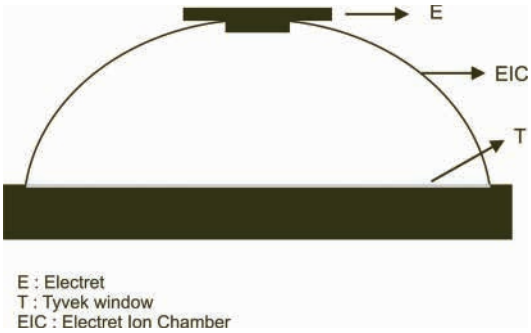

Figure 2.3: Scheme of the ionization chamber type H (E-PERM) used for radon flux measurement. The ionization chamber (EIC) is located on the ground (black space) and the exhaled radon can enter through the Tyvek window (T). The radon concentration is proportional to the potential drop due to radon decay on the positively charged electret (E) located on the chamber top in the air chamber.

ommended for high thoron level areas and areas of high permeability (Kotrappa et al, 2004). In this modified monitor, radon and thoron gas, after being exhaled from the soil surface, diffuse through the Tyvek filter and then pass through a buffer (separator) that contains four filtered holes specifically designed to reduce the influence of any thoron that may be present (Kotrappa and Steck, 2009). The measurement protocol for each of these monitors *in situ* in soil consistes of the following steps:

1. Ground to be measured is cleared of the debris and loosened
2. A paper towel is placed on the sampled soil as can be seen in Figure 2.4
3. The device is located on the paper towel and then the edges of the monitor are covered with the soil from the same area to promote sealing of the edges of the monitor, as it is illustrated in Figure 2.4
4. As soon as the monitor is in position, a pre-measured electret with an initial potential V_i is screwed into the top of the flux monitor.
5. The initial data and time t_i and the location and the electrete code are noted down. It is important not to touch the electrete surface during this operation or allow anything else to touch it.
6. Leave the monitor measuring for a time period T = 4-5 h
7. After the measurement time T, pull the monitor out of the ground and hold it in a low radon area for 3 h to allow radon progeny to decay inside the chamber.

8. Note down the data and time of the end of the sampling (t_f)

9. After these 3 hours the electret is removed from the monitor and the voltage is measured again. The final potential V_f is noted. Close the monitor with a zero electret to prevent dust getting inside and put the monitor into an air-tight bag, which is then closed at a low radon site.

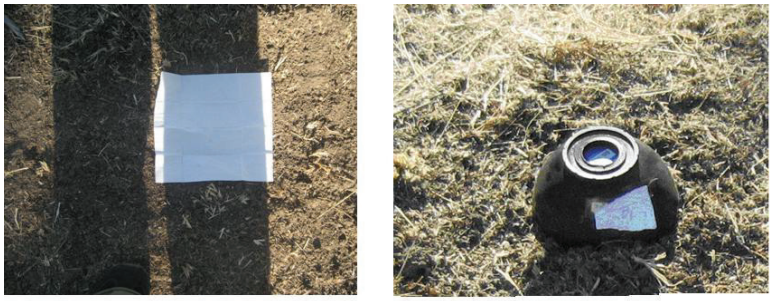

Figure 2.4: A paper towel is placed on the soil after clearing it of debris and loosened soil. The device is located on the paper towel and then the edges of the monitor are covered with the soil from the same area to seal them.

The average of radon accumulated (Bq m^{-3}) in the EIC chamber during the sampling period T and used in Equation 2.4 for radon flux calculation (Bq m^{-2} h^{-1}) can be calculated by Equation 2.5

$$C(\bar{R}n) = \frac{V_i - V_f}{TCF} - BG \tag{2.5}$$

$$CF = A + B\frac{V_i - V_f}{2} \tag{2.6}$$

where CF (Bq m^{-3} h V^{-1}) is the the calibration factor of the EIC monitor with configuration HST, T is the sampling measurement period and it is equal to t_f - t_i (h), V_i is the intial electrete voltage and V_f is the final electrete voltage. BG is the gamma ray component given as an equivalent radon concentration (Grossi et al, 2011). The measurement protocol for the background monitor is the same used for the others monitors. The CF is calculated by Equation 2.6, where the parameters A and B are given by the manufacturer for each EIC monitor configuration (Kotrappa et al, 1993). A typical measurement of radon flux by the EIC monitor is presented in Figure 2.5.

Figure 2.5: Classical EIC monitors configuration for radon flux measurement at *Los Pedrones* site (Spain).

2.3 ARMON: Atmospheric Radon MONitor

The ^{222}Rn concentration monitors for continuous measurements in outdoor air were designed at the laboratory of the Institut de Tecniques Energetiques of the Universitat Politecnica de Catalunya (INTE-UPC). The monitors were named ARMON (Atmospheric Radon MONitor). The monitor is based on alpha spectrometry of positive ^{218}Po which are electrostatically collected on a Passivated Implanted Planar Silicon (PIPS) detector surface by an electrostatic field inside a spherical volume. Each monitor consists of three modules: a detection volume, an acquisition system for alpha spectrum analysis and an automatic drying system to keep humidity low inside the detection volume.

2.3.1 Detection volume

As can be seen in Figure 2.6, the detection volume consists of a glass volume divided into two regions by a metal wire-screen and the detector. The lower region of the instrument is a glass sphere of approximately 20 L volume, which is uniformly covered internally with silver. A dew point instrument model Vaisala DRYCAP DMT340 is located in the uppermost part next to the sensor where the electrical connections are located. The preamplifier/amplifier is on the outside of the detection volume and it is connected to the

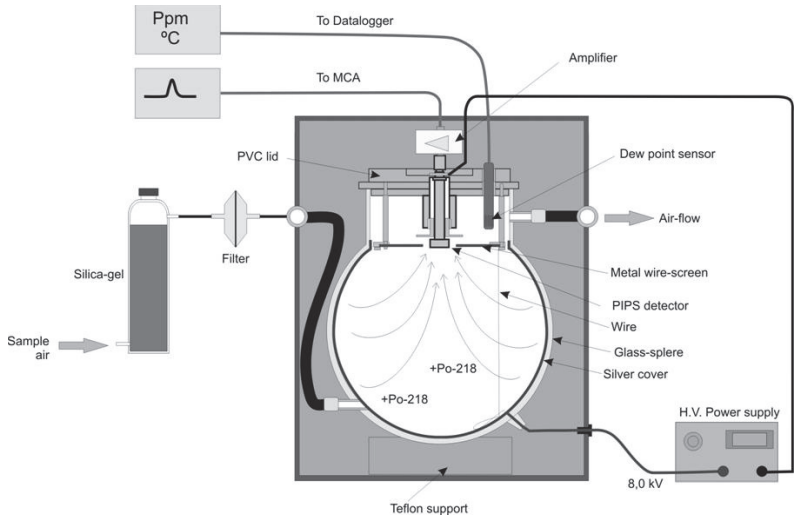

Figure 2.6: Scheme of an electrostatic sphere used for ^{222}Rn concentration measurements in the atmosphere.

α-PIPS detector through connections on a PVC lid. The wire screen and the silver surface are equipotent and the α-PIPS detector is connected to ground. An 8 kV potential is applied between the detector base and the glass sphere walls. The whole sphere is located inside a wooden box in order to prevent breakage and electrical discharges to the soil as reported in Figure 2.7, which shows the spherical detection volume located in the box and the PIPS detector located in the centre of the cap. The air sample is pumped inside the sphere with a flow rate of about 5 L min^{-1}. Before entering the sphere, the air goes through a silica gel tube in order to reduce humidity and then through a Millex-FA50 filter to prevent radon progeny entering the sphere.

2.3.2 Acquisition system and Spectra Analysis

The acquisition system to perform alpha spectrometry consists of a preamplifier model 7401 and an α-PIPS detector model A300 both from the CANBERRA company. A multichannel (MCA) EASY-USB-2K and the MAESTRO-32 version 6 from ORTEC were used for the spectra acquisition and analysis. A typical alpha spectrum analysis is shown in Figure 2.8. Together with ^{218}Po, ^{214}Po and ^{210}Po α decays from ^{222}Rn, α decays from ^{216}Po and ^{212}Po from ^{220}Rn can also be identify. This could also enable thoron to be analysed in the atmosphere in future studies.

^{222}Rn gas concentration in air is calculated by hourly counting of total alpha decay from ^{218}Po on the PIPS detector surface. ^{218}Po decays by emitting alpha particles with an

Figure 2.7: Detection volume of the electrostatic sphere ARMON used for ^{222}Rn concentration measurements in the atmosphere. The spherical detection volume is illustrated together with the volume cap which is made up of a wire screen with a PIPS detector located at its center

energy of 6.004 MeV. The presence of ^{210}Po, which decays with a half life of 138 d by emitting an alpha particle with an energy of 5.304 MeV, does not influence the ^{218}Po analysis because they do not overlap in the spectrum (Figure 2.8). However, the presence of ^{220}Rn in the detection volume could reduce the Minimum Detectable Concentration (MDC) of ^{222}Rn measurement because of the thoron product ^{212}Bi on the detector surface. Indeed, ^{220}Rn decays with a half-life ($T_{1/2}$) of 56 s via alpha emission into ^{216}Po, which immediately decays into ^{212}Bi ($T_{1/2}$ is 0.14 s) by α particle emission. ^{212}Bi has a $T_{1/2}$ of 61 min and decays in 65 % of the time via beta emission into ^{212}Po, which has a half life of only 0.3 μs and decays into stable ^{208}Pb by alpha particle emission with an energy of 8.784 MeV. For 36 % of the time, ^{212}Bi decays into ^{208}Tl by alpha particles emission with energies of 6. 051 MeV and 6.090 MeV, respectively. There is a branch in these alpha emissions of 25.4 % and 9.6 % per decay of the parent nucleus. Thallium then immediately decays into stable ^{208}Pb (Porstendorfer, 1994). Therefore, as consequence of the above explanation, when radon and thoron are present in the detection volume of the electrostatic monitor there is a sum effect between the total counts of alpha particles emitted on the α-PIPS detector surface by ^{218}Po decays, with an energy of 6.004 MeV, and the total counts due to α particles emitted by ^{212}Bi with an energy of 6.051 MeV and 6.090 MeV.

Anyway, the high spectrum resolution and the prior thoron calibration of the electrostatic sphere at the INTE laboratory enabled improvements in device sensitivity by reducing the minimum detected concentrations (MDC) of 25 %, as explained below. Indeed, as it can be seen in Figure 2.9, the three alpha energy contributions from ^{218}Po and from ^{212}Bi can be partially resolved. The total counts due to ^{212}Bi decay, which must be subtracted

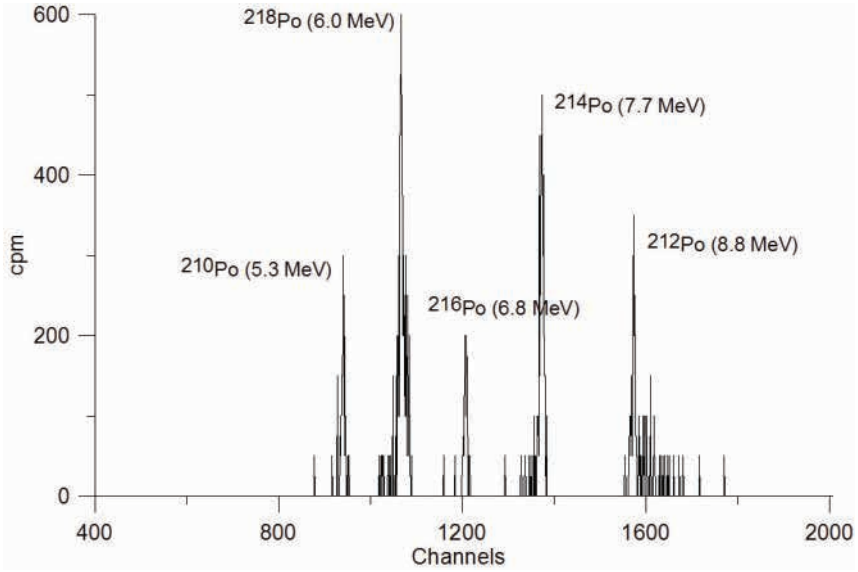

Figure 2.8: Typical alpha spectrum analysis of ^{222}Rn and ^{220}Rn in the outdoor atmosphere.

from the total net area from ^{218}Po decay, can be reduced by selecting a specific upper channel for the Region of Interest (ROI) for ^{218}Po. This leads both to a reduction in MDC device uncertainties and of radon concentration measurements.

Since ^{212}Bi has an alpha energy higher than ^{218}Po, the upper channel for the ROI of ^{218}Po (C_u) can be carefully chosen in order to subtract only half of the net area from ^{212}Bi interference, as presented in Figure 2.9. The net area of ^{212}Bi alpha was previously analyzed by a thoron calibration. The upper channel C_u was then selected by dividing the total bismuth area. The ratio between the total counts of ^{212}Bi and the partial counts of ^{212}Bi was found to be always 0.56. On the other hand, the proportion of ^{212}Bi / ^{212}Po is known to be 0.57. It is now possible to measure ^{218}Po using these two prior relations. Hence, considering a typical atmospheric air measurement with electrostatic radon monitors, the total counts of ^{212}Po is measured to be equal to N. This means that the total counts of ^{212}Bi will be $0.57 \cdot N$. Using the selected C_u, it can be estimated that the counts of ^{212}Bi which interfere with the ^{218}Po area, are equal to $0.57 \cdot 0.56 \cdot N$. This means that 32 % of the total measured counts of ^{212}Po must be subtracted from the measured counts of ^{218}Po.

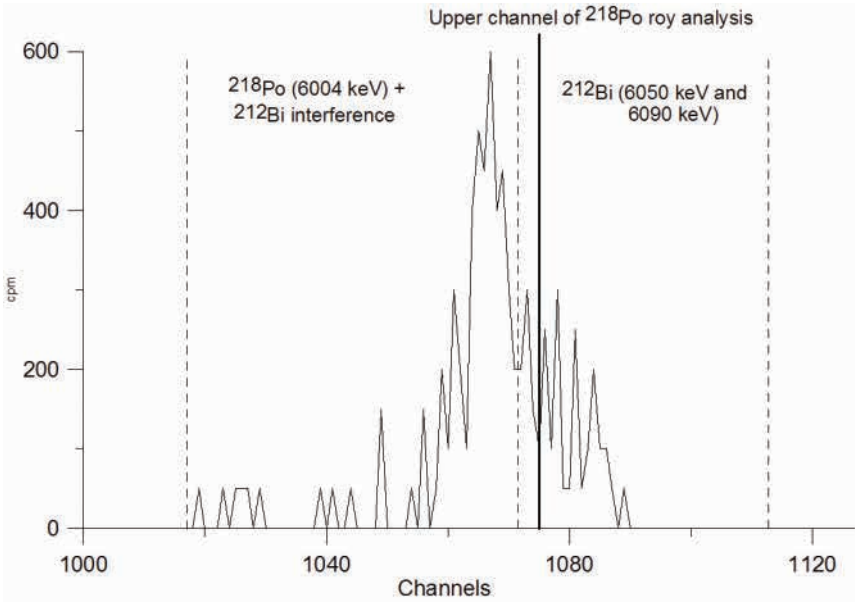

Figure 2.9: Spectrum analysis shows a sum of ^{218}Po (6004 keV), ^{212}Bi (6050 keV) and ^{212}Bi (6090 keV).

2.3.3 Drying system

In order to maximize ^{218}Po collection and, hence, increase detection efficiency, it is necessary to dry the sampled air as much as possible before it enters the detection volume. This will reduce positive ^{218}Po neutralization due to recombination with OH^- (Hopke, 1989). Transport and collection of ^{218}Po ions on the detector surface are strongly influenced by humidity in the chamber due to the increase of the probability that they will be neutralized by OH^- ions. The interval time, τ_{H_2O}, for ^{218}Po recombination during the $[H_2O]$ concentration variations, in an electrostatic chamber was found by Hopke (Hopke, 1989), who obtained a value of 0.879 $[H_2O]^{-1/2}$ s when the water vapour concentration is less then 1800 ppm and of about 0.021 s when $[H_2O]$ is more than 1800 ppm (Hopke, 1989), where 1800 ppm correspond to 10% of relative humidity for pressure condition of 1 atm and 300 K of temperature (Hopke, 1989). The number of ^{218}Po ions which are not neutralized at time t are given by Equation 2.7.

$$N(t) = N_0 \Lambda t \tag{2.7}$$

N_0 is the initial ^{218}Po isotopes number from the radon decay inside the chamber and $\Lambda = \frac{1}{\tau_{H^2O}}$ is the neutralization probability, which is influenced by the humidity chamber.

The environmental conditions of temperature and pressure inside the detection volume can theoretically influence the collection efficiency due to the increase of the kinetic energy of the ions (PhD thesis Esposito, 2000). Nevertheless, experimental measurements have been done at the Casaccia (ENEA, Italy) radon chamber for smaller electrostatic chambers and the results have shown negligible influence of the pressure and temperature parameters (Roca et al, 2004).

Therefore, the drying system module was designed at the INTE-UPC to automatically maintain the sampled air as dry as possible inside the detection volume. The whole module consists of two silica gel tubes and several valves and resistors in order to control air circulation and heating. The air sample goes alternatively through one of the two silica gel tubes to be dried, while the other silica gel tube is being regenerated by hot air at 130 °C passing through it. Each tube is regenerated for 16 hours and then cooled down to ambient temperature for 8 hours for a total cycle of 24 hours. In this way, each silica gel tube will work for one day before being automatically changed and regenerated.

2.4 HYSPLIT: Hybrid Single Particle Lagrangian Integrated Trajectory Model

The usefulness of radon as a tracer for atmospheric studies has been previously commented on. In environmental science such studies usually require the use of modelling tools, either in meteorological studies or in dispersion issues (PhD thesis Arnold, 2009).

In order to analyze the qualitative origin of distant radon observed at the *El Arenosillo* station by a set of back trajectories the model HYSPLIT, version 4 (Draxler and Hess, 1998) was used. The HYSPLIT4 model computes simple air mass trajectories as well as complex dispersion and deposition simulations. The HYSPLIT (HYbrid Single-Particle Lagrangian Integrated Trajectory) model was chosen for this analysis because it has been widely validated (Draxler and Hess, 1998) and it is currently one of the most used models by the scientific comunity (Chambers et al, 2008; Omori et al, 2009; Chan et al, 2010; Hawkins et al, 2010).

Furthermore, the HYSPLIT model can be run interactively on the READY web site (www.arl.noaa.gov) or installed on a PC and run using a graphical user interface (GUI). The PC version comes with a visualization package for results plotting. The trajectory-only model has no restrictions and forecast or archive trajectories may be computed with either version. The HYSPLIT Model can run with multiple nested input data grids, on the website there are links to the ARL and NWS meteorological data server and the access to forecasts and archives including NCAR/NCEP re-analysis. Furthermore, there are additional softwares to convert MM5, RAMS, COAMPS, WRF, and other data to an input for HYSPLIT. Finally, there are several utility programs to display and manipulate meteorological data.

The ARL web server contains several meteorological model data sets already converted into a HYSPLIT compatible format on the public directories. GDAS meteorological data fields were used for back-trajectory analysis in this thesis. The GDAS files can be extracted from the ARL website (http://ready.arl.noaa.gov/archives.php) and they are saved every 6 h on a hemispheric projection at 191-km resolution.

2.5 The *El Arenosillo* station

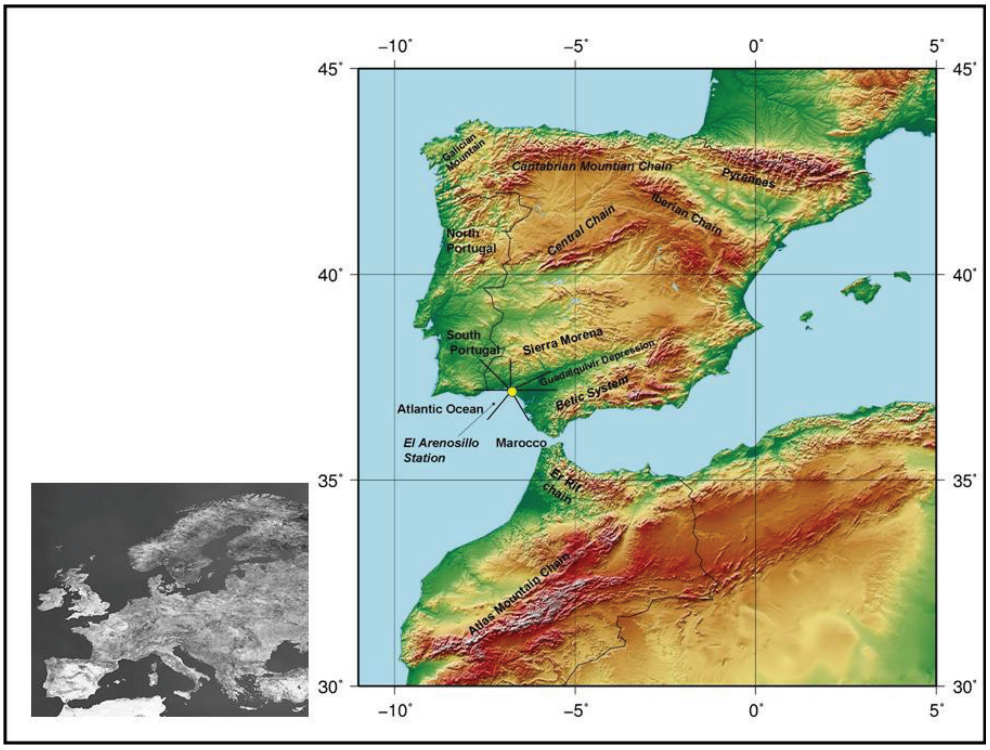

Figure 2.10: Europe (left) and the location of the *El Arenosillo* station on the southern coast of Spain with wind sectors for each specific geographic area (right).

The *El Arenosillo* atmospheric sounding station is part of the National Institute of Aerospace Technology (INTA - www.inta.es) and it is located on the south-west Atlantic coast of Spain (37.1N/6.7E), as shown in Figure 2.10. The *El Arenosillo* station has a 100-m-high tower. This station is located at 25 km from the city of Huelva and only 700 m from the coast as shown by Figure 2.11. The *El Arenosillo* station is sited within the Doñana National Park, a 105-ha national park and wildlife refuge. The *El Arenosillo* station is a strategic point for meteorological studies, since it is located in the far west of Europe and is one of the first areas to receive air masses coming from the Atlantic Ocean. Furthermore, air masses from European regions and from Africa may also cross this area due to the fact that the *El Arenosillo* station is located at the end of the Guadalquivir valley, which acts as a natural channel for the transport of air masses from the Atlantic Ocean towards the Iberian Peninsula.

Figure 2.11: Location of the *El Arenosillo* tower in the Doñana National Park and at 700 m far from the Atlantic coast

A detailed metereological characterization of this area was carried out by Hernández-Ceballos in his doctoral research (PhD thesis Hernandez-Ceballos, 2011) in order to find out the air mass pathways reaching the *El Arenosillo* area. According to this study, this area is typically affected by five different air masses: the Arctic, the Tropical, the Polar, the Continental and the Saharan. The Saharan comes from the Sahara desert, while the Continental air mass arises in the European continent and Mediterranean areas. Another important feature of this location is its proximity to the coast as it is shown in Figure 2.11. Indeed the ^{222}Rn exhalation is usually of the order of 30-50 Bq m^{-2} h^{-1} for land, while it is considered zero for sea (Schery and Huang, 2004). This means that the radon-poor air masses coming from the sea or radon-rich air masses coming from the continent can be identified and can allow studies on synoptic and mesoscale transport (Zahorowski et al, 2004). Finally, the *El Arenosillo* meteorological tower is completely surrounded by pine forest and dunes as illustrated in figure 2.12 which means that the soil is totally made up of sand. Usually, sand is poor in radium and this could possibly mean a low radon flux in this area (Nazaroff and Nero, 1988).

All these characteristics suggest that the *El Arenosillo* area is a natural low radon background zone where analysis of long-distance radon contribution transport can successfully be carried out without any significant contribution from the local radon concentration noise.

Figure 2.12: The 100 m tower located at the *El Arenosillo* station in the South of Spain.

2.6 The Phosphogypsum Pile of Huelva

Only 23 km away from the *El Arenosillo* station, located in the city of Huelva, is a phosphogypsum pile (PG), where phosphogypsum has been accumulated for the last 50 years by a fertilizer company. The phosphogypsum pile has reached a total covered area of 12 km^2 and weighs 80 Mt of weight (Bolivar et al, 1996). It is located in the south-west of Spain, exactly in the estuary formed by the Odiel and the Tinto rivers. Figure 2.13 shows the Huelva phosphogypsum pile. In the 90s the Huelva PG pile was considered to be a radiological surveillance area by the European Union because of a possible radioactive impact on the atmospheric and aquatic environment, due to the high activity of ^{226}Ra in the PG, which is about 600 Bq kg^{-1} (Bolivar et al, 1996; Bolivar et al, 2002). Indeed, the phosphogypsum is a waste product of the phosphoric acid production process. The phosphoric acid (H_3PO_4) is obtained by the chemical processing of phosphate rocks and present high levels of natural uranium radionuclide (Guimond and Hardin, 1989). During the phosphoric acid production process, the phosphogypsum is also co-produced and is

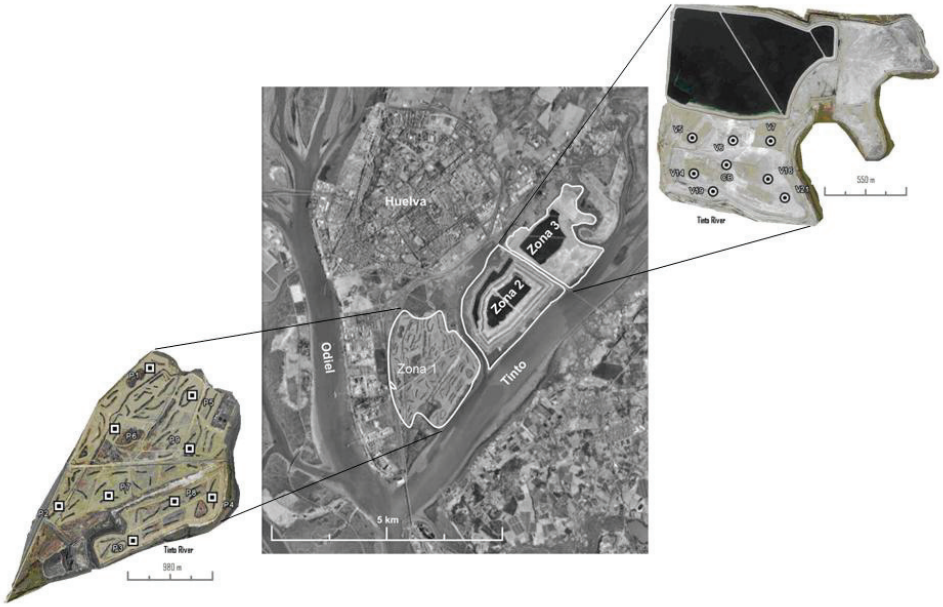

Figure 2.13: Phosphogypsum pile location in Huelva, between the Odiel and Tinto rivers, located 23 km far from the *El Arenosillo* station. The phosphogypsum pile is made up of three different zones: a restored area (Zone 1), an active area (Zone 2) and a not active but not still restored area (Zone 3).

then stored in a pile (Bolivar et al, 1996; Guimond and Hardin, 1989; Bolivar et al, 2002). About 5 tonnes of phosphogypsum are generated for each tonne of manufactured $_3PO_4$ (Perez et al, 2010).

The Huelva phosphogypsum pile is interesting to study in this thesis because it could be a point and remote high radon source on the radon concentration measured at the *El Arenosillo* station due to the high ^{226}Ra activity content in phosphogypsum (Bolivar et al, 1996; Bolivar et al, 2002). Indeed, the ^{222}Rn potentially exhaled from the phosphogypsum pile surface could reach the *El Arenosillo* station due to air mass movement (Arnold et al, 2010).

The Huelva PG pile can be subdivided into three different areas as it is presented in Figure 2.13; Zone 1 which was restored in 1992 by the regional government of Andalusia. It is the oldest pile area and the closest to the Huelva city centre. During the restoration process this area was totally covered with 30-cm-thick natural organic soil. Zone 2 has a size of 238 ha and was the last active zone until the end of 2010 when the phosphogypsum production stopped. This zone is composed of two pools for irrigation and drainage of

phosphogypsum. Each pool is about 75 ha and they are located 10.5 m above sea level. Finally, Zone 3 is 211 ha large. This is an area completely covered with phosphogypsum and is presently used as a safety zone in case of water flooding (Technical Report CSN, 2011; PhD thesis López-Coto, 2011).

The possible radioactive impact due to the presence of the fertilizer industry in the city of Huelva has also been widely evaluated in different studies in the past by measurement of natural radioactivity in water and superficial sediments (Martinéz-Aguirre et al, 1994; Bolivar et al, 1996; Bolivar et al, 2002). Past analyses have shown activity concentrations between 500 and 1500 Bq kg^{-1} for some radionuclides from the decay chain of ^{238}U. These concentrations are averagely 20 times higher than in typical unperturbed soils and sediments. On the other hand, concentrations of ^{232}Th and of ^{40}K seem to show typical values as well as in unperturbed soils and ^{137}Cs activities were below the limit of detection (Bolivar et al, 2002; Dueñas et al, 2007).

Furthermore, Dueñas found out a significant difference between the radon exhaled from different areas of the PG pile in Huelva (Dueñas et al, 2007). Generally, the ^{222}Rn flux from the unrestored area (Zone 2) was observed to be 50 % lower than in the active PG stack (Zone 3) (Dueñas et al, 2007). This study also observed that the radon flux in the restored area (Zone 1) was approximately eight times lower than the active zone. The method used by Dueñas to carry out ^{222}Rn flux measurements involved the adsorption of radon on activated charcoal (Dueñas et al, 2007). The detector was placed on the surface of the soil to be measured and was allowed to collect radon for a time period of up to 24 h. The radon gas collected on the charcoal was then measured by gamma spectrometry of its progeny. ^{222}Rn flux values in the restored pile (Zone 1) were founded between 40 and 700 Bq m^{-2} h^{-1} (Dueñas et al, 2007). In the unrestored area (Zone 3) the radon flux measurement were located in an interval from 180 to 1100 Bq m^{-2} h^{-1}. Finally, in the active pile (Zone 2) the radon flux measured by Dueñas varied between 700 and 5500 Bq m^{-2} h^{-1} (Dueñas et al, 2007). Another study of ^{222}Rn flux from the Huelva PG surface carried out by Abril shows an interval value between 28 and 1000 Bq m^{-2} h^{-1} over the total pile surface (Abril et al, 2009). These cited studies were both performed by activated charcoal.

Nevertheless, it is important to bear in mind that the exhalation of ^{222}Rn from a soil surface is significantly influenced by soil characteristics and, particularly, by the humidity content in the soil material which drastically reduces the diffusion length of the gas in the pore space (Nazaroff and Nero, 1988; De Martino and Sabbarese, 1997). High water content in soil can drastically reduce radon exhalation (Nazaroff and Nero, 1988) and therefore a careful study should be carried out in order to understand how humidity content can influence radon exhalation from the phosphogypsum material. Furthermore, the measurement methods should be properly validated in order to evaluate any possibile influences on the radon flux measurement itself (Grossi et al, 2011).

Chapter 3

EIC and ARMON monitors response under controlled environmental conditions

3.1 Introduction

In this chapter the methods and the results of the EIC E-Perm and of the ARMON monitors calibrations are reported. The EIC monitor, with a chamber H for radon flux monitor measurement, presented in Section 2.2.2, and with a smaller chamber S, of 200 mL volume, were calibrated in the INTE-UPC radon chamber under controlled environmental conditions and were then compared with others continuous and integrated radon monitors. This comparison was done in colaboration with the Universitat Autonoma de Barcelona (UAB). Results will be reported in this thesis only for EIC monitors whereas the whole study will be presented in a future indexed paper in collaboration with the UAB group. The calibration of the ARMON monitors, introduced in the Section 2.3, was also carried out in the INTE-UPC radon chamber and its results will be presented in the following sections of this chapter (Vargas et al, 2004 and Vargas and Ortega, 2006). Particularly, the EIC monitors response under controlled environmental conditions was studied and compared with others integrated and continuous radon instruments of the UAB group. Preliminary results of this comparison study were presented at the II Congress of the Spanish Society of Medical Physics (SEFM)) and the Spanish Society of Radiological Protection (SEPR) on May 2011 (Moreno et al, 2011). Actually, the calibration factor of EIC monitors is given by the producer and theoretically they should not be influenced by environmental parameters (Kotrappa and Stieff, 1994; Vargas and Ortega, 2006; Sorimachi et al, 2009). However, a single study by Mahata found out a linear increase of measured radon concentration with increasing humidity, from 30 % RH up to a value of 85 % RH (Mahata et al, 2001). This last study seems to have not been properly carried

out so a new calibration study should be done to clarify this point. On the other hand, the influence of humidity and temperature on the ARMON monitor efficiency was analyzed for the first time.

3.2 Metods and Results

3.2.1 The INTE-UPC radon chamber

The INTE radon chamber enables stable radon concentrations reference values to be obtained and controlled conditions of temperature (°C) and of humidity to be set (Vargas et al, 2004). In Figure 3.1 the radon chamber, used for the radon instruments response study and its control panel are presented.

Figure 3.1: The radon chamber at the INTE laboratory (UPC) is presented here with its control panel

It is a 20 m^3 chamber located at the INTE-UPC radon laboratory. The chamber walls are made of 2-mm-thick welded stainless steel sheets to make the structure airthight. The radon source inside the chamber consists of a dry powder material containing 2100 KBq of ^{226}Ra, which is enclosed in the source container (model RN-1025 manufactured

by Pylon Electronics). All (100%) of the radon gas produced escapes from the dry powder source material. The generated radon activity is transported by an airflow in which the moisture has previously been removed by silica gel. A programmable logic controler (model Omron ZEN 10C1AR-A) enables control of the radon exhaled from the source to pass into the chamber or go outside by an On/Off signal. This system gives high radon concentration stability during calibration exposures. Furthermore, the chamber has a ventilation rate control system (0-6 m^3 h^{-1}) in order to minimize the radon activity concentration gradients inside the chamber, radon activity exhalation is injected at the inlet of the air conditioning system and is dispersed at the outlet by means of a diffuser for a radon uniformity greater than 5 %. Using the INTE radon chamber, a radon concentration range between 100 Bq m^{-3} to 30 kBq m^{-3} was obtained and measurement cycles were performed with different radon concentration references.

The radon concentration in the reference chamber is measured by alpha spectrometry from the ATMOS 12 DPX monitor (Vargas et al, 2004 and Vargas and Ortega, 2006). The monitor, was calibrated at the Physikalish-Technische Bundesanstalt (PTB) by comparing the reading with a primary standard ATMOS. The alpha-spectra obtained with the ATMOS reference instrument is analysed in order to estimate radon concentrations. The uncertainty in radon concentration measured by the ATMOS monitor is of about 10 % with a coverage factor of K = 2, which corresponds to a coverage probability of the 95 %.

Finally, the temperature in the radon chamber is regulated using a commercial refrigeration unit with an electrical heating. Furthermore, there are an humidifier and a dehumidifier devices which can modify the relative humidity. External PC software continuously controls both the temperature and the relative humidity. The temperature is maintained between ± °C for the 10-40 °C range, and the relative humidity is kept between ± 2.5 % from 15 % to 95 % (Vargas et al, 2004).

3.2.2 EIC monitors calibration and Results

The study of the response of R-EIC and RT-EIC radon flux monitors under controlled environmental conditions was carried out in the INTE-UPC radon chamber. The EIC radon flux monitors with HST configuration, a H chamber and a Short Term electret (ST), and with the HLT configuration, a H chamber with a Long Term (LT) electrete, were calibrated during this study. The R-EIC and the RT-EIC monitors with a HST configuration were compared directly with the ATMOS 12DPX in the INTE-UPC radon chamber with a radon exposure concentration of 5.0 ± 0.5 kBq m^{-3} for an exposure time of 3 h and with standard conditions of temperature (T= 20°C) and humidity (45%). On the other hand, the EIC monitors with a HLT configuration were compared with other integrated and continuous instruments used by the Autonomous University of Barcelona (UAB). The comparison between these devices was made for atmospheric radon concentrations exposure between 18 and 25 kBq with exposure time periods of 70 h. The

temperature conditions ranged between 10°C and 30°C. The humidity interval was from 30% to 85%. Furthermore, together with the two types of EIC monitors, with HLT and HST configurations, the INTE-UPC Group also exposed 10 integrated EIC monitors with an SLT configuration, S chamber of 200 ml and a Long Term electret (LT). To sum up, 21 RT-EIC (HST) monitors, 10 RT-EIC (HST) monitors, 4 R-EIC (HLT) monitors, 5 R-EIC (HLT) monitors and 10 SLT monitors were used during each exposure.

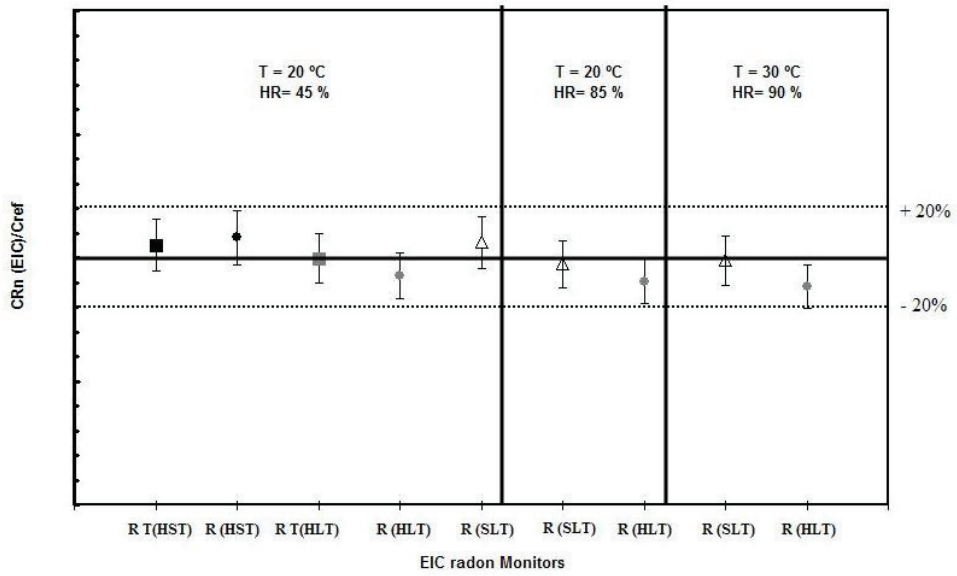

Figure 3.2: Variation of ratio C_{Rn}(EIC)/ C_{Ref} for each SLT (triangle), RT-EIC (square) and R-EIC (circle) monitor with configuration HST (black) and HLT (grey)

The following integrated and continuous detectors were also used by the UAB research Group during the comparison study. Continuous used monitors were: an ATMOS 12DPX (Gammadata Instrument), an AlphaGUARD (Genitron Instruments GmbH, Frankfurt, Germany), a Clipperton (Font et al, 2008) and a RAD7 monitor (Durridge). Furthermore, others integrated radon detectors were used by the UAB Group such as the Makrofol DE (policarbonate) FzK FN, the CR-39 policarbonate (Gammadata Instrument) and the LR-115 films. This part of the study was financed by a contract agreement between the INTE-UPC and the UAB within the framework of the project *Study of Environmental Radiological Surveillance Instruments and Radon Measurement under Extreme Environmental Conditions*, which was commissioned by the Spanish Nuclear Safety Council (CSN) to the Autonomous University of Barcelona (UAB).

In Figure 3.2 the ratio C_{Rn}(EIC)/ C_{Ref} for each R-EIC and RT-EIC monitor with HST, HLT and SLT configurations is shown. C_{Rn}(EIC) is the radon average concentration mea-

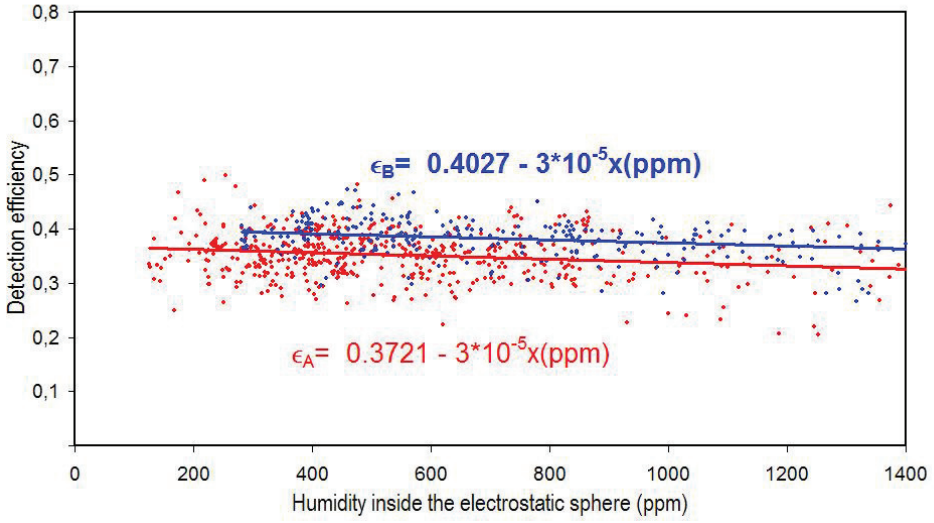

Figure 3.3: Efficiency detection of two ARMON monitors calibrated at the INTE-UPC radon chamber

sured by the EIC monitor for each configuration type in the INTE-UPC radon chamber during exposures under standard environmental conditions (T = 20°C and U = 45 %). C_{Ref} is the radon reference concentration in the INTE-UPC radon chamber measured by the ATMOS monitor. The ratio $C_{Rn}(EIC)/C_{Ref}$ is equal to 1 with an uncertainty of 20 %, which confirms they are not significantly influenced by environmental conditions (Kotrappa et al, 2004).

3.2.3 ARMON Monitors Calibration and Results

The two atmospheric continuous radon monitors (ARMON) were calibrated directly using the radon reference concentration obtained inside the INTE-UPC radon chamber measured by the ATMOS 12DPX. Monitors calibration was performed under different humidity and temperature conditions which were setted inside the radon chamber in order to study the ARMON monitor detection efficiency. Air sampled from the INTE radon chamber was pumped inside the detection volume of the monitors to be calibrated, which were located outside the chamber. The automatic drying system enabled absolute humidity values to be kept below 1500 ppmV. The continuous radon monitor calibration results performed at the INTE-UPC laboratory using the National Spanish Radon Chamber are shown in Figure 3.3. The monitor efficiency was 0.37 cpm per Bq m^{-3} and 0.40 cpm per

Bq m^{-3} with a correction factor for the humidity inside the sphere of $3 \cdot 10^{-5}$ per ppm. The Minimum Detectable Concentrations (MDC calculated by Currie, 1968) are 202 mBq m^{-3} and 219 mBq m^{-3}, respectively. The most sensitive device was used to analyze radon air at 100 m of height, where a lower radon concentration was expected, while the other monitor was used at 10 m.

Chapter 4

EIC radon flux response study by laboratory measurement

4.1 Introduction

Both the reproducibility and the reliability of the EIC radon flux monitor results were also tested by laboratory measurement on soil samples of phosphogypsum, which is a material with a high radium activity concentration, at the INTE-UPC radon laboratory. Subsequently, the influence of water content on the soil sample and the measured radon flux was tested with a reference method. Finally, the theoretical radon accumulation curve on soil samples and on a radon exhalation bed was studied. Results and conclusions of this study are presented in this chapter.

4.2 Material and Method

In order to study the EIC monitors response and to analyze the radon flux variation due to the humidity content in the soil or the environmental conditions present in the accumulation volume, a set of laboratory measurements were carried out using phosphogypsum material samples. Three different dried samples from the same source material were selected, with weights of 10 kg, 280 g and 44 g respectively. The radium activity concentration of the source material was 550 Bq kg^{-1} and it was collected from the Huelva phosphogypsum pile presented in the section 2.6. The phosphogypsum material was selected for this laboratory measurement because of its high radium activity concentration and because the phosphogypsum pile is located close to the *El Arenosillo* station, the site which will be characterized during this thesis work. This laboratory study will also aim to better understand the radon exhalation process from phosphogypsum.

4.2.1 EIC ^{222}Rn flux monitor response

The reproducibility of the EIC monitor response was studied using a 10 kg phosphogypsum sample which was used to built a radon exhalation bed and could therefore approximately represent an "in situ" measurement. The 10 kg of material was previously separated into 40 different parts and dried at T = 110 °C for 12 h. When the separate parts had cooled down, they were mixed together and placed in a rectangular plastic box of dimension 20 cm x 20 cm x 40 cm. The ^{222}Rn flux measurements by RT-EIC monitors, with a HST configuration, following the protocol measurement presented in Section 2.2.2, were carried out each day for 9 days and at the same time (10 am - 15 pm). A typical measurement is shown on the right-hand side of Figure 4.1. These RT-EIC monitor results were compared with a reference radon flux method, which was devised at the INTE-UPC radon laboratory. The method uses a 3.72 L Glass Measurement Jars with a circular opening of 9.4 cm of diameter (http://radelec.com). The glass bottle is located upside down on the soil surface. An EIC monitor in the SST configuration is located on the top of the bottle as is illustrated on the left-hand side of Figure 4.1. This method is based on the accumulation theory introduced in the Section 2.2.2. The radon concentration increased during 8 h is measured by the voltage difference on the electret ST. The SST monitors had been previously calibrated in the radon chamber of the INTE-UPC laboratory as described in Section 3.2.2. The glass bottle prevents any possible radon leak.

Figure 4.1: Reference method for radon flux study on the exhalation bed (on the left) and RT-EIC radon flux monitor measurement (on the right).

4.2.2 Specific Results: EIC ^{222}Rn flux monitor response

The ^{222}Rn flux measurement results by RT-EIC monitors with a HST configuration are reported in Figure 4.2 together with the reference radon flux measurements by EIC monitor with an SST configuration in a glass bottle which is indicated by a violet bar. The ^{222}Rn flux results by EIC monitors with a HST configuration are perfectly reproducible and are in agreement with radon flux measured by the sealed method with an SST chamber. The average radon flux for this dry phosphogypsum soil sample was estimated to be 33 $\pm$ 5 Bq m^{-2} h^{-1}.

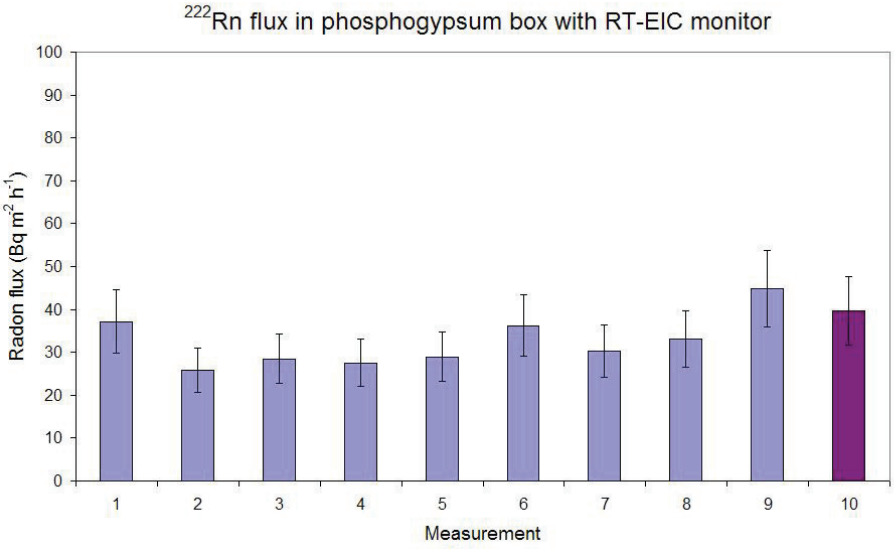

Figure 4.2: Radon flux with RT-EIC monitor was measured several times (N= 1-9) in laboratory condition on the same soil sample (dry weight W_d = 10 kg) and compared with the reference radon sflux method (measure N=10) to confirm the monitor response.

4.2.3 Influence of water content on ^{222}Rn exhalation

The radon exhalation rate (Bq h^{-1}), which represents the velocity of radon to escape from the pore material, was measured using phosphogypsum soil samples of 44 g and 280 g , rispectively. A study on the variation of the radon exhalation rate in relation to the soil water content was carried out on both soil samples. Each of the two soil samples was located in a 3.72 L glass measurement jar with a rubber sealing collar as presented in the Figure 4.3. This method is based on the measurement of radon concentration

accumulated in the closed volume for 24 h, with the hypothesis that the sample size was small enough to measure all the emanated radon (De Martino and Sabbarese, 1997). The radon concentration inside the volume was measured with a EIC monitor in the SST configuration, located on the top of the volume as shown in Figure 4.3. The sample humidity is given in percentage of weight present in the soil sample due to the water. It is calculated as (W_w - W_d)/W_d, where W_w is the wet sample weight and W_d is the dry sample weight (Nazaroff and Nero, 1988).

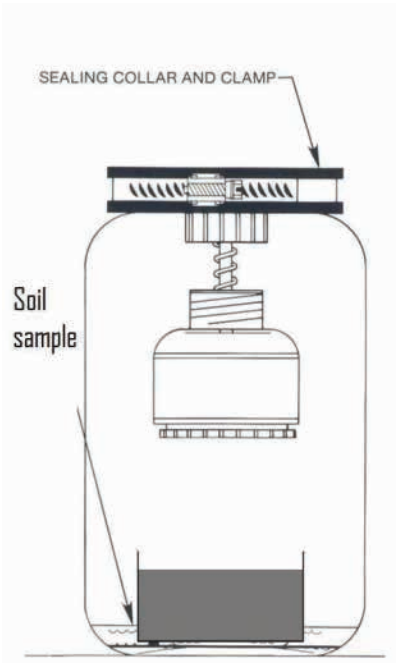

Figure 4.3: Measurement system for radon exhalation rate of small soil sample by EIC monitor with an SST configuration.

4.2.4 Specific Results: The influence of water content on ^{222}Rn exhalation

The ^{222}Rn exhalation rate (Bq h^{-1}) results from two phosphogypsum soil samples of 44 g and 288 g are reported in relation to the soil sample humidity content in Figure 4.4. The initial increase observed in the exhalation rate of the soil sample in Figure 4.4 is then followed by a significant decrease when the water content in the sample is above 25 %. This result is in agreement with results from the literature such as those of Morawska and Phillips, 1980; Nazaroff and Nero, 1988; De Martino and Sabbarese, 1998). Obviously,

the radon exhalation rate, which represents the Bequerels exhaled per hour from the material, seems to increase when the soil sample size increases as it can be observed in Figure 4.4 when the hypothesis of small volume is still real (Morawska and Phillips, 1980). Neverthless, the 288 g soil sample shows the same exhalation rate, of about 0.6 Bq h^{-1}, of the whole 10 kg phosphogypsum sample which has shown an exhalation rate of 0.59 $\pm$ 0.11 Bq h^{-1}. This confirms the fact that when the soil sample is large, not all emanated radon in the pore material will be able to travel to the soil-air interface (Nazaroff and Nero, 1988).

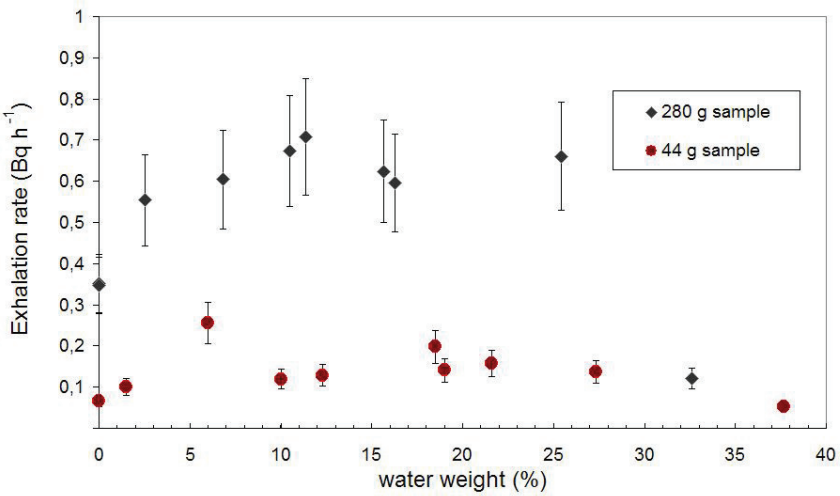

Figure 4.4: Total radon exhalation rate was measured on two phosphogypsum soil samples with different weights (44g and 280 g) by laboratory measurement in relation to their humidity content.

In Figure 4.5 the curve of radon exhalation rate per unit of mass is obtained from the results in Figure 4.4 by dividing by the soil sample mass. Values for both soil samples are in agreement, which confirms the fact that all radon emanated in these two small soil samples is still able to diffuse in the sealed bottle volume. In addition, values observed for radon exhalation rate per unit of mass in this soil material are between 0.002-0.004 Bq kg^{-1} h^{-1} which is in agreement with lowest values reported by Nazaroff of 0.002-0.02 (Nazaroff and Nero, 1988).

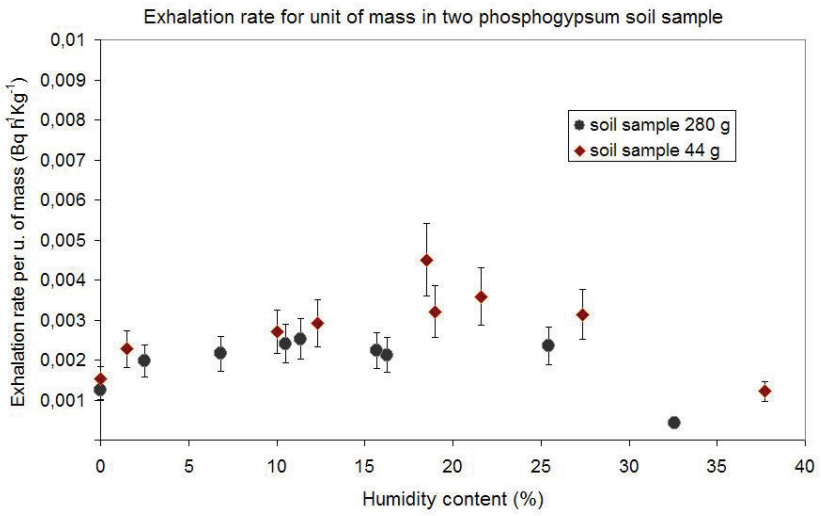

Figure 4.5: Total radon exhalation rate for unit mass on two phosphogypsum soil samples with different weights (44g and 280 g) in relation to their humidity content.

4.2.5 Influence of environmental conditions on ^{222}Rn flux measurement

In order to investigate the possible influence of environmental condition variation inside the accumulation chamber several experiments were carried out at the INTE-UPC laboratory. The ^{222}Rn flux from the phosphogypsum material was continuously measured by a DOSEman monitor (SARAD GmbH) which was located iniside the 3.72 L Glass Measurement Jars instead of the integrated EIC monitor used for the previous experiments. An EasyLog USB (Lascar Electronics) sensor was also included inside the volume in order to check the temperature and humidity variation inside the volume. Measurements of radon concentration inside the glass bottle were done using the configuration presented in Figure 4.3, with the phosphogypsum sample located inside the sealed volume, and with the configuration presented in Figure 4.1, with the glass bottle located upside down on the soil surface of the phosphogypsum exhalation bed. Hourly measurement of ^{222}Rn gas concentrations inside the volume were performed for several days in both experiments, in order to observe evolution in time. The DOSEman monitor measures the ^{222}Rn concentration by α spectroscopy of ^{218}Po and ^{216}Po.

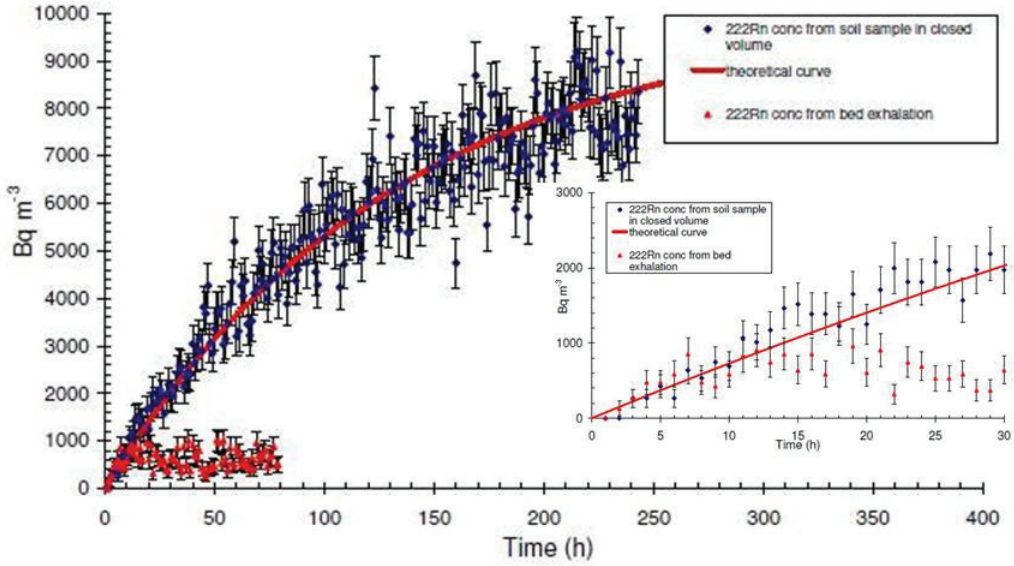

Figure 4.6: ^{222}Rn concentration exhaling from a phosphogyspum soil sample and from a phosphogypsum exhalation bed measured hourly by a DOSEman monitor.

4.2.6 Specific Result: Influence on the ^{222}Rn flux measurement

Results of ^{222}Rn concentration measured inside the glass volume when the phosphogyspum soil sample is sealed inside it and when the glass volume was located upside down on the posphogypsum exhalation bed are presented in Figure 4.6. It is evident how the theoretical accumulation curve properly describes the case where the soil sample is sealed inside the closed volume and the only affecting term to the radon diffusion inside the volume is the radon concentration gradient between the pore material and the free air. On the other hand, when the material/air system is not sealed, such as for in situ measurement, there is an air exchange between the accumulation air volume and the external air which can significatly reduce the radon exhalation. Several measurements were carried out to confirm this behaviour of radon concentration when it is accumulated from in situ measurement as shown in Figure 4.6 and in Figure 4.7.

4.3 Specific Conclusions

The radon flux results measured on the exhalation bed of phosphogypsum soil by RT-EIC radon flux monitors with a HST configuration located directly on the soil surface and with an SST configuration, located inside a sealed glass bottle, show reproducible results and a good agreement which confirms the reliability of RT-EIC HST radon flux monitors for in situ measurement. The radon flux measured for the phosphogypsum soil was quite low, only about 33 ± 5 Bq m^{-2} h^{-1}, if compared with material ^{226}Ra activity concentration of 550 Bq kg^{-1}. This result was confirmed by hourly radon concentration measurements performed by DOSEman monitor which show a slope during the first 5 hours in the radon concentration accumulation of a sealed soil sample and on the exhalation bed which shows a radon flux of 39 ± 8 Bq m^{-2} h^{-1}. These results could be explained by the low diffusion coefficient of radon gas in the phosphogypsum, which has been discussed elsewhere (Nazaroff and Nero, 1988). Furthermore, the radon exhalation rate, which represents the bequerel exhaled per hour from the material, seems to increase when the soil sample dimensions increase from 44 g to 248 g (Morawska and Phillips, 1980). Neverthless, the 288 g soil sample shows the same exhalation rate observed from the exhalation bed, with a values of 0.6 Bq h^{-1}, which confirms that not all the radon emanated in the pore material will reach the soil-air interface and then exhaled to the free air.

In 1986, Andrew found out that if C_0 is the initial radon concentration, only under diffusive transport, at distant x the concentration C(x) will be given by Equation 4.1

$$C(x)=Co\ e^{-x/L} \tag{4.1}$$

L is the diffusion length (m) and is equal to the square root of the ratio between the diffusion coefficient D_c and the radon decay constant λ. Solving this equation it shows that only the 37 % of the initial radon concentration will travel a distance L, only the 13 % of Co will reach the distance 2L and so on (Andrew and Wood, 1972). The diffusion coefficient of ^{222}Rn gas in common soils is of about 10^{-7} m^2 s^{-1} (Nazaroff and Nero, 1988). This means it will be able to travel a lenght of 30 cm. Laboratory results for different phosphogypsum soil samples show an exhalation rate for phosphogypsum soil of 0.5 Bq h^{-1} (Figure 4.4) also for the largestsoil sample of 10 kg in weight and 0.02 m^3 of volume. This will confirm the small radon diffusion coefficient in phosphogypsum which, qualitatively, is the order of 10^{-8} m^2 s^{-1}. Finally, results of radon flux measurements carried out by continuous DOSEman monitors on an exhalation bed show a very rapid saturation of the radon concentration inside the accumulation volume which occurs in the first 8-10 hours. Although more detailed studies are needed to understand this phenomenon, it seems to be due to a pressured gradient presence between the internal air volume and the external free air. However, fast radon flux measurements during the first 1-3 hours are recommended in order to avoid this problem of saturation.

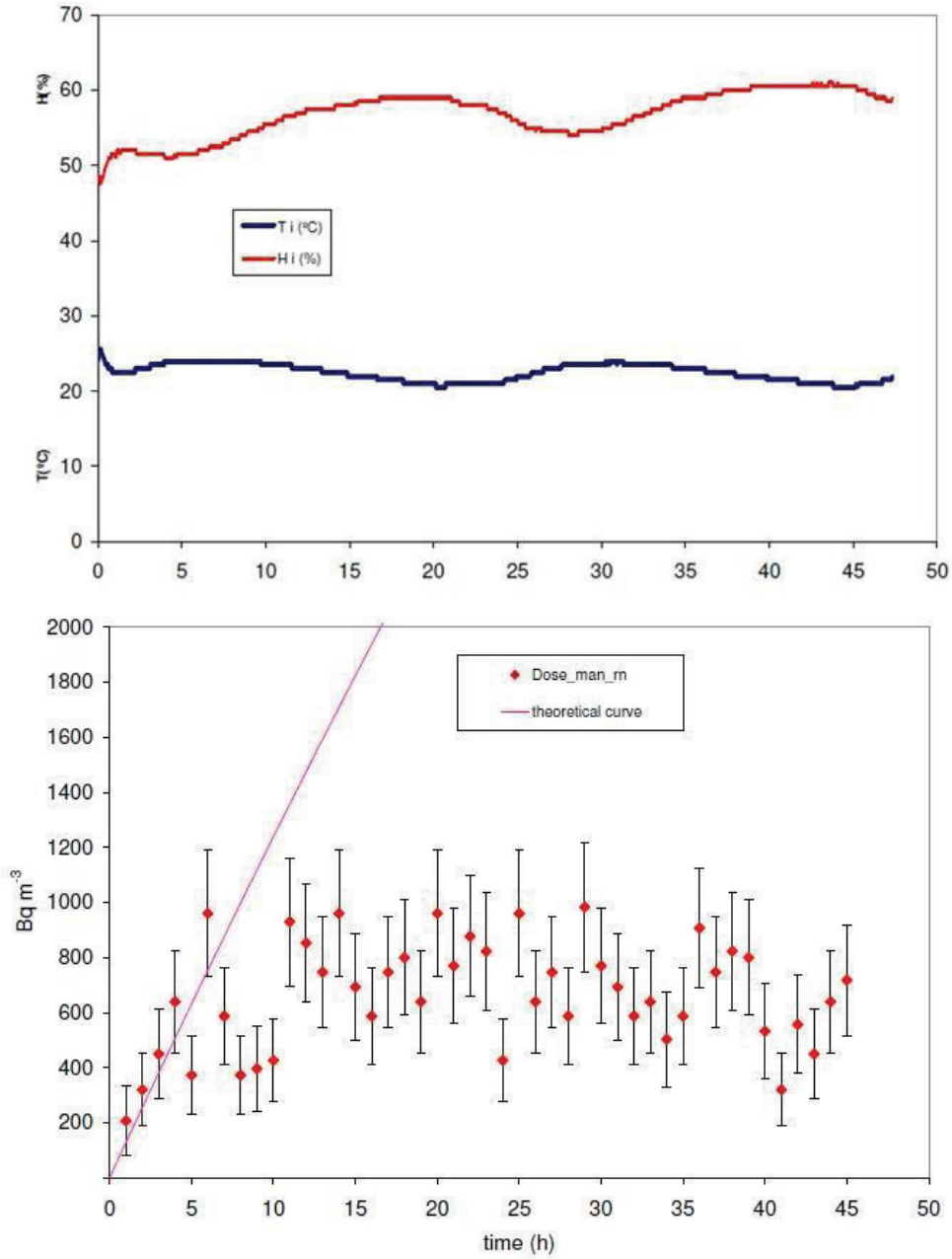

Figure 4.7: ^{222}Rn concentration exhaling from a phosphogypsum exhalation bed measured by a DOSEman monitor. Environmental parameters inside the accumulation volume were also measured by EasyLog USB sensor.

Chapter 5

in situ EIC monitor response study in soils

5.1 Introduction

The EIC Radon flux monitor reliability was tested by an *in situ* inter-comparison campaign in soil, which was performed in the summer of 2008 in the centre-east of Spain. Different systems to directly measure radon flux from the soil surface and to measure the related parameters of terrestrial γ dose and of ^{226}Ra activity in soil, for indirect estimation of radon flux, were compared during this campaign. Four eastern Spanish sites with different geological and soil characteristics were selected: Teruel, Los Pedrones, Quintanar de la Orden and Madrid. The participating members involved in the campaign study were the Institute of Energy Technology (INTE) of the Technical University of Catalonia (UPC), the Huelva University (UHU) and the Basel University (BASEL).

The measurement campaign of radon flux, across Eastern Spain, was performed in the middle of July, 2008. In order to avoid rainy episodes that may influence the soil humidity (Nazaroff and Nero, 1988) described in the Chapter 4 of this thesis, the terrestrial γ dose rate (Szagvary et al, 2007) or the radon flux. The campaign was carried out during the most typical eastern Spanish climate conditions. The radon flux (Bq m^{-2} h^{-1}) and the terrestrial gamma dose rates (nSv h^{-1}) were measured at each site by several monitors and at different points in order to get average analysis values. ^{226}Ra activity (Bq kg^{-1}) was determined in the laboratory by gamma spectrometry on soil samples collected during the campaign. Each parameter was determined with different equipment by the campaign members in order to compare results.

5.2 Material and Methods

5.2.1 Sites

Four eastern Spanish sites were selected in this measurement campaign. The chosen locations were Teruel, Los Pedrones, Quintanar de la Orden and Madrid. The location characteristics, the average humidity and the temperature conditions during the measurement campaign are shown in Table 5.1. These locations are included within the Spanish Automatic Surveillance Network (REA - www.csn.es) which allows an evaluation between our measurements of terrestrial γ-dose rates with the routine REA data. Furthermore, this choice of sites promised a wide range of radon flux values to be obtained, as suggested by the European radon map which will be introduced in Figure 6.1 (Szagvary et al, 2009). Finally, direct measurements were considered a validation of the anomalously high radon flux values indicated by this map in comparison to the rest of Europe.

Table 5.1: Overview of Sites

Site	Latitude	Longitude	Height (m)	R.H. (%)	T (°C)
Teruel	40.45	-1.06	1082	33-36	30-33
Los Pedrones	39.47	-0.77	678	50-60	22-25
Q. de la Orden	39.79	-3.54	693	48-53	22-26
Madrid	40.58	-3.62	682	37-50	25-31

5.2.2 Terrestrial γ-dose rate

The total gamma dose measurements were performed at each station at 1 m above ground level with the following portable monitors. A High Pressure Ionization Chamber RS-112 (HPIC, GE Reuter-Stockes, Inc.) was used by the INTE-UPC. This model has a volume of 4.2 litres. It is filled with argon gas at a pressure of 25 atm. Its measurement range is between 10 nGy h^{-1} and 5 μGy h^{-1} with a precision of 5 %. A GammaTRACER (Genitron Instruments GmbH, Frankfurt, Germany) with a dual Geiger-M*ü*ller tube was used by the Basel University. This device has one tube with 110 pulses per min at 100 nSv h^{-1} and another tube with 0.2 pulses per min at 100 nSv h^{-1}. The measurement range is between 10 nSv h^{-1} and 10 Sv h^{-1}. A proportional counter probe LB 123D by the Berthold company was used by the UHU. Its sensitivity is 0.20 μSv h^{-1} per 1 cps. The energy range is from 30 keV to 2 MeV. The dose rate range covers 6 decades from 50 nSv h^{-1} to 10 mSv h^{-1}. All devices were located within 5 m of each other. The measurements represent the total γ dose rate. They include a terrestrial component, mainly from ^{40}K,^{238}U, ^{232}Th and their progeny, a cosmic component, principally muons, an anthropogenic component, largely from ^{137}Cs, and an inherent background due to

the measurement devices. The terrestrial natural gamma dose rate was obtained by subtraction of all the other components such as the cosmic component. The cosmic component subtracted at all sites, which have an altitude ranging between 680-1080 m, was of 30 $\pm$ 5 nSv h^{-1} (Wissmann et al., 2007).

Terrestrial dose-rate data have also been used, for indirect radon flux calculations, from the MARNA map (Quindós et al, 2004), which has a spatial resolution of 1 km, and from the European radon map (Szagvary et al, 2009). The REA Network has an automatic radiological station (REA) at each site which consists of dual Geiger-Müller tubes, model BAI9305 from the Berthold company, to observe both low and high γ doses. Two data series were extracted from the REA Network, one is directly provided by the Spanish Nuclear Safety Council (CSN) and the other was corrected according to an optimization quality study carried out by Saéz-Vergara (Sáez-Vergara et al, 2002). This last correction was effectively done by a comparison between the reference CIEMAT dose-rate monitors, located at a standard height of 1 m above ground level, and the REA dose-rate monitors.

5.2.3 ^{226}Ra Activity

Soil samples were collected at each campaign station at different depths between 0 and 70 cm by rock sampling techniques. The soil samples of 100 g in weight were then put into air-tight Petri dishes of 100 ml in volume. The Petri dishes were kept for 30 days to allow the ^{226}Ra to reach secular equilibrium with its short-lived progeny. The soil samples were then analyzed at the INTE-UPC and at the UHU laboratories by ^{214}Pb and ^{214}Bi radium progeny γ-spectrometry. ^{226}Ra activity was also measured with another method. This method uses acquired terrestrial γ dose from all the natural radio nuclides (D_{tot}) to obtain the ^{226}Ra contribution to the dose (D_{Ra}) by the empirical equation, $D_{Ra} = 0.24 * D_{tot}^{1.01}$ (Mahou et al, 2005). This result is then employed to derive the radium activity in the soil using the hypothesis that ^{226}Ra activity is closely related to ^{238}U activity and thus a $D_{Ra} = 62.19$ nSv h^{-1} corresponds to an activity concentration in the soil of ^{226}Ra equal to 12.21 Bq kg^{-1} (Quindós et al, 2004).

5.2.4 ^{222}Rn flux

The radon flux at the selected Spanish locations measured during this campaign by the integrated EIC radon flux monitor was compared with measurements done by another integrating system and two continuous monitors. The integrated method was the activated charcoal method. The continuous devices were an AlphaGUARD (Genitorn Instrument Gmbh, Frankfurt, Germany) and a Sun Nuclear model 1027. All these integrated and continuous systems are based on the previously presented accumulation method (Morawska, 1989).

A number of 8 H chambers of RT-EIC monitors were used in this campaign at each site following the measurement protocol presented in Section 2.2.2. Three of them were used to subtract the radioactive background. The chambers were located at 50 cm distance from each other, covering a total area of 2 m^2. In Figure 2.5 a typical measurement configuration of the EIC monitors is presented for the *Los Pedrones* site. The other integrating system used to determine the radon flux, involved ^{222}Rn adsorption on activated charcoal, has been explained in detail elsewhere (Countess, 1976; Fremman and Hartley, 1986). The charcoal response is influenced by environmental conditions as previous studies have shown and this should be taken into account to properly estabilish its calibration factor (Ronca-Battista and Gray, 1988; Vargas et al, 2004a). The ^{222}Rn collector is placed on the soil surface over a time period T. ^{222}Rn is then determined through its progeny ^{214}Pb (295 KeV and 352 KeV) and ^{214}Bi (609 KeV) in secular equilibrium conditions by gamma spectrometry (Kaplan, 1963). A number of 3 charcoal canisters were exposed at each site for 6 hours and covered a total surface area of around 0.5 m^2. Each charcoal canister was made of a cylindrical box with a circular surface of 10 cm diameter and 1 cm of height. The canisters were located directly on the soil surface, thus avoiding void volume between this and the absorbent material. The ^{222}Rn activity concentration will accumulate inside the closed volume located on the soil surface.

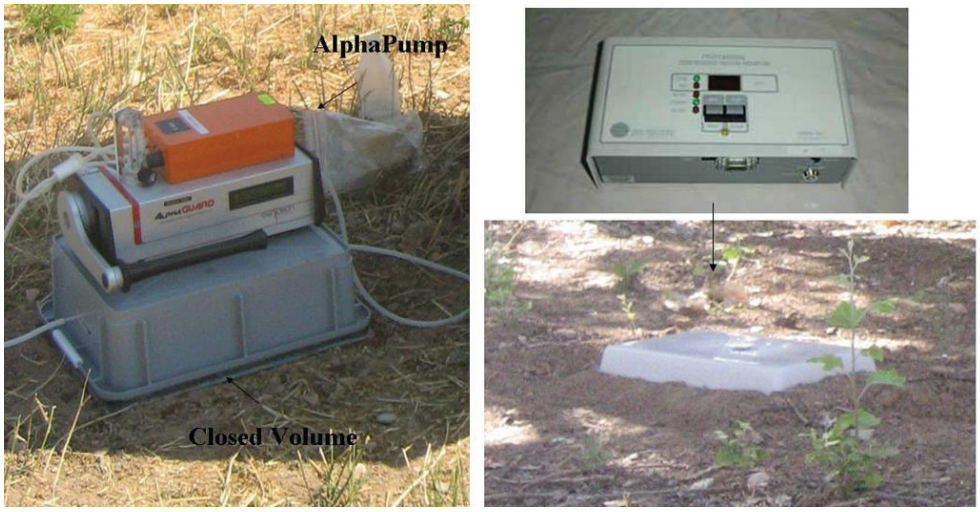

Figure 5.1: Continuous ^{222}Rn flux monitors: the AlphaGUARD (on the left-hand side) and the Sun Nuclear model 1027 (on the right-hand side) during a typical measurement.

The ^{222}Rn gas, in the chamber volume was measured continuously by the AlphaGUARD monitor (Genitron) and the Sun Nuclear model 1027 monitors presented in Figure 5.1. The Sun Nuclear monitor is a patented electronic detecting device using a diffused-junction photodiode sensor to measure ^{222}Rn gas concentration by radon progeny electrodeposition. The monitor was located directly under the accumulation volume and the

radon flux was measured by ^{218}Po (6 MeV) alpha spectrometry for 6 h at one point in each measurement location. The AlphaGUARD monitor was placed near the accumulation volume chamber. The sampling air was pumped inside the monitor at a flow rate of 0.3 l min^{-1} and concentration values were provided for each 10 min interval. A small 1-l plastic bottle was used to prevent aerosols and ^{220}Rn from entering into the AlphaGUARD (Lehmann et al, 2003). The AlphaGUARD was acquiring for 2 h at 3 different points at each measurement location.

The four different systems were located close to each others, covering a circular surface area with a radius of about 5 m. Table 5.2 summarises the device characteristics and their geometrical position during the campaign measurements. Radon flux was also estimated using two indirect methods. Table 5.2 resumes the indirect methods characteristic and reference. The first method, presented in the Table 5.2 as a GDR reference method, consists of the empirical Equation 5.1, derived by Szagvary et al, 2007.

$$y = 0.89x - 11.01 \tag{5.1}$$

The previous relationship was extrapolated using the local terrestrial γ-dose rate data, which has a resolution depending on the European Radiological Data Exchange Platform, EURDEP (www.eurdep.jrc.ec.europa.eu) data (Szagvary et al, 2007). The y, in the empirical Equation 5.1, represents the estimated radon flux (Bq m^{-2} h^{-1})) and x is the available terrestrial γ-dose in nSv h^{-1}. The gamma dose-rates measured during the present campaign by RS-112 (GDR-1) and by the GammaTRACER (GDR-2) were also used as input data to be compared with the reference Radon map method, GDR.

The other indirect method is named ^{226}Ra in Table 5.2 and is based on the calculation of ^{222}Rn flux using the Nazaroff diffusion Equation 5.2.

$$F = C_{Ra}\lambda f \rho \sqrt{\frac{D_c}{\lambda \varepsilon}} \tag{5.2}$$

where C_{Ra} is the ^{226}Ra activity (Bq kg^{-1}), F is the radon flux, f is the emanation material coefficient, ρ is the soil density, D_c is the bulk material diffusion coefficient, which is influenced by soil characteristics and conditions (T and HR), and ε is the material porosity. Typical geological parameters, for common soil with characteristics similar to the soil sites campaign, were chosen for f (0.23), r (1.5 10^3 kg m^{-3}), D_c (2.0 10^{-7} m^2 s^{-1}) and ε (0.25) (Nazaroff and Nero, 1988).^{226}Ra activity used as an input for this method was obtained directly by gamma spectrometry measurement of campaign soil samples and from the terrestrial dose rate data from the MARNA map and its conversion to activity concentration by the empirical equation introduced in the Section 5.2.3.

Table 5.2: Characteristics of direct and indirect measurement methods to determine ^{222}Rn flux from soil

Methods	Principle	Technique	N. of device/ meas. replicate	N. of location for each meas. site	Single Meas. period	Reference
Direct Methods						
Charcoal	^{222}Rn accumulation in canister	γ spectrometry	3/1	1 on ground surface	6	(Dueñas et al, 2007)
E-Perm	^{222}Rn accumulation in chamber	Voltage discharge	8/1	1 on ground surface	6	(Kotrappa and Steck, 2009)
AlphaGUARD	^{222}Rn accumulation in closed chamber	α spectrometry	1/3	1 on ground surface	1	(Lehmann et al, 2003)
Sun Nuclear	^{222}Rn accumulation in chamber	α spectrometry	1/1	1 on ground surface	4	- -
Indirect Methods						
GDR1 Szagvary-RS112	Empirical relation with measured γ dose	dual Geiger-M*üller*	1/1	1 at 1 m above ground	5	(Szagvary et al, 2009)
GDR2 Szagvary-Gamma Tracer	Empirical relation with measured γ dose	Ionization Chamber	1/1	2 at 1 m above ground	2	(Szagvary et al, 2009)
^{226}Ra (INTE/UHU)	Empirical relation with ^{226}Ra in soil	Laboratory γ spect.	1/1	1 at 0-30 cm under ground	1	(Nazaroff and Nero, 1988)
Indirect Reference Methods						
GDR ^{222}Rn Map	Empirical relation with EURDEP γ dose	dual Geiger-M*üller*				(Szagvary et al, 2009)
^{222}Rn MARNA Map	Empirical relation with ^{226}Ra from MARNA map	Ionization Chamber				(Nazaroff and Nero, 1988)

5.3 Results

In the following section results for the terrestrial γ-dose rate, ^{226}Ra activity and radon flux are presented and discussed.

5.3.1 Terrestrial γ-dose rate

Figure 5.2 shows the terrestrial dose rate results obtained by the different equipment and methods after subtracting the cosmic component. The measured data from the RS-112 (INTE-UPC) and the LB-1236 (UHU) monitoring were in good agreement with the MARNA map for each campaign site. The measured value from the uncorrected REA is too high in comparison with the other measured values. However, the same REA are significantly closer to the other measured values after the correction developed by Sáez-Vergara et al, 2002. The values measured by GammaTRACER tended to be higher than the other data.

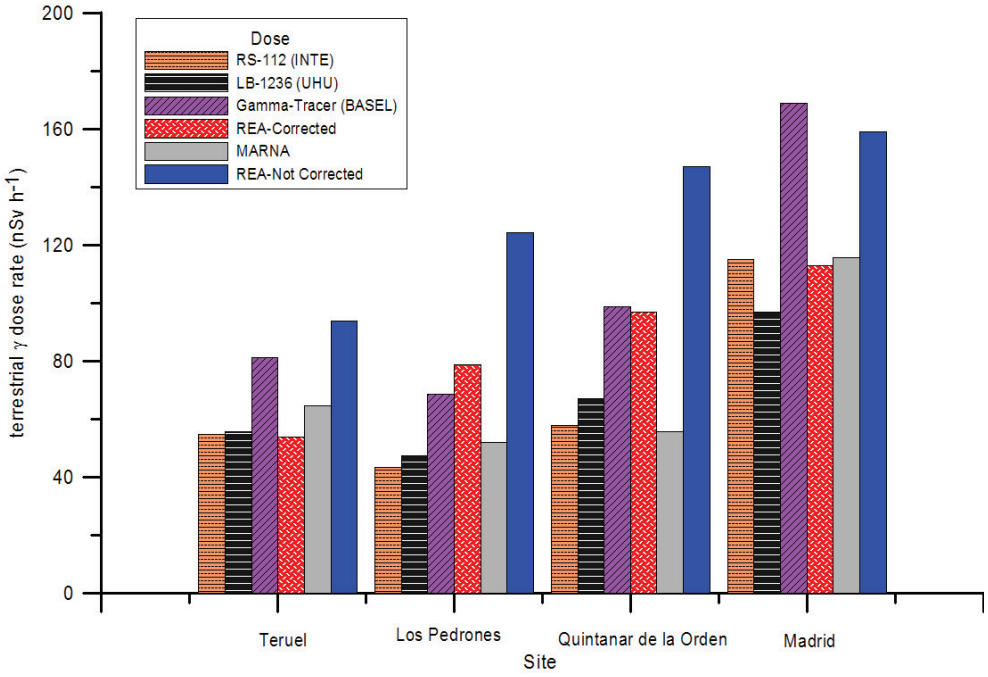

Figure 5.2: The terrestrial gamma dose rate measured at each site by RS-112 (INTE), LB-1236 (UHU) and GammaTracer (BASEL) monitors are shown. The dose rate for each REA station and their corrected values are also reported in according to Sáez-Vergara et al, 2002. Furthermore, the values obtained from the MARNA map are included.

5.3.2 ^{226}Ra soil activity mass

^{226}Ra soil activity mass in soil samples from each campaign site was analyzed at the INTE-UPC and the UHU laboratories. The ^{226}Ra activity results in the soil samples from the first terrain layer, which ranges between 0 and 30 cm, were compared as shown in Figure 5.3. ^{226}Ra activities were also measured for deeper soil samples, up to a depth of 70 cm, showing quite a homogeneous distribution. The radioactivity concentrations measured at the aforementioned laboratories are in agreement to within a confidence level of 95 %. An evaluation was also done between previous data and the ^{226}Ra activity calculated by the empirical equation introduced in the Section 5.2.3, where the input terrestrial dose rate was measured by subtracting the cosimc component from the environmental gamma dose measured by the RS-112 (INTE) monitor . These last values were within a range of $\pm$ 5% of the directly measured ^{226}Ra activity average for Teruel, Q. de la Orden and Los Pedrones soil samples. The results show less agreement for the Madrid soil sample, where the ^{226}Ra activity obtained by the empirical Equation was within a range of $\pm$ 15 % of the directly measured average concentration. In order to explain this difference, the gamma

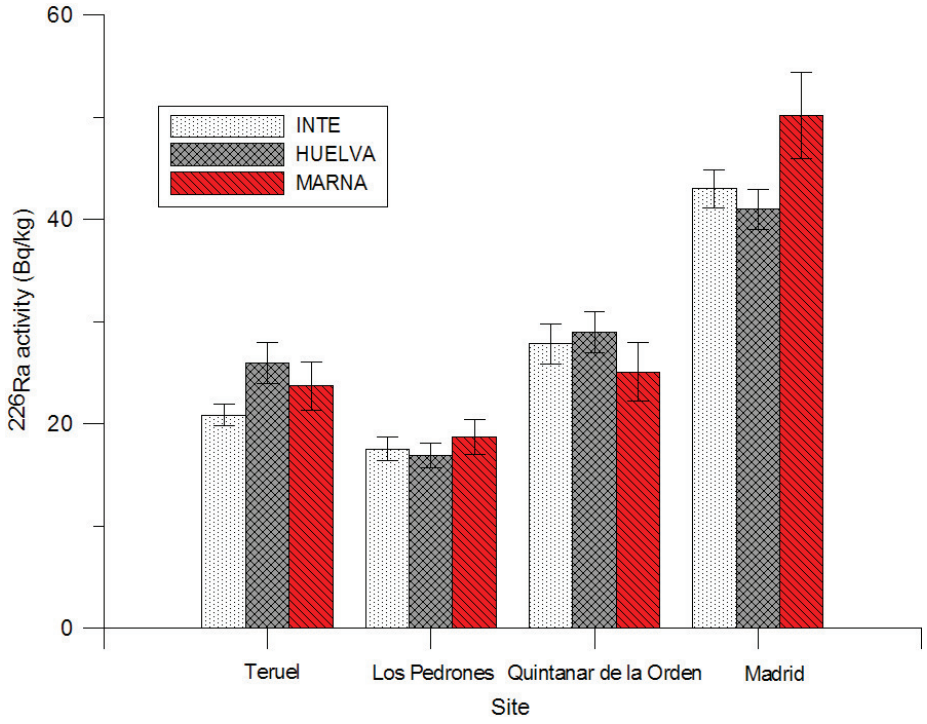

Figure 5.3: Radium activity concentration measured by the INTE-UPC laboratory (white), UHU laboratory (grey) and that obtained by using the MARNA equation D_{Ra}= 0.24∗ $D_{tot}^{1.01}$ (red) are shown.

spectrum obtained form the soil samples in Madrid was analyzed. The analysis showed a high activity concentration of ^{40}K (1200 Bq kg^{-1}) and of ^{228}Ra (50 Bq kg^{-1}) at the Madrid site, which could influence the reliability of the empirical Equation by Szagavary et al, 2009. The ^{40}K and the ^{226}Ra activity at the other sites have a mean value, respectively, of 300 Bq kg^{-1}and 23 Bq kg^{-1}, which are commonly expected in Spain (UNSCEAR, 2000). Therefore, the high ratio between the ^{40}K and the ^{226}Ra activity found in Madrid undermines the hypothesis of obtaining at least 65 % of contribution from ^{226}Ra. It could explain the difference between ^{226}Ra derived values and the campaign results observed in Madrid.

5.3.3 ^{222}Rn flux

The results of radon flux data by direct measurements and indirect methods are shown in Figure 5.4. ^{222}Rn flux data calculated by the equation obtained from Szagvary et al, 2009

(GDR (EURDEP), GDR-1 (Geiger-Müller) and GDR-2 (RS-112)) and by the Nazaroff diffusion equation (226Ra MARNA map and 2226Ra (INTE/UHU), both described in previous sections, are also reported. The data measured by continuous monitors, Alpha-GUARD and Sun Nuclear, and by integrated methods, EPERM and charcoal, show that the agreement among the participants was about 10 % (SD/mean) at the Los Pedrones and Q. de la Orden sites, and about 23 % at the Teruel and Madrid sites.

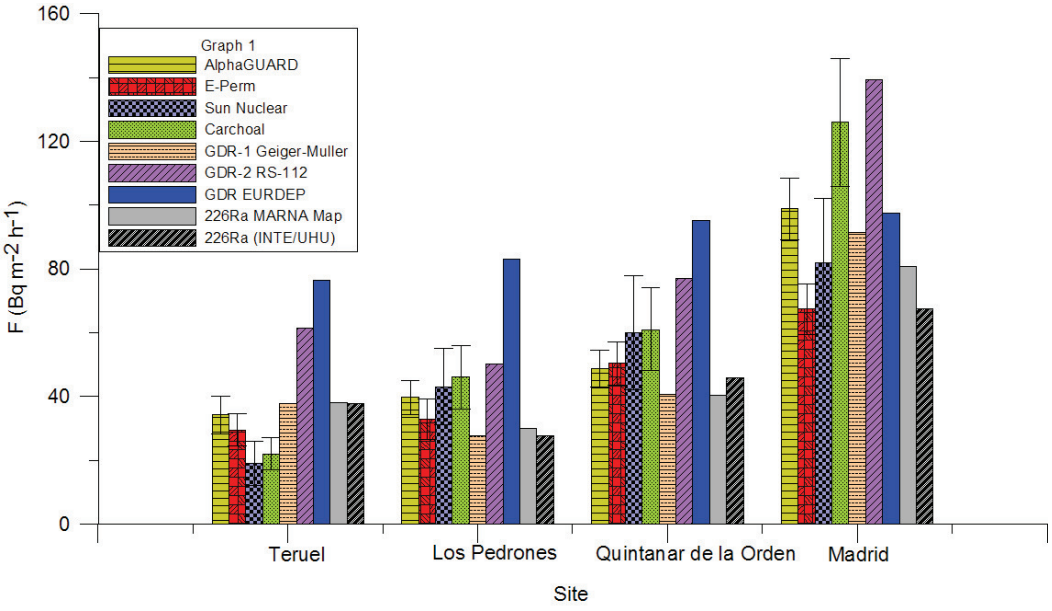

Figure 5.4: Radon flux levels measured at each site by direct and indirect methods are presented. Values measured by the continuous Sun Nuclear (UHU) and AlphaGUARD (BASEL) monitors, and by the integrated detectors E-PERM (INTE) and charcoal (UHU), are compared. Radon flux (y) estimated in order to apply the equation proposed by Szagavary et al, 2009, with dose rate (x) data from measurements by EURDEP data (GDR), RS-112 (GDR-1) and Gamma-Tracer (GDR-2) are also reported. Furthermore, radon flux is also estimated using the equation $F = C_{Ra}\ \lambda\ f\ \rho\ [D_c/(\lambda\ \varepsilon)]^{1/2}$ at each site with radium concentration obtained from the MARNA project with the empirical relation to obtain the radium (226-MARNA map) and by laboratory measurements (226Ra INTE).

The activated charcoal gives some differences, compared to the other systems, at the Madrid and in Teruel sites. Nevertheless, these values fall within 2σ and they have not been rejected. Indirect radon flux estimation, obtained by applying the empirical equation by Szagvary et al, 2009, were within a range of +/-30 % of the directly measured radon flux average when they were based on the terrestrial dose directly measured by

RS-112 (GDR-1).These indirect radon flux estimates were larger than the direct radon flux measurements when we used dose-rates from the EURDEP (GDR) data base or from GammaTRACER (GDR-2) measurements. This is due to the high dose-rate values shown in Figure 5.2.Indirect radon flux values, obtained by applying the empirical equation, presented in Section 5.2.3, were within 20 % and 40 % of the directly measured radon flux averages when ^{226}Ra activity in the soil was obtained from the literature (^{226}Ra MARNA map) and by laboratory measurements (^{226}Ra INTE/UHU), respectively.

5.4 Specific Conclusions

The EIC radon monitor response for the determination of radon flux directly from soil have been compared with other direct and indirects radon flux methods during an inter-comparison campaign carried out at four selected Spanish sites in summer 2008 under the most typical climate conditions for the eastern Spain. The geological characteristics of the object sites allowed a wide range of radon flux values ranging from 40 Bq m^{-2} h^{-1} and 90 Bq m^{-2} h^{-1} to be observed. Direct methods to determine radon flux, including both continuous and integrated systems, showed a good agreement with a coefficient of variation between 10 % and 23 %. This value is in accordance with the 34 % found out in the study by Hutter and Knutson, 1998.

Indirect methods based on the measurement of terrestrial gamma dose rate, or ^{226}Ra soil activity, and their empirical correlation with radon flux, were applied and evaluated. Results show that these correlations give radon flux values within 20 % and 40 % respectively of the directly measured radon flux average when the ^{226}Ra activity and the terrestrial γ dose-rate measurements are accurately measured. This results was observed both for ^{226}Ra activity obtained by MARNA map terrestrial dose data, or by direct measurement at the INTE and UHU laboratories on soil samples, and for terrestrial dose rate measured by RS-112 and by LB-1236 monitors at each campaign site. However, it was found that the terrestrial γ dose-rate values from the Automatic Spanish Surveillance network (REA) and those obtained by GammaTRACER lead to an overestimation of radon flux.

Part III

El Arenosillo station characterization

Chapter 6

^{222}Rn Flux characterization of the *El Arenosillo* area on a regional and local scale

^{222}Rn flux maps are useful in order to obtain informations about the possible origin of radon concentrations measured at a particular site (Arnold et al, 2010). In this work the radon flux of the Iberian Peninsula and of North Africa are of particular interest to estimate because the *El Arenosillo* station is located on a coastal area close to Africa as it is shown in Figure 2.10. It is particularly important to define the local radon flux of the *El Arenosillo* station itself and other areas close to this station which could influence the radon background. Hence, in this chapter both direct and indirect radon flux methods have been used in order to evaluate the radon flux contibution at the *El Arenosillo* station area on a regional and local scale.

6.1 ^{222}Rn flux of *El Arenosillo* area on a regional scale

Knowledge of ^{222}Rn flux from the ground is useful as regards studying the radon source in radioactive transport processes in the atmosphere.

Several indirect methods to estimate ^{222}Rn flux on a regional scale with high spatial resolution have been developed such as studies carried out by the European ^{222}Rn flux map (Szagvary et al, 2009), by the MARNA project (Mahou et al, 2005) and by the PhD work of Lopéz-Coto, 2011 as discussed in the first chapter of this thesis. The first method is based on an empirical relation found out between the radon flux and the terrestrial γ dose rate as it has been described in Chapter 4. Figure 6.1 shows the European ^{222}Rn flux map

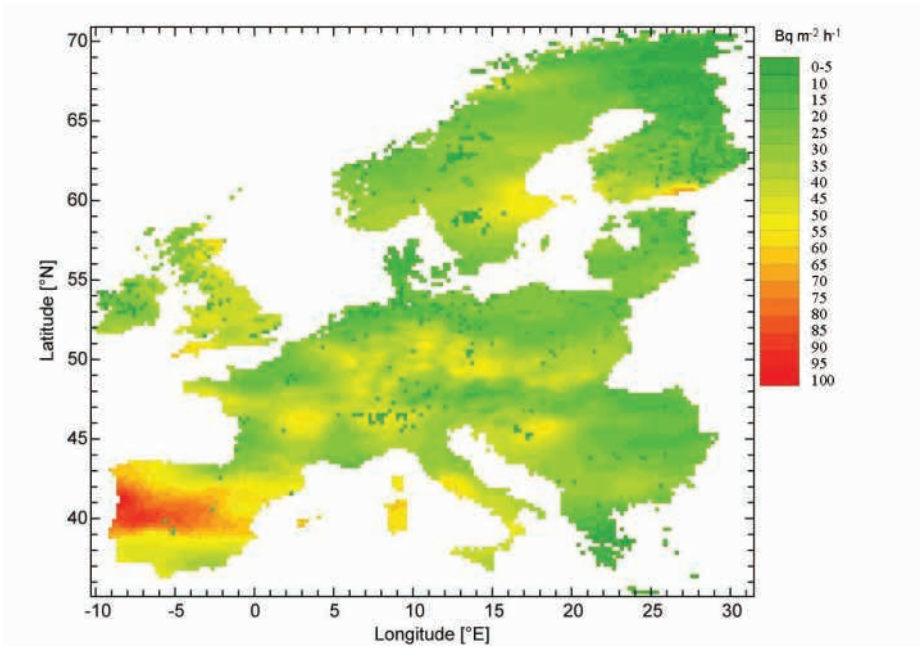

Figure 6.1: European ^{222}Rn flux map obtained using a relation with terrestrial γ-dose values of EURDEP Network (Szagvary et al, 2007).

(Szagvary et al, 2009). The second method gives useful information on the terrestrial γ dose rate in Spain with a spatial resolution of 0.02 degrees. This map was cronstructed within the framework of the Spanish National Uranium Exploration and Investigation Plan (Quindós et al, 2004). This data can be used in order to obtain the radium content from the soil and then calculating the ^{222}Rn flux by the Nazaroff equation as it has been presented in the Chapter 4 of this thesis. The map presented in Figure 6.2 was obtained in the PhD work of Arnold, 2009 , which downscaled the Spanish terrestrial γ dose map (MARNA) and combined it with the empirical relationship observed by Szagavary et al, 2009. The weakness of these two previous methods is that they do not take into account the environmental conditions at each site which can strongly influence the radon flux (Nazaroff and Nero, 1988; Grossi et al, 2011). Furthermore, these methods which do not include the gelogical soils parameters such as porosity, permeability and viscosity of each area which affect the radon diffusion in the soil. Finally, the radon emanation factor and the radon diffusion coefficient for each soil type and under different environmental conditions have not been taken into account in these methods. The new model for mapping the radon flux on a global scale presented in 2011 by Lopéz-Coto tried to solve all of these deficiencies (PhD thesis López-Coto, 2011). Indeed, in this method the real-time metereological conditions are also included in the radon flux estimation together with some

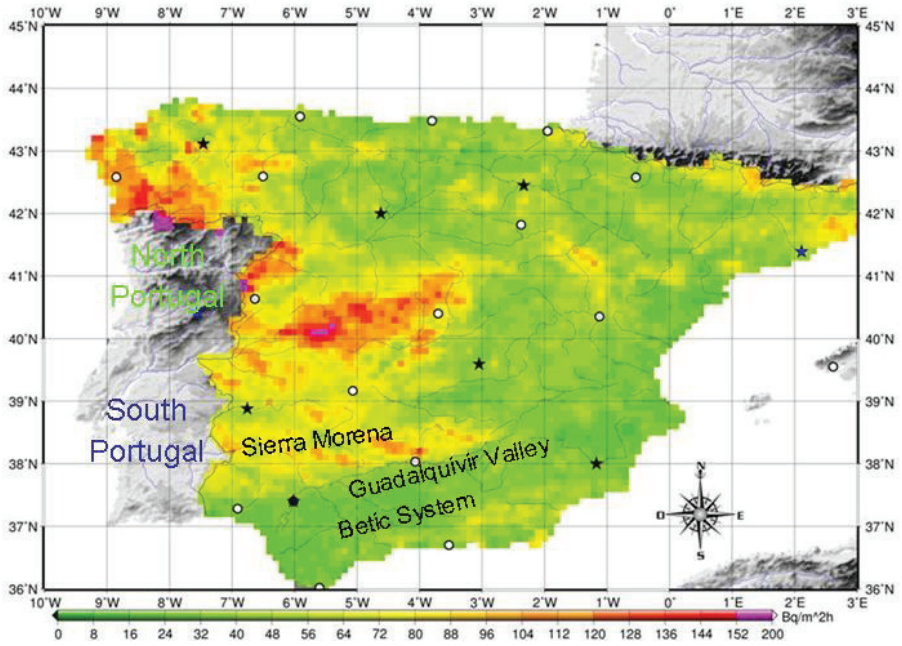

Figure 6.2: Radon flux map of Spain, downscaled by Arnold in her doctoral research (PhD thesis Arnold, 2009) and wind sector legend for the *El Arenosillo* station.

gelogical soil parameters for each region with a spatial resolution of 1 km^2. Unfortunately, all these methods are not able to include any possible contribution to the ^{222}Rn flux due to non-negligible gradient pressure except in the Lopéz-Coto model which offers this information but it does not give any information about the presence of faults in the soil surface.

A visual inspection of the map in Figure 6.2 and the geographic map of the *El Arenosillo* area in Figure 2.10, allows us to carry out a classification of several homogenuous ^{222}Rn flux areas. The Sierra Morena area, NNE of the *El Arenosillo* station, presents an average radon flux of 60-70 Bq m^{-2} h^{-1}, the Betics System, E of the *El Arenosillo* station and on the south-easternn coast of Spain has an average radon flux of 40-50 Bq m^{-2} h^{-1}, the Guadalquivir valley, between the Sierra Morena and the Betics system, which acts as a preferential channel for air masses reaching the Iberian Peninsula with an average radon flux of 5-10 Bq m^{-2} h^{-1}. Finally, the highest radon flux area is seen in the western centre of Spain with an average radon flux of 120-140 Bq m^{-2} h^{-1}. Portugal is not shown on this map, but an estimation of the radon flux in this area can be obtained from the European Radon Flux map 6.1, which shows an average radon flux of 50 Bq m^{-2} h^{-1} for South Portugal and 60-80 Bq m^{-2} h^{-1} for the North. Unfortunately, there are no

radon flux maps for North Africa. Nevertheless, direct measurements of radon flux for different Moroccan areas near the Atlas mountain system, in the Errachidia and Beni-Mellal regions, have shown high radon fluxes of about 150 Bq m^{-2} h^{-1} (Oufni, 2003) which can be used as a first estimation of exhalation in these areas.

6.2 ^{222}Rn flux of the *El Arenosillo* area on a local scale

6.2.1 ^{222}Rn flux method

The ^{222}Rn flux term was directly and indirectly measured at the *El Arenosillo* tower and at the Huelva phosphogypsum pile, which was considered as a possible high radon source due to its proximity to the *El Arenosillo* station. The ^{222}Rn flux was directly measured by the EIC monitors described in the Chapter 2, characterized under controlled environmental conditions in the Chapter 3 and 4, and for *in situ* soil in the Chapter 5 of this thesis. The radon flux characterization campaigns at the *El Arenosillo* area was performed in July 2010 and in May 2010 in order to check exhalation differences for sand. Seven measurement points were chosen for performing direct radon flux measurements. The first point (1) was located at the tower base. The additional six points from (2) to (7) were distributed around the surrounding area and covered a circular area with a radius of 200 m.

The radon flux was also directly measured at the phosphogypsum pile in the restored area (Zone 1) and the unrestored area (Zone 3) always by the EIC monitor (Kotrappa and Steck, 2009). At each measurement point one of these RT-EIC monitors, was used together with a new, slightly modified version, named R-EIC monitors, which could additionally minimize the response to thoron in the case that it is present in the analyzed soil due to ^{232}Th decay, as previously explained. A third sealed monitor was located at each measurement point in order to evaluate the environmental background in order to subtract it from the measurement. Figure 2.13 shows the measurement points locations in both phosphogypsum pile areas. Furthermore, in Figure 6.3 a typical measurement with the related detectors deployed at the phosphogypsum pile is shown. A detailed explanation of the EIC monitor method and the measurement protocol have already been reported in Section 2.2.2 of the this thesis.

6.2.2 Radionuclides activity method

In order to estimate the ^{222}Rn flux of the *El Arenosillo* area by indirect methods too, soil samples were collected at the same points where ^{222}Rn flux measurements were carried out. The radiation concentration activity of ^{226}Ra, ^{232}Th and ^{40}K was analyzed for each of

Figure 6.3: Typical measurement of ^{222}Rn flux by EIC E-Perm monitors at the unrestored area (Zone 3) at the Huelva phosphogypsum pile.

the 30 soil samples collected at the Huelva phosphogypsum pile and at the *El Arenosillo* station. In the case of the phosphogypsum pile, the soil samples were collected during the campaign at both restored and unrestored areas (Zones 1 and 2). Ten soil samples were collected at each pile zone with a spatial resolution of 500 m. The radiation activity content for natural radionuclides was then measured at the INTE-UPC laboratory by γ-spectrometry with a HPGe coaxial detector for each collected soil sample. The soil samples were warmed up to 150 °C in order to dry them and then put into air-tight Petri dishes of 50 ml volume. The Petri dishes were stored for 30 days to allow the ^{226}Ra to reach the secular equilibrium with its short-lived progeny. ^{226}Ra activity concentration for unit of weight (Bq kg^{-1}) was evaluated by measuring the net count and calculating the weighted average of its progeny ^{214}Pb (352 keV) and ^{214}Bi (609 keV). ^{232}Th activity was obtained using net counts of ^{212}Pb (238 keV), ^{208}Ac (911 keV) and the corrected counts of ^{208}Tl (583 keV). Corrected counts for ^{208}Tl are obtained by dividing the measured cps for 0.36. ^{40}K was measured by directly using its gamma peak at 1460 keV.

6.2.3 Terrestrial γ-dose rate method

The indirect method proposed by Szagavary et al, 2009 was also applied and a proportional counter monitors LB 123 D-H10 (Berthold) and integrated TLD detectors were used by

the research group of INTE-UPC for measurement of terrestrial γ-dose rate at at *El Arenosillo* tower area and at the Huelva phosphogypsum pile. The Berthold probe has a temperature interval which ranges from -10 °C to 60 °C. The measuring range is between 0.05 μSv h^{-1} and 10 mSv h^{-1}. The TLD used werethermoluminescence passive detectors widely employed for dose exposure estimation (Piesch and Burgkhardt, 1983; ISO, 1997). The TLD detectors were arranged in a holder for environmental dosimetry and located in the measurement field at 1 m above ground level (Ortega et al, 2008). The terrestrial gamma dose rate was measured at each site along with radon flux measurements and soil samples collection. The cosmic component to the dose was subtracted.

6.3 Results at *El Arenosillo* tower

Single radon flux results for both RT-EIC and R-EIC monitors, measured during dry and wet periods, are shown in Figure 6.4. Normally, the EIC monitors are used to estimate radon flux values that are much higher then 5 Bq m^{-2} h^{-1} (Grossi et al, 2011). Therefore, high uncertainties were observed for these low radon flux values. In any case, the difference between the dry and wet season can be considered really small at the *El Arenosillo* area. Indeed, taking into account the monitor uncertanties, Figure 6.4 shows radon flux results slightly higher during the wet period for the RT-EIC monitors. This result could be explained because of the influence of water content on radon flux for low water presence, as presented by past studies (Nazaroff and Nero, 1988; Grossi et al, 2011) and as found out during laboratory analyses presented in this thesis in the Chapter 4. Finally, the difference between RT-EIC and R-EIC monitors could indicate some contribution from ^{220}Rn exhalation. These results also confirm low local radon flux, in agreement with the low radon flux area found by indirect methods in Figure 6.2. The mean value of the all 23 measurements is 4.9 Bq m^{-2} h^{-1} with a standard deviation of 2.3 Bq m^{-2} h^{-1}.

The average radiation activity concentration for unit of weight (Bq kg^{-1}) in soil samples collected at the *El Arenosillo* station is 5.6 $\pm$ 1.3 Bq kg^{-1} for^{226}Ra and it is 5.3 $\pm$ 1.2 Bq kg^{-1} for ^{232}Th. Average activity for ^{40}K is 100 $\pm$ 15 Bq kg^{-1}, which is normally observed in organic soils (Bolivar et al, 1996; Grossi et al, 2011). Furthermore, the average terrestrial gamma dose measured in this area, after the cosmic component subtraction, is 42 nSv h^{-1}.

Using these results of the terrestrial gamma dose rate and of the radium activity concentration it is possible to indirectly calculate the ^{222}Rn flux at the *ElArenosillo* station using the Szagvary and the ^{226}Ra methods, introduced in Chapter 5. The European radon flux map in Figure 6.1 gives a ^{222}Rn flux value of 50 Bq m^{-2} h^{-1}. However, the same Szgevary equation with measured terrestrial gamma dose gives a ^{222}Rn flux value of 20 Bq m^{-2} h^{-1}, this difference could be due to the interpolation method used by the European radon flux map. On the other hand, the radon flux value obtained by the ^{226}Ra methods leads

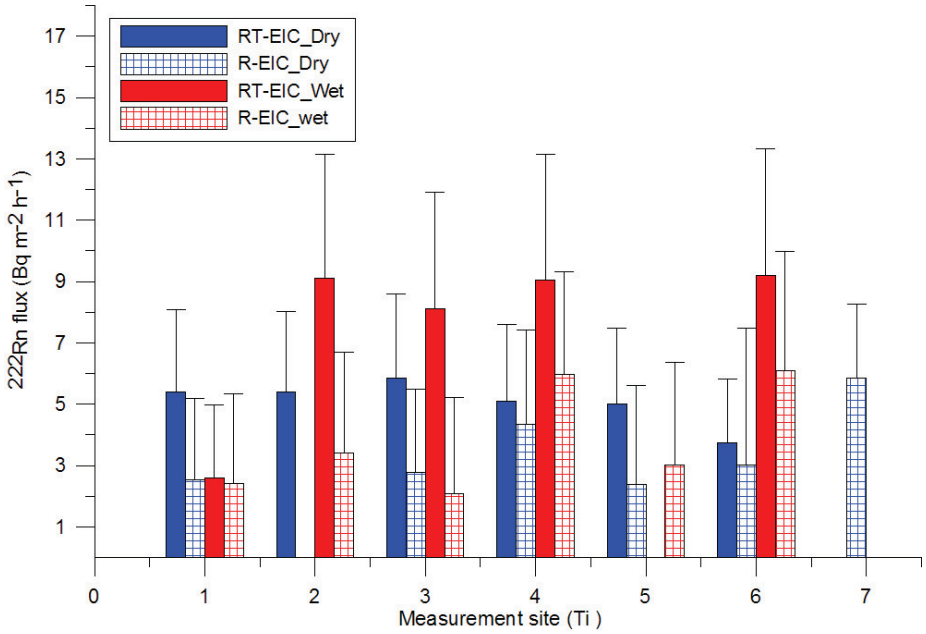

Figure 6.4: Radon flux results at the *El Arenosillo* station measured by RT-EIC and R-EIC monitors with thoron filters during dry and wet conditions.

to a radon flux value of 8 Bq m^{-2} h^{-1}, which is in agreement with experimental results reported in Figure 6.4.

6.4 Results at the Huelva phosphogypsum pile

Two measurement campaigns were carried out in spring and summer 2010 in order to realize a complete evaluation study of the ^{222}Rn flux on the restored and unrestored areas of the pile surface. Access to the active zone of the phosphogypsum pile was not available during the campaigns. The campaigns included the analysis of radiation activity content in soil samples collected at the restored and unrestored areas, the environmental γ-dose rate measured on the restored and unrestored pile surface area and the measurement of ^{222}Rn flux directly *in situ* at the restored and unrestored areas and under different environmental conditions.

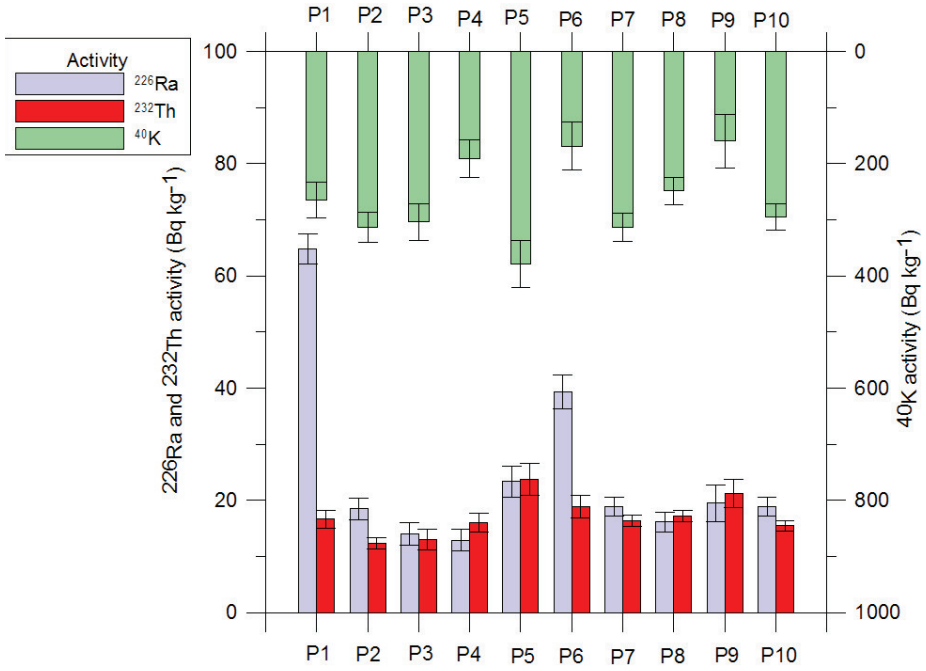

Figure 6.5: Activity concentration for unit of weight (Bq kg^{-1}) of ^{40}K (dark bar), ^{226}Ra (grey bar) and ^{232}Th (white bar) in soil samples from Zone 1 of the phosphogypsum pile.

6.4.1 Radiation activity results

The radiation activity concentration for unit of weight (Bq kg^{-1}) of different natural radionuclides measured in soil samples collected at Zone 1 and at Zone 3 of the Huelva phosphogypsum pile are shown in Figure 6.5 and in Figure 6.6. Figure 6.5 presents results for the restored area which was covered in 1992 with a 25-com-stick layer of organic soil. The ^{40}K activity concentration for soil samples from this zone is commonly 300 Bq kg^{-1}, which is normally observed in organic soils (Guimond and Hardin, 1989; Bolivar et al, 2002; Grossi et al, 2011). ^{226}Ra and ^{232}Th present a similar average activity concentration of 20 Bq kg^{-1}. Measurements at points P1 and P6, which are both located in the north-east of Zone 1, as shown in Figure 2.13, present a higher activity of ^{226}Ra of 65 Bq kg^{-1} and 38 Bq kg^{-1}, respectively. This could be due to the utilization of a different layer for the covering of this part of the restored pile as explained in the PhD thesis of Lopéz-Coto, 2011. Figure 6.6 shows the results of natural radionuclides activities at the unrestored area, Zone 3, which is still entirely covered by phosphogypsum. ^{40}K activity values were under 40 Bq kg^{-1}, which was the minimum detected activity for this radionuclide for a gamma spectrum of 24 h. The ^{226}Ra activty results present an average activity of 500 Bq

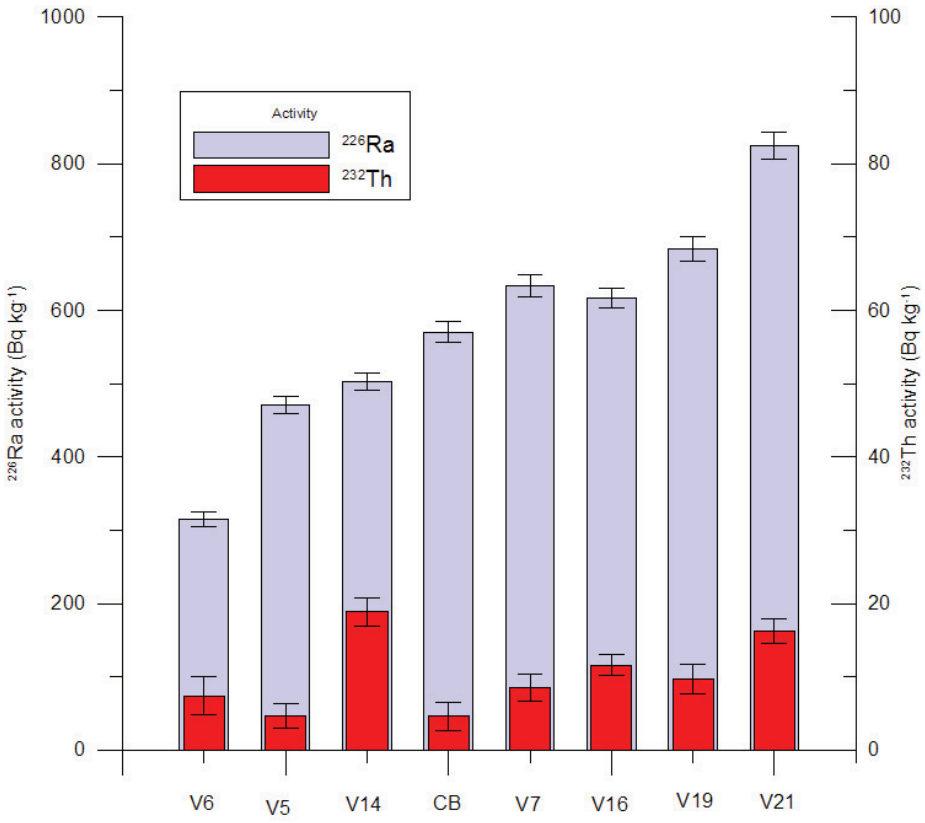

Figure 6.6: Activity concentration for unit of weight (Bq kg^{-1}) of ^{226}Ra (gray bar) and ^{232}Th (white bar) in soil samples from Zone 3 of the phosphogypsum pile.

kg^{-1} which is in agreement with results from the literature (Bolivar et al, 2002; Dueñas et al, 2007). Furthermore, a new significant increase of ^{226}Ra activity, from 200 Bq kg^{-1} to 800 Bq kg^{-1}, was observed in soil samples collected closer to the Tinto river such as at the points V21 and V19 (Figure 2.13). This could be due to the water transport of soil material to the riverside (Bolivar et al, 2002). Finally, ^{232}Th activity concentration was measured in a range interval between 5 and 10 Bq kg^{-1} and the same activity increase was observed near to the Tinto riverside. This material transport by the water could be explained by the presence of a 5-6 m slope between the centre of Zone 3 and the riverside, which facilitates water flow.

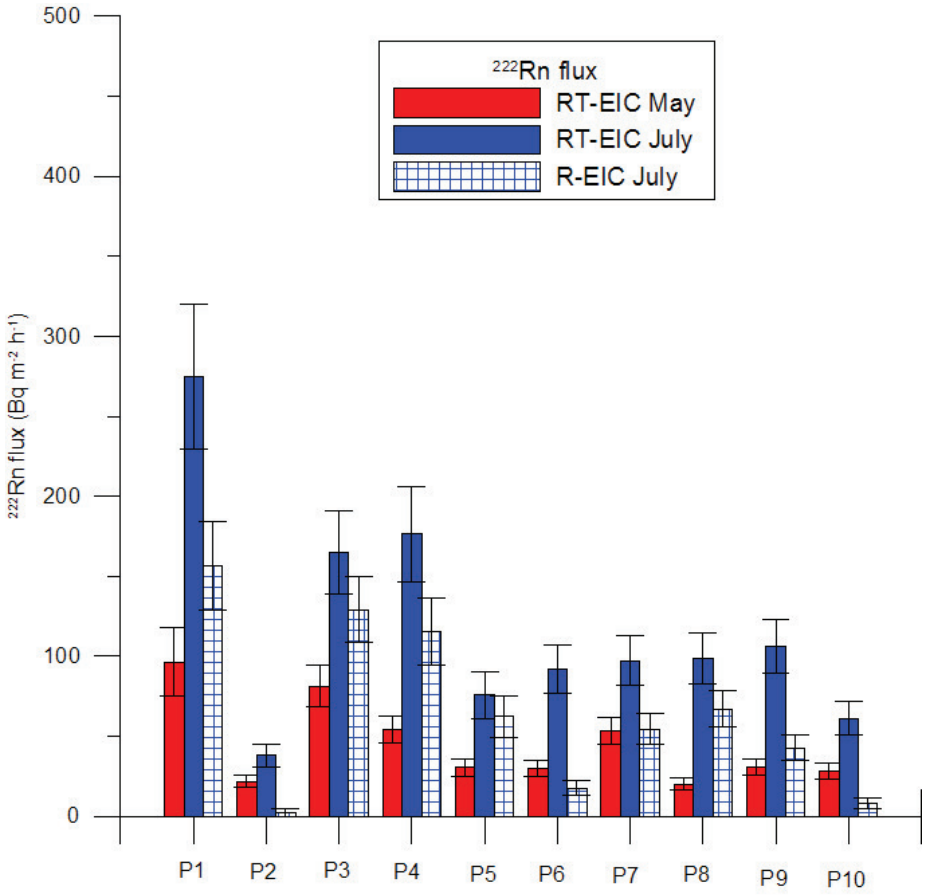

Figure 6.7: Radon flux results at the restored phosphogypsum pile zone by RT and R-EIC monitors during the May and July 2010 campaign.

6.4.2 ^{222}Rn flux results

Direct radon flux measurements performed at Zone 1 and Zone 3, which are the restored and unrestored pile areas respectively, are shown in Figure 6.7 and in Figure 6.8. Figure 6.7 shows the results of ^{222}Rn flux measured at the restored pile (zone 1). The radon flux values observed in this area during the wet period, in May 2010, are lower than those measured during the dry period, in July. Furthermore results of RT-EIC monitors show higher values compared with results of R-EIC monitors which do not take into account the thoron contribution. This could indicate the presence of ^{220}Rn exhalation from the soil surface, due to ^{232}Th decay, which is not yet quantifiable. An average radon flux of

118 ± 20 Bq m^{-2} h^{-1} was measured in this zone during the dry period which is double the typically observed radon flux (Grossi et al, 2011) and an average value of 45 ± 8 Bq m^{-2} h^{-1} during the wet period as was expected due to the influence of humidity content on the soil. Figure 6.8 shows the high radon flux values measured at the points P1, P3 and P4. Point P1 also presents a ^{226}Ra activity of 60 Bq kg^{-1} which could explain the high measured radon flux, the points P3 and P4 are close to the Tinto river and perhaps there is a contribution due to the radon emanated after the decay of ^{226}Ra accumulated in the phosphogypsum located at the bottom of the pile. Figure 6.8 presents the radon flux results for the unrestored area (Zone 3). The results range between 20 and 110 Bq m^{-2} h^{-1}, they show a small difference between dry and wet periods, which is of about 20 % higher during dry period. This fact could be due to the ability of phosphogypsum to retain water for a long time. The average radon flux in this zone seems to be of about 45 Bq m^{-2} h^{-1} and the standard deviation is of 20 Bq m^{-2} h^{-1} which is not as high as would be expected in phosphogypsum.

The activity concentration of the ^{226}Ra in Zone 1 and at Zone 3 can be used to indirectly evaluate the radon flux. Indeed, the restored zone presents an average activity of ^{226}Ra in the soil samples of 24 Bq kg^{-1} as reported in Figure 6.5. Using the Nazaroff equation the estimated radon flux is of about 40 Bq m^{-2} h^{-1} which is in agreement with directly measured radon flux during the wet period. Unfortunately, this method is not able to estimate the radon flux difference between dry and wet periods because it does not take into account values of metereological conditions. On the other hand, the radium content of the soil sample in the unrestored zone presents an average value of 500 Bq Kg^{-1} which, using the Nazaroff equation with standard soil parameters leads to a radon flux of 800 Bq m^{-2} h^{-1}. This is definitively much higher than the observed average value in Figure 6.8. This difference between the direct and indirect methods can be explained because in the Nazaroff equation does not take into account neither the humidity content in the phosphogypsum material or its exact radon diffusion coefficient, which drastically reduce the radon exhalation from the material surface (Nazaroff and Nero, 1988; MSc thesis Grossi, 2006).

6.4.3 Terrestrial γ-dose results

The measurements of environmental gamma dose rate include only the terrestrial component, mainly from the ^{40}K and the ^{238}U and the ^{232}Th series, because the cosmic component had been subtracted. The restored Zone 1 presents an average environmental dose rate of about 100 nSv h^{-1} where the unrestored area shows an average dose rate of 270 nSv h^{-1}. These data can be also used for evaluating the radon flux by the empirical equation of Szagvary et al, 2009. The terrestrial γ-dose rate measured at each point in the restored and unrestored areas have been plotted against the measured radon flux in Figure 6.9 in order to compare their relationship with the empirical relation found out by Szagvary et al, 2009. The radon flux measurement at the unrestored pile is definitively

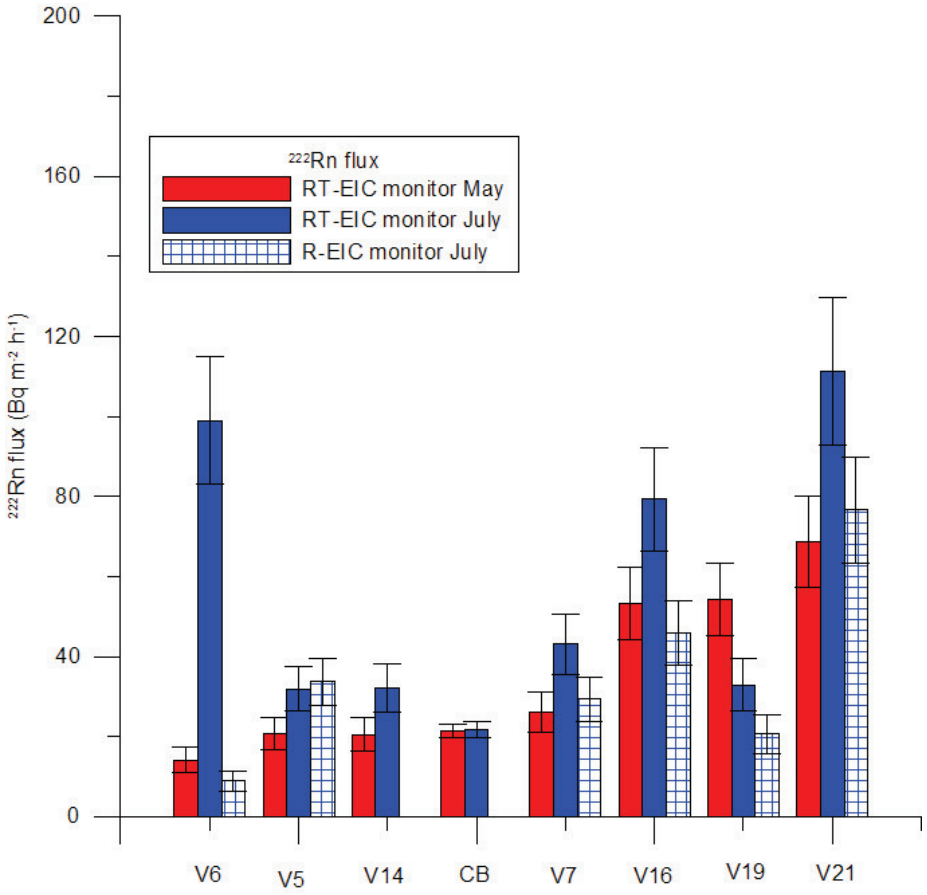

Figure 6.8: Radon flux results at the unrestored phosphogypsum pile zone by RT and R-EIC monitors during the May and July 2010 campaign.

lower than that expected for the Szagvary empirical equation (Szagvary et al, 2009). Nevertheless, radon flux results in this zone are proportional to measured terrestrial gamma dose rate. On the other hand, the radon flux results in the restored area seem to follow a linear relationship found by Szagvary et al, 2009. However, the points P1, P3 and P4 show higher radon flux than those expected, which could be due to a contribution to the gamma dose because of phosphogypsum material deposited at the bottom of the pile and which is closer to the Tinto river as is seen in the radon flux results.

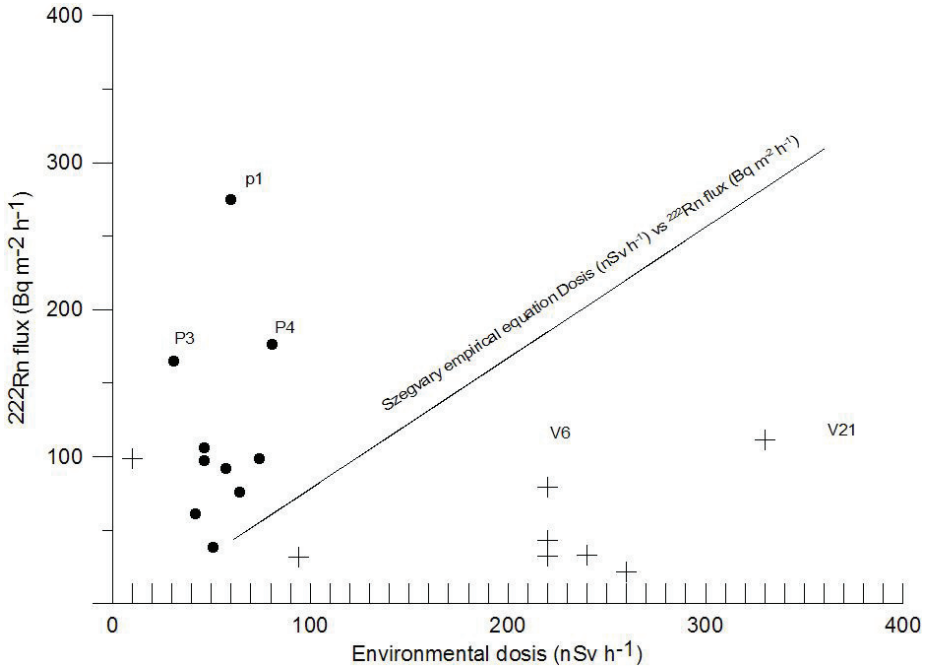

Figure 6.9: Linear relationship between environmental gamma dose rate (nSv h^{-1}) and radon flux (Bq m^{-2} h^{-1}) measured at each point in the restored (square point) and unrestored (cross point) areas. Comparison with Szagvary et al, 2009 empirical relation.

6.5 Specific Conclusions

Direct radon flux measurements at the *El Arenosillo* tower show quite low radon exhalation from the soil with an average of 5.3 ± 1.8 Bq m^{-2} h^{-1}. This result is in agreement with indirect radon flux methods for the same area obtained in the PhD thesis of Arnold, 2009 which used the Szagvary equation together with terrestrial gamma dose data obtained by the MARNA map. However, the radon flux results obtained at the *El Arenosillo* tower by the European radon flux map are of about 50 Bq m^{-2} h^{-1} and they are certainly too high (Szagvary et al, 2009). This fact could be due to the high terrestrial gamma dose rate used by Szagvary for this area, which came from the REA station. Ra and it has been shown to be overestimated (Grossi et al, 2011).

The radon flux results during dry and wet periods do not show significant differences due to the high permeability of sand which allows the water to permeate through it quickly (Nazaroff and Nero, 1988). Indeed, the permeability is an important parameter since soils with high permeability have a lower humidity, whereas water can accumulate in soils with low permeability (Levin et al, 2002). The *El Arenosillo* tower is exclusively surrounded

by pine forest and sand. The sand has an intrinsic high permeability of the order of 4 $\cdot$ 10^{-11} m^2, which is one or two orders of magnitude higher than for other typical soils (Nazaroff and Nero, 1988) and could explain the lack of a marked difference of radon flux observed between dry and wet periods.

The ^{222}Rn flux results at the phosphogypsum pile do not seem to show high values which means that the PG is not a high radon flux source to be used for inverse modelling applications, which include the reconstruction of the source term by use of atmospheric transport models in backward mode. In spite of the high activity of ^{226}Ra measured in the phopshogypsum soil, the laboratory experiments and the direct *in situ* measurements of radon flux have shown that the high humidity content of this material does not allow the radon to be exhaled from the surface. Furthermore, the phosphogypsum material does not exhale high radon concentration even when it is completely dry because of a very small radon diffusion coefficient in this material. Indeed, radon flux measurements at the phosphogypsum pile were carried out in dry and wet periods and results show a significant difference between the two season. Nevertheless the phosphogypsum soil always appeared really wet to the touch. Lopéz-Coto comments this is due to a high rain season in 2010 which meant that the phosphogypsum did not get completely dry (PhD thesis López-Coto, 2011). A laboratory analysis of radon flux from phosphogypsum soil samples was carried out with totally dried samples, as presented in the Chapter 4, and no difference was observed in the radon flux results.

In any case, experimental radon flux results found out at the Huelva phosphogypsum pile during this study are not in agreement with previous studies by Dueñas et al, 2007 and by Abril et al, 2009. These studies, which were carried out using the charcoal canisters method, found out extremely high radon flux values in the Huelva phosphogypsum pile with a great great dispersion between 100-1000 Bq m^{-2} h^{-1}. This discrepancy is presently under study and will be published in a future paper. On the other hand, the indirect radon flux maps of regions of Europe and of Spain offer useful informations in order to evaluate the possible radon source contribution reaching the *El Arenosillo* station, but these methods, in special zones such as the Huelva phosphogypsum pile, have not been shown to be completely reliable. Indeed, indirect radon flux maps need to take into account the possible environmental conditions and the geological material parameters which can influence radon exhalation.

However, indirect radon flux methods have been usefull on a regional scale to point out several *hot spot* areas, with a high radon flux, such as Sierra Morena, the Bethic System and central Spain. Furthermore, a literature study shows a possible high radon flux in the North of Morocco due to the presence of the Atlas Mountains. All these high radon sources could be really usefull to perform inverse modelling studies and need to be confirmed by experimental atmospheric radon concentration analyses and atmospheric backtrajectory studies. Finally, all these previous results confirm the possibility of using the *El Arenosillo* station for atmospheric studies which use radon as a tracer because this station does not present a significantly noisy radon background due to the local contribution.

Chapter 7

^{222}Rn atmospheric concentration at 100-m-high tower of the *El Arenosillo* station

7.1 Introduction

Two ARMON monitors for atmospheric radon concentration measurement, which were presented in Section 2.3 and were calibrated in the INTE-UPC radon chamber as explained in the Chapter 3, were installed on the 100-m-high tower of the *El Arenosillo* station, on the Spanish south-west coast. The station is managed by the National Institute for Aerospace Technology (INTA). The ^{222}Rn concentration time series at 10 m and at 100 m were measured hourly for two years at this meteorological station. In this chapter the seasonal analysis of atmospheric radon concentration performed at the *El Arenosillo* station during 2009-2011 are presented. Results for each season present evidence associated with the origin of air masses reaching the *El Arenosillo* station.

7.2 Material and Methods

The atmospheric radon concentration variability was measured at two different levels on the *El Arenosillo* tower. Meteorological parameters were also available at this site during the analysis. Data for one year were analysed and the radon behaviour for different seasons and under different local meteorological conditions was studied at this coastal area. Furthermore, both the diurnal and nocturnal behaviour of radon gas was also analysed.

7.2.1 Site

The *El Arenosillo* station is the site selected in this thesis work for performing a complete radon characterization. The *El Arenosillo* site is located in the South of Spain (37.10N/6.79E), as shown in Figure 7.1 and its characteristics have been described in details in Section 2.5. The 100-m-high tower of the *El Arenosillo* station is only 25 km from the city of Huelva, where the phosphogypsum pile described in the Chapter 2 is located and it is only 0.7 km from the Atlantic coast. The *El Arenosillo* station is sited within the Doñana National Park.

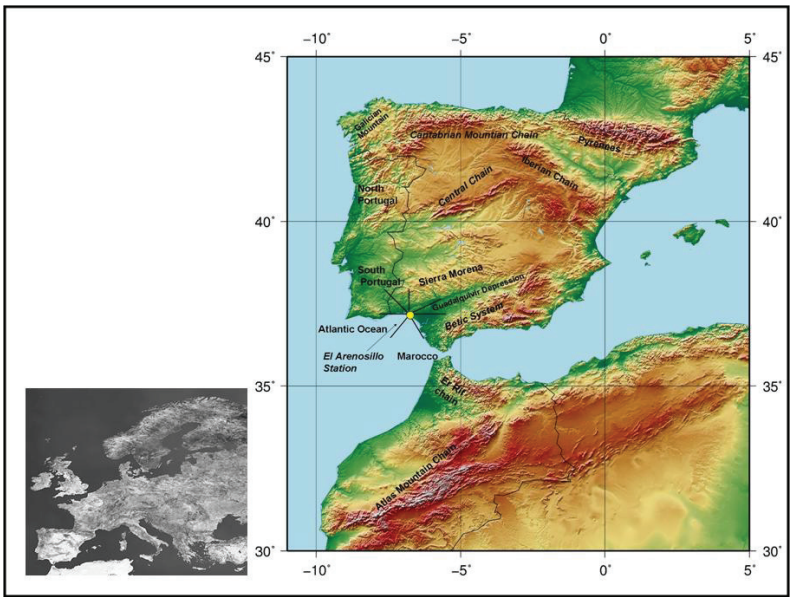

Figure 7.1: Europe (left) and the location of the *El Arenosillo* station on the southern coast of Spain with wind sectors for each specific geographic area (right).

7.2.2 Meteorological parameters

Meteorological parameters with a time resolution of 10 minutes are continuously measured at *El Arenosillo* station. The instrumentation used was a Vaisala WXT520 with sensors located at 10 m. The measurement interval for wind speed was between 0 and 60 m s^{-1}. The accuracy is 3 % for wind speeds between 0 and 35 m s^{-1} and 5 % when the wind speed ranges from 35 to 60 m s^{-1}. Accuracy in wind direction measurement is ± 38 and response time is 250 ms. Average data results at 10 m tower were used in this study for a statistical analysis of seasonal hourly radon concentration from November

2009 till November 2010. The seasons were defined as winter, December to February, spring from March to May, summer from June to August and autumn, from September to November. The data analysis of wind direction frequencies was done to study the direction of incoming air masses using characteristic source sectors at the *El Arenosillo* station, as illustrated in Figure 7.1. The Sierra Morena sector includes N and NEE winds; The Guadalquivir Valley sector ranges between NEE and E; The Bethics System sector is defined between E and SSE; the Moroccan sector includes winds coming from SSE to SSW; the Atlantic Ocean sector is defined from SSW to SWW, the South Portugal sector includes wind coming from SWW to NW. Finally, North Portugal was defined as winds coming from NW to N. The wind speed study was carried out by dividing seasonal data into 5 speed divisions: speeds below 1 m s^{-1} is defined as calm, from 1 to 3 m s^{-1}, from 3 to 5 m s^{-1}, from 5 to 7 m s-1 and above 7 m s^{-1}.

7.3 Seasonal atmospheric ^{222}Rn concentrations

A summary of results of radon concentrations time series at two different heights and their relation with local wind conditions is given in Figures 7.2, 7.4, 7.6 and 7.8 for each season for a period of one year. On each plot the wind-rose and the bar chart for average radon concentrations, at 10 m and at 100 m, are shown for different *source* wind sectors and several wind speed ranges. Although this is a simple local correlation, it may provide a hint on the possible distant sources affecting measurements. Furthermore, the statistical analysis of measurement results for each season shows a bimodal lognormal distribution given in Figures 7.3, 7.5, 7.7 and 7.9 with the geometrical mean and the standard deviation obtained by a Gaussian fit. The average hourly measured concentrations of radon gas obtained over a year at the 10 and 100 m heights at the *El Arenosillo* station were 3.51 Bq m^{-3} and 2.61 Bq m^{-3}, respectively. At 10 m, the standard deviations for the hourly, daily, weekly, and monthly data amounted to 2.87 Bq m^{-3} (N=3382), 2.35 Bq m^{-3} (N=169), 1.69 Bq m^{-3} (N=34), and 1.10 Bq m^{-3} (N=10), respectively. For 100 m, these standard deviations were 2.02 Bq m^{-3} (N=3684), 1.47 Bq m^{-3} (N=164), Bq m^{-3} (N=35) and 0.53 Bq m^{-3} (N=10), respectively.

7.3.1 Autumn Season

Results for autumn 2009 with average radon concentrations under specific wind direction conditions are reported in Figure 7.2, as it will be done in the following sections for each seasonal analysis. The average radon concentration in the atmosphere, for each of the defined season, presents similar behaviour when the wind flows from specific sectors and with the same speeds intervals. These wind sectors include specific geographic areas such as:

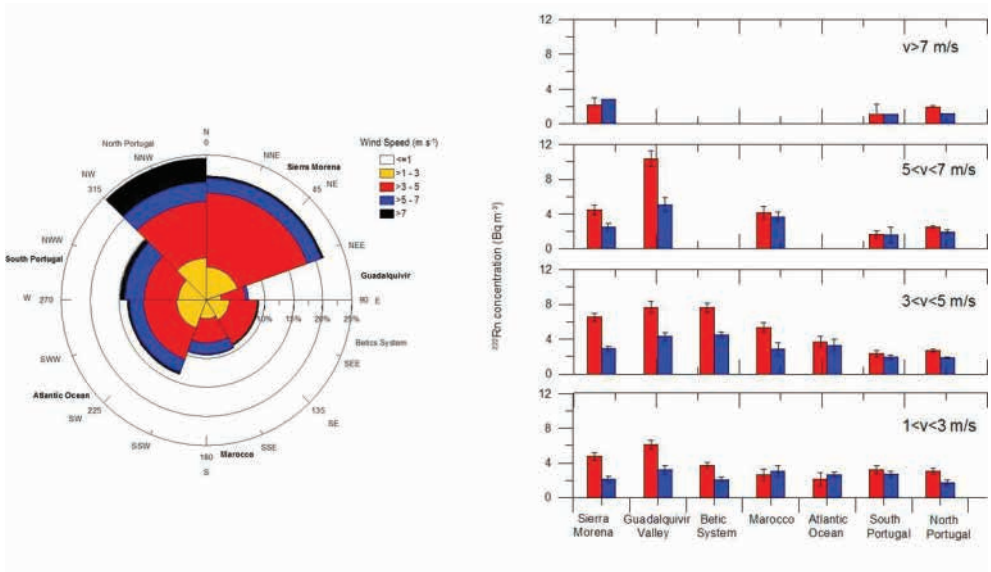

Figure 7.2: Wind-rose and average ^{222}Rn concentrations at 10m (white bar) and 100m (gridded bar) during autumn.

The Sierra Morena Sector. The most statistically relevant cases during autumn are observed when the prevailing wind comes from the first quadrant with wind speed intervals of 1-3 m s^{-1}, 3-5 m s^{-1} and 5-7 m s^{-1}. An increase of average radon concentration can be observed at 10 m and at 100 m in autumn in Figure 7.2, as well as during other seasons, when the wind comes from the Sierra Morena Mountains. This area has an average radon flux of 60-70 Bq m^{-2} h^{-1}, which is much higher than the average radon flux observed at the *El Arenosillo* station, as seen in Figure 6.2 and in the direct radon flux results of Figure 6.4. A radon concentration increase, when the wind comes from Sierra Morena, has also been observed in Seville, which is 66 km east of the *El Arenosillo* station, by Arnold et al, 2009. Average radon concentrations at 10 m and at 100 m are significantly different even for high wind speeds, which shows the possibility of an important advected contribution at the lower level. This difference is also present when wind flows from the Guadalquivir and the Bethics region. This can be explained by the fact that most of the cases, in these sectors, are during nighttime. Nighttime conditions help both the accumulation of locally exhaled radon in the vicinity of the station within a shallow boundary layer, as well as the development of downslope cold and shallow flows that would carry radon coming from the mountains to the sea due to the southwest-northeast Guadalquivir depression axis (PhD thesis Hernandez-Ceballo, 2011).

The Guadalquivir sector. Radon concentration increases during autumn when the wind comes from the Guadalquivir valley sector, as shown in Figure 7.2. Average radon

concentration at 10 m is about 10 Bq m^{-3} when the wind speed is between 5 and 7 m s^{-1}, which could indicate air masses coming from inland regions of Spain, characterized by high radon flux as shown in Figure 6.2. As can be observed in the following sections, the average radon concentrations at 10 m and at 100 m are significantly different when the wind comes from NW to E, including the North of Portugal, the Sierra Morena and the Guadalquivir valley sectors. As in the previous sector, as well as in the winter season, most of the cases are nighttimes occurrences. This shows both the possibility of a shallow nocturnal boundary layer, which allows the accumulation of radon, and the advection due to the drainage flows down the Guadalquivir valley to the *El Arenosillo* station that carry the radon exhaled inland.

The Bethics System Sector. An increase of average radon concentration at 10 m when the wind comes from the E-SE sector can be seen in Figure 7.2. This fact is due to the presence of the Bethics System, characterized by radon flux between 50-60 Bq m^{-2} h^{-1}. Average radon concentration at 10 m is 7.6 Bq m^{-3} when the wind reaches the *El Arenosillo* station with a velocity between 3 and 5 m s^{-1}. There is a relative difference between radon results at the two heights, as seen in Figure 7.2 probably due to the proximity of the Bethics area source as explained in the previous section for the Sierra Morena.

The North Portugal Sector. More frequently wind comes from North Portugal during autumn, as can be seen in Figure 7.2. The North Portugal area has an average radon flux of 70 Bq m^{-2} h^{-1}, which is much higher than the local radon flux measured during this study at the *El Arenosillo* station, of around 5-10 Bq m^{-2} h^{-1}. It is also different to the value estimated from the European radon flux map (Szagvary et al, 2009). A relative increase is observed in average radon concentrations at both levels when the wind comes from the North of Portugal instead of from the South of Portugal. This slight increase in radon concentration can probably be explained by air masses crossing Portugal until they reach the *El Arenosillo* coastal area. In this sector most of the cases fall in the late afternoon until the early hours of the morning. Nevertheless, air masses passing over the South of Portugal come from the ocean and are not rich in radon. As regards the nocturnal cases, they are composed of well-mixed air passing over the warmer sea surface, which could explain similar average radon concentrations at both levels.

The Atlantic Ocean and South Portugal sector. Average radon concentrations are lower, about 2 Bq m^{-3}, and are similar for both heights when the wind comes from the Atlantic Ocean sector and from South Portugal (Figure 7.2). This could indicate radon-poor, well-mixed air masses travelling over the ocean and along the South Portugal coast.

The Morocco sector. Figure 7.2 shows how average radon concentrations are similar for both heights and they present values between 3-4 Bq m^{-3} when the wind comes from the Morocco sector. This relative radon increase, compared with the sea sector, could be due to the presence of the Atlas mountain system on the Moroccan coast, in the Errachidia

and Beni-Mellal regions, which have shown a high radon flux of about 150 Bq m^{-2} h^{-1} (Oufni, 2003). Neverthless, similar radon concentrations at both levels could be due to well mixed air masses coming from the warm Sahara surface and passing over the Atlas mountains.

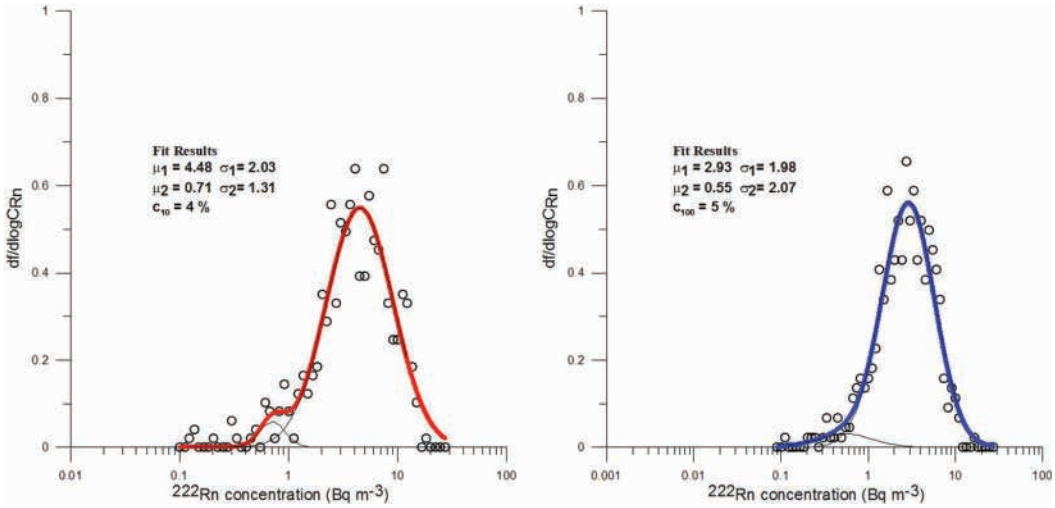

Figure 7.3: Bimodal lognormal distribution of radon concentration measurement at *El Arenosillo* station during autumn at 10 m (left) and at 100 m (right).

The statistical analysis of hourly radon concentration results at 10 m and at 100 m during the autumn season show a bimodal lognormal distribution either at 10 m or at 100 m, Figure 7.3. Experimental data were fitted with a double Gaussian function to calculate the geometric mean and the standard deviation of each distribution. The geometric mean $\mu_{1,10}$ of radon concentration data at 10 m and for the larger distribution in Figure 7.3 is 4.48 Bq m^{-3} with a standard deviation $\sigma_{1,10}$ = 2.03 Bq m^{-3}. The geometric mean $\mu_{1,100}$ for the larger distribution of Figure 7.3 at 100 m is 2.93 with $\sigma_{1,100}$ = 1.98 Bq m^{-3}. The larger distribution at both heights represents the total radon concentration hourly values which were measured under all wind conditions. The difference between previous values $\mu_{1,10}$ and $\mu_{1,100}$ indicates a good separation of atmospheric layers during the autumn season.

A second smaller Gaussian in Figure 7.3, with an area of c_{10} = 4 % and c_{100} = 5 % of total bimodal distributions, are visible at both heights with values lower than 1 Bq m^{-3}. This distribution includes all radon concentration hourly values measured when the wind comes from between 200 and 300 degrees, which corresponds to the Atlantic Ocean area. The geometric means are $\mu_{2,10}$ = 0.71 Bq m^{-3} with standard deviation 1.31 Bq m^{-3} and $\mu_{2,100}$ = 0.55 Bq m^{-3} with standard deviation 2.07 Bq m^{-3} at 10 m and at 100

m, respectively. These previous geometric means $\mu_{2,10}$ and $\mu_{2,100}$ indicate no significant differences, as was to be expected.

7.3.2 Winter Season

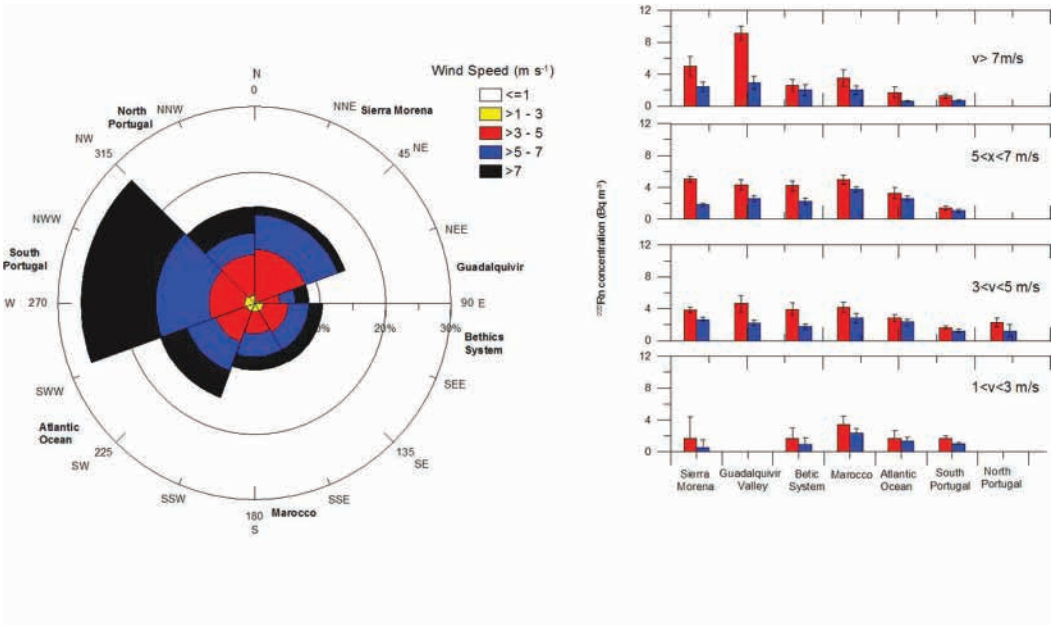

Figure 7.4: Wind-rose and ^{222}Rn concentration at 10 m (white bar) and 100 m (gridded bar) during winter

Most incidents occur during the winter season when the wind comes from SWW-NW with a frequency of 23 %, corresponding to South Portugal, with a wind speed higher than 7 m s^{-1} and an average radon concentration of 2 Bq m^{-3} at both levels, as it can be seen in Figure 7.4. Furthermore, the wind comes from the Sierra Morena and from the Guadalquivir valley with a frequency of 12 % and a velocity between 3 and 5 m s^{-1}. Under these conditions, the average radon concentration at both heights is significantly different from that observed during autumn. Average values of 8 Bq m^{-3} and of 3 Bq m^{-3} were measured at 10 m and at 100 m, respectively. This, as in autumn, could be explained by the frequently occurring stable atmosphere during winter which allows level separation and radon accumulation in the lower layers of the atmosphere. In addition to this, there is the contribution of advected radon from either Sierra Morena or inland regions channelled during nighttimes down the Guadalquivir valley. No significant occurrence of calm conditions, with wind speeds lower than 1 m s^{-1}, were observed at

the *El Arenosillo* station during winter. There were a large number of occurrences for wind velocities between 1 and 3 m s^{-1} from all wind sectors. These low wind cases show radon concentration observations significantly similar, as illustrated in Figure 7.4. Average radon concentrations of 3 Bq m^{-3} at 10 m and 2 Bq m^{-3} at 100 m were measured. These low average concentrations, related to low wind speed, could be essentially due to a local distribution from the *El Arenosillo* soil with a radon flux of 4 Bq m^{-2} h^{-1}.

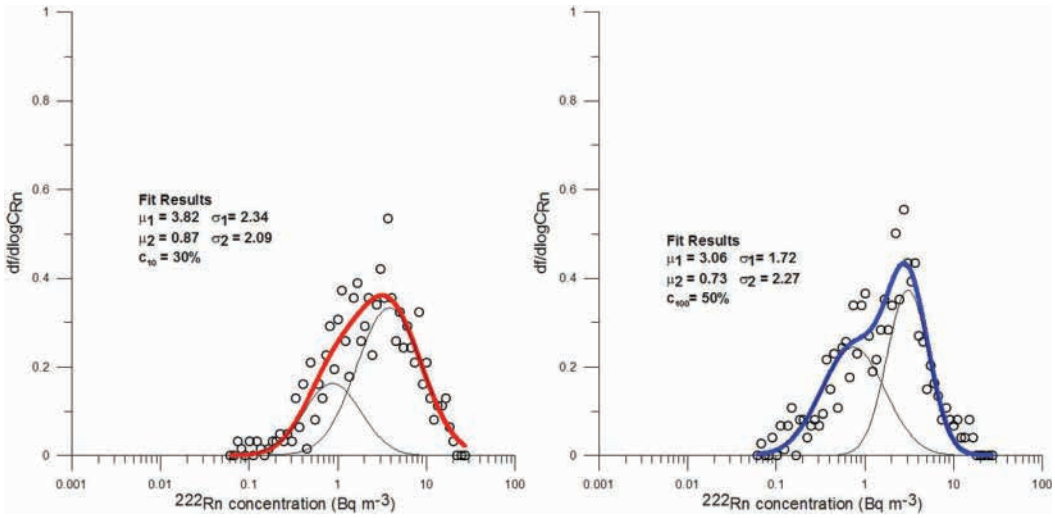

Figure 7.5: Bimodal lognormal distribution of radon concentration measurement at *El Arenosillo* station during winter at 10 m (left) and at 100 m (right).

The geometric mean $\mu_{1,10}$ of radon concentration data at 10 m is 3.82 Bq m^{-3} with a standard deviation $\sigma_{1,10} = 2.34$ and $\mu_{1,100} = 3.06$ with $\sigma_{1,100} = 1.72$ at 100 m, Figure 7.5. These radon concentrations are not as high as would be expected for winter and could be explained by the high frequency of radon-poor air masses coming from the Atlantic Ocean and from South Portugal during this season, as observed in Figure 7.4, which contribute to the total seasonal average. The small Gaussian distributions due to pure sea air masses are 30 % and 50 % of the total distribution area, Figure 7.5. The geometric means are $\mu_{2,10} = 0.87$ Bq m^{-3} and $\mu_{2,100} = 0.73$ Bq m^{-3} at 10 m and at 100 m, respectively.

7.3.3 Spring Season

Most radon concentration measurements were made with the wind coming from the SWW-NW sector with a wind velocity of up to 7 m s^{-1}, which includes the South Portugal area, Figure 7.6. Average radon concentrations at both heights are similar and quite low, ranging between 0.5 and 1 Bq m^{-3}. These low average results could be explained by well-

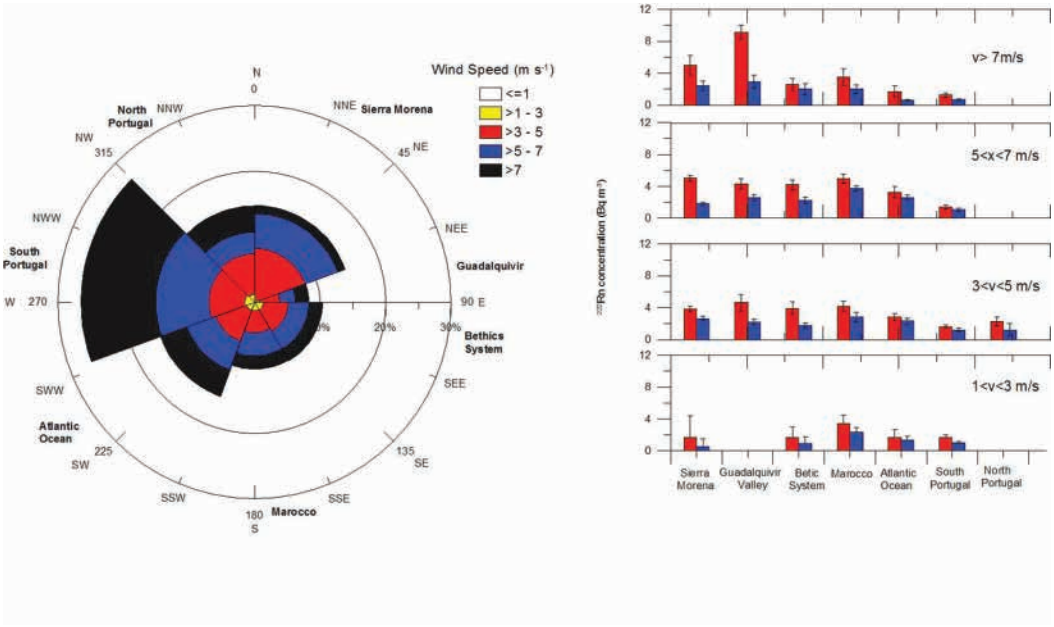

Figure 7.6: Wind-rose and ^{222}Rn concentration at 10 m (white bar) and 100 m (gridded bar) during spring.

mixed radon-poor air masses in strong wind coming from the Atlantic Ocean and passing over South Portugal. The radon flux is lower than 5 Bq m^{-2} h^{-1}, as shown in Figure 6.4 and as was discussed in the Section 7.3.1. The average relative radon contribution increase for the Moroccan sector which, as explained in the Section 7.3.1, could be due to the presence of the Atlas Mountains, which is a high radon flux area, Figure 7.6. Furthermore, during the spring season, the average radon concentration values in the Moroccan sector are higher than during winter. This result could be due to an increase in temperature in spring in this zone and a consequent radon flux increase from this area. In addition to this, spring is an unstable season and thus nighttimes inversions or semi-permanent inversions do not occur as often as in winter and autumn.

The geometric mean $\mu_{1,10}$ of radon concentration data at 10 m is 3.60 Bq m^{-3} with a standard deviation $\sigma_{1,10} = 2.18$. The geometric mean is $\mu_{1,100} = 2.05$ with $\sigma_{1,100} = 2.20$ at 100 m, Figure 7.7. These average radon concentrations indicate good atmospheric layer separation during this season. The small Gaussian distributions have areas of 10 % and 4 % of the total bimodal area with similar geometric means of $\mu_{2,10} = 0.73$ Bq m^{-3} and $\mu_{2,100} = 0.20$ Bq m^{-3} at 10 m and at 100 m, respectively, Figure 7.7.

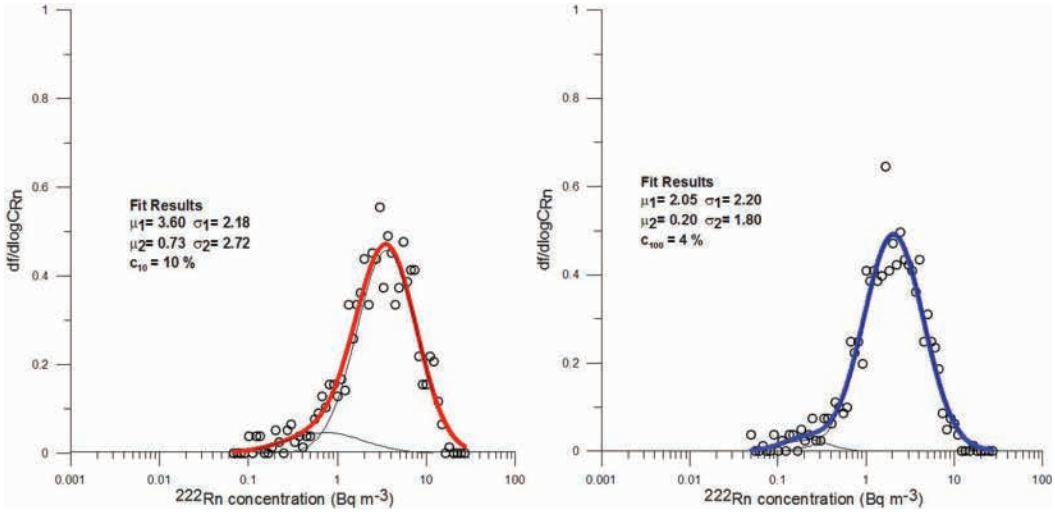

Figure 7.7: Bimodal lognormal distribution of radon concentration measurement at *El Arenosillo* station during spring at 10 m (left) and at 100 m (right).

7.3.4 Summer Season

Results for average radon concentrations at the *El Arenosillo* station together with local wind conditions for summer show the predominant occurrence of wind coming from ocean during this season with air masses poor in radon and well-mixed, Figure 7.8. During most of the measurements the wind came from the SWW-NWW direction, which represents the Atlantic Ocean and South Portugal areas. Wind speed ranged between 1 and 5 m s^{-1} during the summer. The average radon concentration is 2 Bq m^{-3} at both heights. This last result shows good layer mixing conditions and incoming air poor in radon. Low average radon concentrations are in agreement with what would be expected for summer when the wind comes mainly from the sea. A relative increase of radon concentration was measured, as was seen for each season, when the wind came from Morocco with a speed of 3-5 m s^{-3}. There were no significant cases of high wind speed in this season, which are more relevant when wind flows from the first quadrant, as explained previously.

The geometric mean $\mu_{1,10}$ of radon concentration data at 10 m is 2.64 Bq m^{-3} with a standard deviation $\sigma_{1,10} = 1.86$. $\mu_{1,100}$ is 2.41 with $\sigma_{1,100} = 1.88$ at 100 m, Figure 7.9. These values indicate really good statistics for this season and a strong mixing layer, as was expected for an unstable summer. The small Gaussian distributions due to radon concentration measured when wind came from the sea are also reported. Their total areas are only 5 % and 1 % of the total distribution areas. The geometric means are $\mu_{2,10} = 0.62$ Bq m^{-3} with a standard deviation of 1.35 at 10 m and $\mu_{2,100} = 0.35$ with a standard deviation of 1.35 at 100 m. A summary of results is shown in Table 7.1.

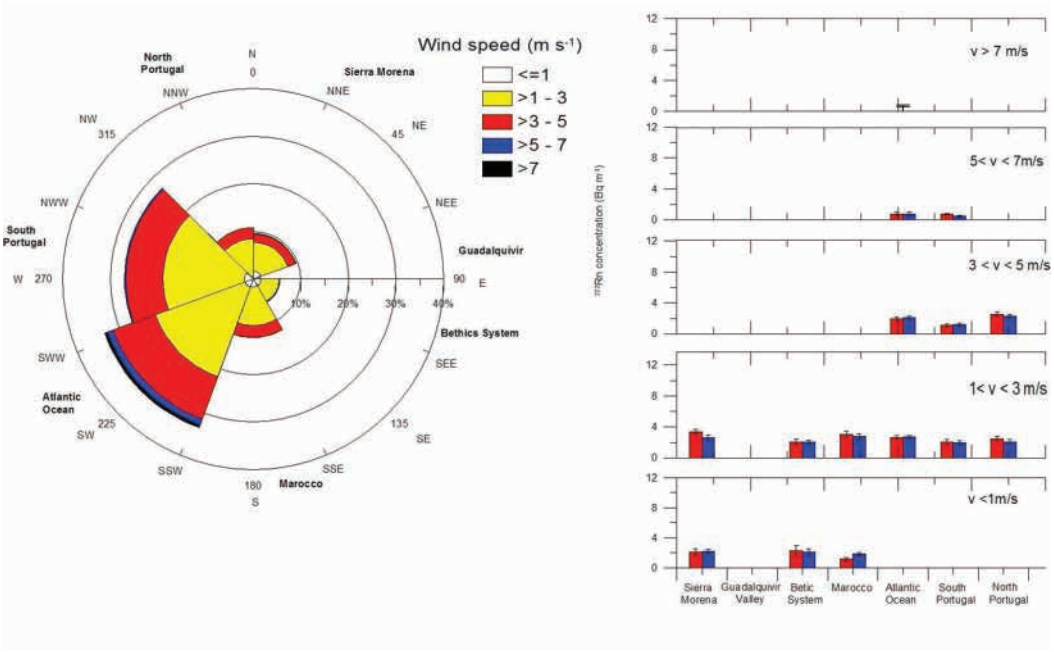

Figure 7.8: Wind-rose and ^{222}Rn concentration at 10 m (white bar) and 100 m (gridded bar) during summer.

Table 7.1: Bimodal Lognormal Distributions of ^{222}Rn concentration at *El Arenosillo* station

	Bimodal Lognormal Distribution at 10 m					Bimodal Lognormal Distribution at 100 m				
	$\mu_{1,10}$	1,10	$\mu_{2,10}$	$\sigma_{2,10}$	c_{10}	$\mu_{1,100}$	$\sigma_{1,100}$	$\mu_{2,100}$	$\sigma_{2,100}$	c_{100}
Autumn	4.48	2.03	0.71	1.31	4	2.93	1.98	0.55	2.07	5
Winter	3.82	2.34	0.87	2.09	30	3.06	1.72	0.73	2.27	50
Spring	3.60	2.18	0.73	2.72	10	2.05	2.20	0.20	1.80	4
Summer	2.64	1.86	0.62	1.35	5	2.41	1.88	0.35	1.35	1

The geometric mean ($\mu_{i,j}$) for each lognormal distribution due to the total radon concentration measurement (i=1) and due to radon concentration measurement coming from the sea (i=2) and its geometric standard deviation ($\sigma_{i,j}$) is reported for each season and for each measurement height (j=10 or j=100). Furthermore, the percentage of area c (%) of the smaller lognormal distribution with respect to the larger area is given for all bimodal distributions.

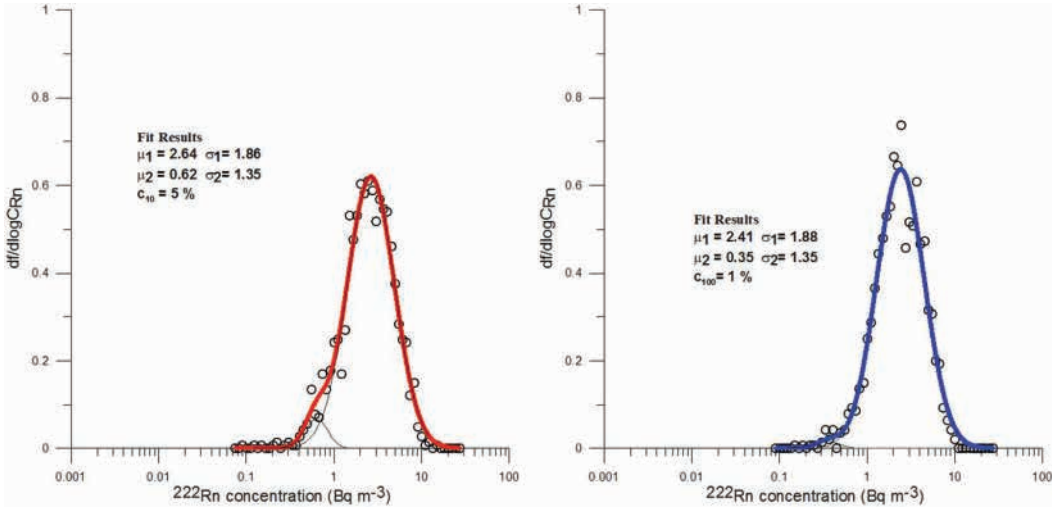

Figure 7.9: Bimodal lognormal distribution of radon concentration measurement at *El Arenosillo* station during summer at 10 m (left) and at 100 m (right).

7.4 Daily ^{222}Rn concentration

The daily cycles of ambient radon concentration at the *El Arenosillo* station were analyzed for each season and at two different measurement heights. Results are presented in Figure 7.10, where the hourly evolution of average radon concentrations throughout the day at 10m (solid line) and at 100m (dashed line) are given. Figure 7.10 shows that ^{222}Rn concentration at 10m is normally higher than at 100m, as expected (Levin et al, 2002). Radon concentration behaviour at 10 m shows a well-defined diurnal cycle for each season with variable amplitude, characterized by an accumulation of radon during the night and a subsequent dilution during daytime (Stull, 1988). During the night a shallow stable layer develops close to the ground due to the faster cooling of the surface of the Earth. Radon exhaled from the soil then accumulates in the lower layers of the atmosphere. After sunrise, and until sunset, radon concentration in the atmosphere decreases due to the development of a deep mixing layer (Zanetti, 1990; Vinuesa et al, 2007; Vinuesa and Galmarini, 2007). In addition to the local contribution, and the accumulation during nighttimes, there is also the contribution of the advected radon during the shallow nighttimes flows that occurs in the Guadalquivir valley. This carries the radon exhaled inland towards the station contributing to the lower level measurements.

Average ^{222}Rn concentrations at 100 m do not normally have a pronounced diurnal cycle, as opposed to those at 10m, as can be seen in Figure 7.10. This lack of a cycle at 100 m is due to the fact that it is above the inversion that defines the nocturnal stable boundary

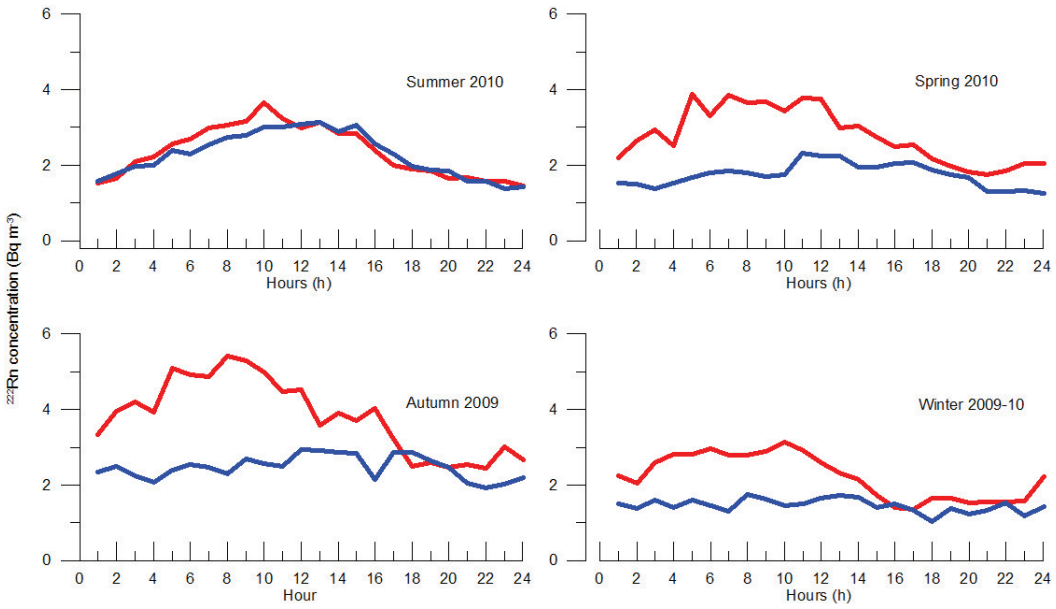

Figure 7.10: Hourly (UTC) evolution of ^{222}Rn concentration at the *El Arenosillo* station at 10m (solid line) and at 100m (dashed line).

layer (SBL). At this height, there is usually a reservoir layer in between the nocturnal boundary layer and the top of the daily mixing layer. Radon which reaches the mixing layer on the previous day may be kept in this layer and effectively preserved through the night and is only influenced by the combined effect of the decay and sink process (Vinuesa et al, 2007).

The Figure 7.10 shows that highest average radon concentrations at 10m recorded during autumn and spring, shown in Table 7.1, which could indicate a lower stable atmospheric layer during the night and air masses transporting radon exhaled from distant sources during the day, as has been detailed above. Daily average radon concentrations at 10m observed during winter are not as high as expected for this season. This could be explained by a considerable frequency of radon-poor air masses coming from the Atlantic Ocean and from South Portugal, as has been shown in Figure 7.4. On the other hand, the unstable summer atmosphere with strong mixing during the day shows no significant difference between radon concentrations at either height and a cycle that is not so pronounced in Figure 7.10. Most of the air masses in the summertime come from the sea, with well mixed and radon-poor air.

7.5 Specific Conclusions

Atmospheric ^{222}Rn concentration behaviour has been characterized at the *El Arenosillo* station on the south-west coast of Spain. The work has been done on a 100 m meteorological tower where two ARMON radon monitors for continuous gas concentration measurement were installed. The influence of local wind speed and direction on radon concentrations observed at 10 m and a 100 m, at the *El Arenosillo* station, were studied and an analysis of seasonal behaviour and diurnal cycle was done.

The 100-m-high tower provides an opportunity to carry out a qualitative analysis of possible distant radon contribution sources using hourly radon concentrations at 10 m and at 100 m with the wind conditions at the *El Arenosillo* station. Indeed, this analysis has pointed out several possible sources of high radon flux close to the *El Arenosillo* station in the Sierra Morena range. A remote eventual source has also been found in the Moroccan area. Furthermore, the significant contribution of the Guadalquivir Valley as a channel of air masses coming from inland regions with high radon flux has been studied. A significant difference was observed for average radon concentration at both heights when wind flows from the M-NE quadrant, which includes the Sierra Morena, the Guadalquivir Valley and the Bethics systems, also with high speeds. This could prove the existence of an important advected contribution at the lower level during the nocturnal hours along the southwest-northeast Guadalquivir depression axis could help to explain these previous cases.

The *El Arenosillo* tower also offers the opportunity to study the hourly variation of atmospheric radon at 10 m and at 100 m which allows meteorological and atmospheric studies. The diurnal cycle of ambient radon for most of the seasons is in agreement with past studies. An unusual hourly evolution of radon concentrations was observed during the summer, when radon concentrations at 10 m and at 100 m show similar values, but with a diurnal cycle. Finally, the characteristic air masses transport behaviour and itsinfluence on hourly radon concentrations observed during this study at *El Arenosillo* station will be analyzed by the atmospheric transport model HYSPLIT4 in the following chapter.

Chapter 8

Qualitative analysis of radon transport patterns to the *El Arenosillo* station

8.1 Introduction

An atmospheric radon concentration analysis of measurements at the *El Arenosillo* station done based on one year of continuous measurements as it has been presented in the previous chapter. The aim of this study was to acquire knowledge of the seasonal and diurnal/nocturnal behaviour of radon gas at a coastal site such as the *El Arenosillo* station and at different heights. As previously discussed, several possible radon source regions have been set up; the Morocco area, to the South of the *El Arenosillo* station, 300 km away; the Bethics System 110 km East from the *El Arenosillo* station and the Sierra Morena, which is to the North, 150 km away, as can be seen in Figure 7.1. This previous study was carried out using meteorological measurements obtained at 10 m above sea level which actually only give information on a local scale. The results need now to be confirmed by an integration with meteorological information on a regional scale, which definitively influences the air masses movement. Indeed, the atmospheric transport patterns that may occur in one region are defined by the main synoptic situations affecting it and its local topography and surface meteorological measurements could not be enough to study such complex situations as has been shown elsewhere (PhD thesis Arnold, 2009; Arnold et al, 2010; PhD thesis López-Coto, 2011; Crawford et al, 2009).

Within this framework, some specific episodes of atmospheric radon concentration, at the *El Arenosillo* station, have been analyzed in this chapter by back-trajectory analysis with the Lagrangian model HYSPLIT4 in order to visualize the air masses origin under specific synoptic conditions and to identify the possible radon transport pathways at the *El Arenosillo* station. In Chapter 2, we commented on how back trajectories have been

widely used to infer geographic regions that contribute to pollution events (Stohl, 1996; Stohl et al, 2003; Considine et al, 2005; Seibert et al, 1998, Stach et al, 2007; Cecchi et al, 2007). Furthermore, it has been also pointed out how the strong vertical gradient of atmospheric radon at coastal sites makes it an ideal indicator for processes in the atmospheric boundary layer (ABL). In addition, the great contrast between terrestrial radon flux and oceanic radon flux, which is basically taken equal to zero, is really useful to differentiate between oceanic and continental air masses (Iida et al, 1996; Pearson and Moses, 1966; Ikebe, 1970).

The present qualitative analysis aims to confirm the radon source regions which have been found out during the experimental radon characterization of the *El Arenosillo* station presented in the previous chapter. Furthermore, the study of back trajectories and wheatear maps can help to better understand transport of radon under different synoptic situations at *El Arenosillo* station.

8.2 Material and Methods

8.2.1 Back Trajectory Analysis with the HYSPLIT4 model

In this chapter the dispersion model HYSPLIT4 has been used in order to define the origin of air masses coming to the *El Arenosillo* station and their possible relation with observed highest/lowest radon concentration episodes. Each back trajectory was calculated using the meteorological file GDAS as an input file. The HYSPLIT model, version 4, and the GDAS file have already been presented in Chapter 2 of this thesis. In this section the use and limitations of the back trajectory analysis made by HISPLIT4 model will be presented.

The reliability of a trajectory calculation depends also on the spatial resolution of the used input file (PhD thesis Arnold, 2009). It is important to take into account the relation between the spatial evolution of the meteorological files and the spatial covering of atmospheric movement under study. In our case, GDAS files have a spatial horizontal resolution of 111 km (1x1 degree) and they can be enough for carrying out a qualitative analysis of radon transport on a synoptic scale. Furthermore, the GDAS files have 23 pressure levels and the first 12 levels are under 500 hPa. The vertical information on meteorological parameters in the GDAS files, for the El Arenosillo station area, have been validated by HYSPLIT4 trajectories by Hernandéz-Ceballo, 2011 in his doctorate research. A comparison between meteorological parameters reported in the GDAS file and meteorological parameters measured during 45 radio sounding campaigns done at the *El Arenosillo* station was carried out by Hernandéz-Ceballo. Wind speed and wind directions were compared in this work at 200 m, 800 m, 1500 m and 3000 m heights. The total vertical temperature profile was also compared. However the correlation between GDAS data and experimental values becomes better at high level and during nocturnal

hours, Hernandéz-Ceballo concluded that correlation of GDAS data and radio sounding values is still valid at 200 m and above and during diurnal hours.

The back trajectories in the present analysis, as well as in the PhD thesis of Hernandéz-Ceballo, 2011 were calculated with the kinematic method (3D). This method uses the meteorological model vertical velocity fields and allows a better description of the air mass pathways to be achieved. Back trajectory length was of 5 days in order to analyze synoptic air mass movement and to reduce the model uncertainties (Draxler et al, 2009). Furthermore, the back trajectories were calculated at different height levels: 300 m, 500 m, 1000 m, 1500 m and 3000 m. The lowest level of 300 m was used in order to ensure a model that is representative at lower atmospheric layers which could be influenced by the topography (PhD thesis Hernandez-Ceballo, 2011). Finally, the highest levels of 1500 m and of 3000 m were used for analysis of high atmospheric layers and to observed their separation during different episodes. For each radon episode, two back trajectories per day were calculated and each back trajectory started at observed maxima/minima radon concentration time (UTC). Furthermore, for each episode the corresponding weather charts obtained from the archive of the Wetterzentrale (www.wetterzentrale.de)
are also given in order to better understand the possible air masses transport patterns.

8.2.2 Episodes Description

The episodes selected for this study present the most frequently occurring synoptic conditions observed at the *El Arenosillo* station. This high occurrence of air masses was found out during experimental characterization of radon behaviour in this area as presented in the previous chapter. The high occurrence of several type of air masses has been also confirmed by Hernandéz-Ceballo et al, 2011 who performed a meteorological characterization of the *El Arenosillo* station by a cluster analysis of 7000 back trajectories with the HYSPLIT4 model during the period 1997-2007 (PhD thesis Hernandez-Ceballo, 2011). Following the characterization of radon behaviour presented in the previous chapter of this thesis and the meteorological characterization done by Hernandéz-Ceballo, 2011, it is clear that the most frequent air masses coming to *El Arenosillo* station proceed from the Atlantic/North American region, from the North of Europe, from the Mediterranean area and from the North of Africa.

An example for each most frequent radon episodes was selected for this analysis related to high/low observed radon concentration during the measurement period and both the pronounced and not so pronounced relative differences between radon concentration at 10 m and at 100 m heights. Back-trajectory analysis with a GDAS file resolution of 111 km does not have sufficient resolution on the vertical and horizaontal scale in order to explain the different radon behaviour at 10 m and at 100 m. However, this analysis is useful to give a hint of synoptic air mass movement for radon-rich and radon-poor air masses reaching the *El Arenosillo* station. Furthermore, the measured atmospheric radon concentrations

at 10 m and at 100 m levels have been used in order to obtain more informations about mixing layers and the depth of the nocturnal stable layer.

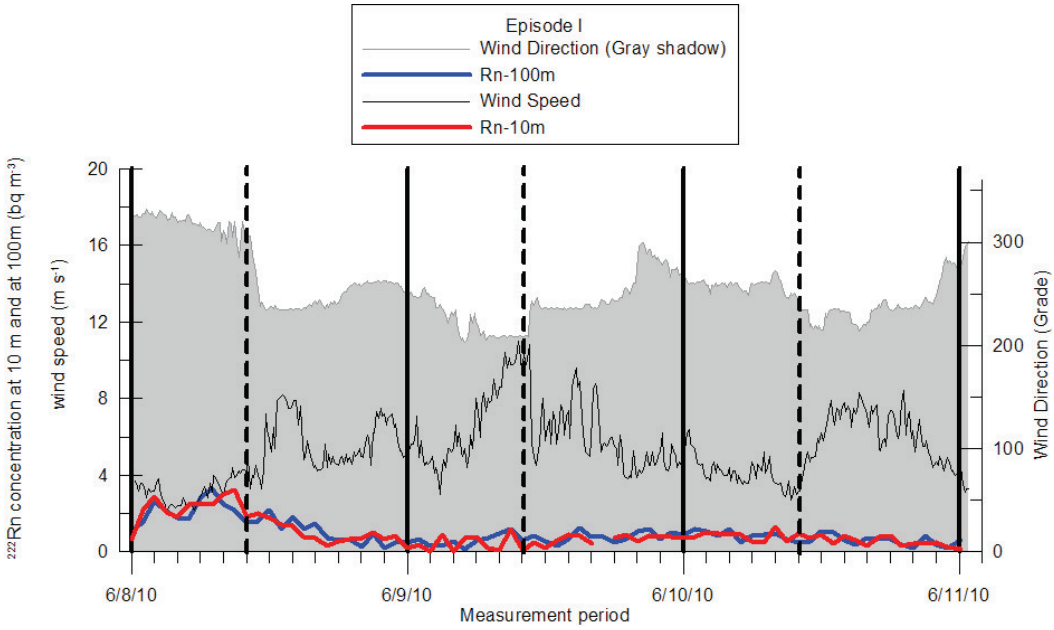

Figure 8.1: ^{222}Rn concentrations measured at 10 m (red line) and at 100 m (blue line) heights from the 8^{th} to 11^{th} of June 2010 at *El Arenosillo* station. Experimental values of wind direction and wind speed at 10 m height are also reported.The continuous and dotted lines represent the maxima and minima atmospheric radon concentration in each day, rispectively.

Episode I is presented in Figure 8.1, It occurred during June 2010 which is part of the summer season. The summer season, as explained in the previous chapter, is characterized by the presence of air masses coming from the Atlantic Ocean. A small initial increase is observed in the radon concentration in Figure 8.1 during the 8^{th} of June where values at both levels reach on average 2 Bq m^{-3} and the wind speed is of about 3 m s^{-1}. Figure 8.1 shows that during the rest of the episode the average radon concentration is very low, of around 0.8 Bq m^{-3} and t*El Arenosillo* ind speed is quite high with an average value of 6 m s^{-1}. The ^{222}Rn concentrations at both heights are quite similar and there is an absence of a good representative diurnal cycle for radon which is usually observed (Levin et al, 2002; Zahorowski et al, 2004; Lambert et al, 1970) with maxima concentrations seen during the nocturnal period and with minima concentrations measured during sunny hours, as has been explained above. Experimental observations show a meteorological wind direction between 200-300 degrees which seems to coincide with the Ocean area and the South of

Portugal area. All these observations confirm the arrival of radon-poor air masses coming from the Atlantic Ocean at high speed, which can drastically scavenge the local radon.

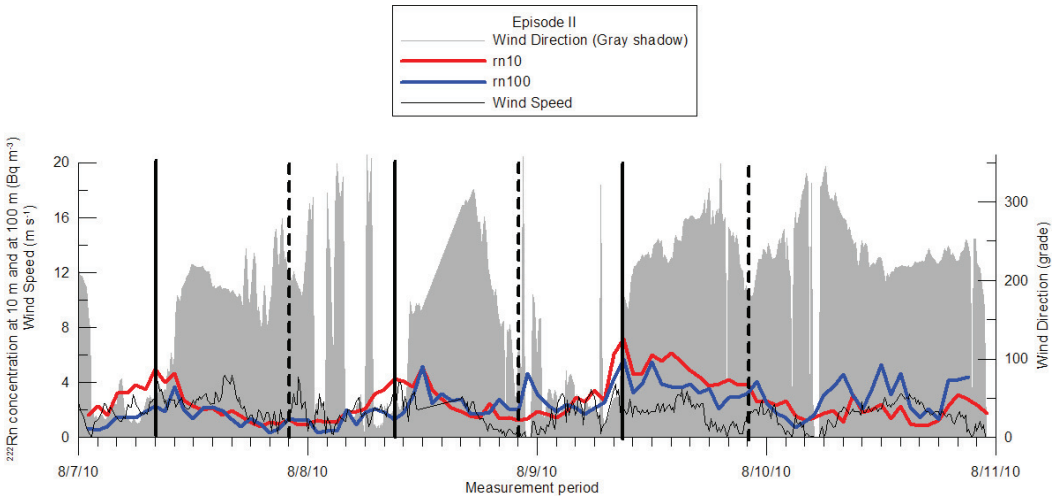

Figure 8.2: ^{222}Rn concentrations measured at 10 m (red line) and at 100 m (blue line) heights from the 7^{th} to 11^{th} of August 2010 at the *El Arenosillo* station. Experimental values of wind direction and wind speed at 10 m height are also reported. The continuous and dotted lines represent the maxima and minima atmospheric radon concentration for each day, respectively.

Episode II is presented in Figure 8.2. It was recorded in August 2010 during the summer season at the El Arenosillo station with a well-mixed layer as discussed in the previous chapter. Figure 8.2 shows that radon concentration at both levels is still quite similar during this episode and it increases to an average value of 3 Bq m^{-3} with really low wind speeds on average of 2 m s^{-1}. The diurnal cycle of radon is finally evident in this episode and it is in inverse relation with wind speed variation as would be expected (Levin et al, 2002; Zahorowski et al, 2004). The wind direction is between 50 and 200 degree which seems to come from the Ocean area and from the Bethics Area. Figure 8.2 shows a cumulative radon concentration during the nocturnal hours (black line) which indicates stable conditions. The atmospheric ^{222}Rn concentration at 10 m height is higher than the concentration at 100 m, during the night. This could be due to the radon accumulation in the nocturnal boundary layer as it was previously explained in Chapter 7.

Episode III is presented in Figure 8.3. It was recorded in March 2010,which is part of the spring season at the El Arenosillo station with a transition condition between winter and summer and an homogeneous wind rose similar to the one presented in the previous chapter for this season. Figure 8.3 shows that the diurnal cycle of radon concentration is much more evident now especially at 10 m height which could indicate a higher actvity

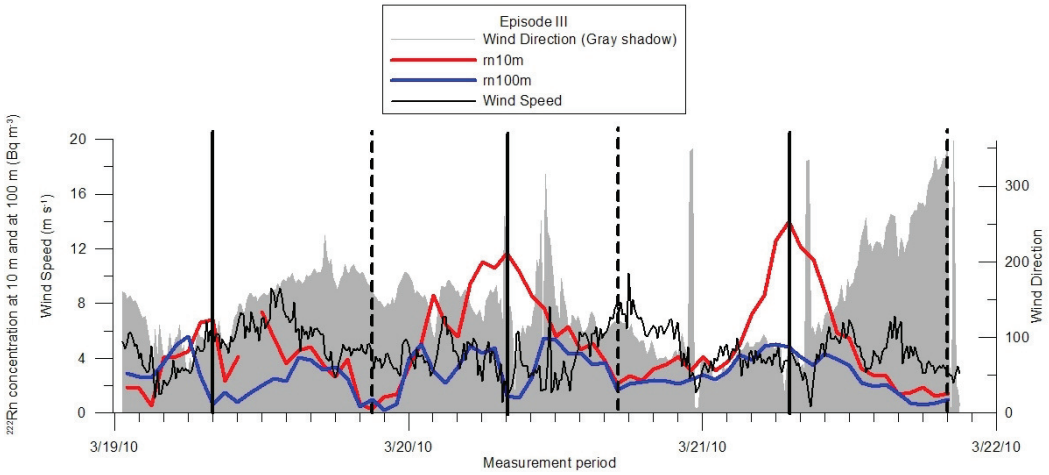

Figure 8.3: ^{222}Rn concentrations measured at 10 m (red line) and at 100 m (blue line) heights from the 19^{th} to 22^{th} of March 2010 at the *El Arenosillo* station. Experimental values of wind direction and wind speed at 10 m height are also reported. The continuous and dotted lines represent the maxima and minima atmospheric radon concentration for each day, respectively.

of tranported radon or a deeper nocturnal boundary layer (Galmarini, 2006; Vinuesa and Galmarini, 2007). The absolute difference between the radon concentration at both levels is more pronounced in the accumulation period as would be expected (Galmarini, 2006; PhD thesis Arnold, 2009). The wind speed is on average between 4 and 5 m s^{-1} and the wind direction is between 100 and 200 degree which indicates the origin of the air masses is the North of Africa and the Bethics System, including the Strait of Gibraltar. The wind speed values observed during this episode confirm that the air mass coming from the Morocco area could be rich in radon.

Episode IV is presented in Figure 8.4. It was recorded in November 2009, which is part of the winter season at the *El Arenosillo* station, as shown in the previous chapter. Figure 8.4 shows that the diurnal cycle of radon cncentration is visible. The absolute difference between the radon concentrations at both levels is more pronounced in the accumulation period which coincides as would be expected. The wind speed is on average 5-6 m s^{-1} and the wind direction is between 0 and 70 degrees which indicates it comes from the North, e.g. from the Sierra Morena area.

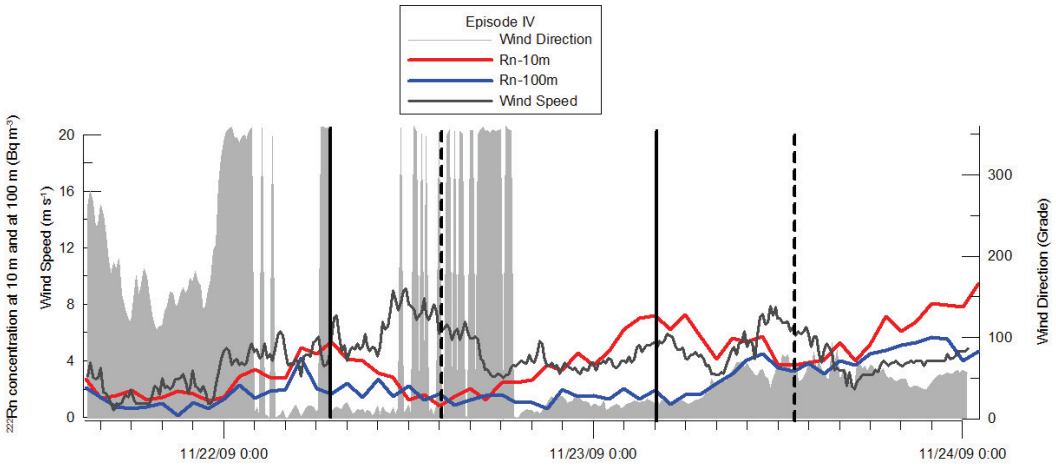

Figure 8.4: ^{222}Rn concentrations measured at 10 m (red line) and at 100 m (blue line) heights from the 21^{st} to 24^{th} of November 2009 at the *El Arenosillo* station. Experimental values of wind direction and wind speed at 10 m height are also reported. The continuous and dotted lines represent the maxima and minima atmospheric radon concentration for each day, respectively.

8.3 Back-trajectory results and discussion

8.3.1 Episode I: June 2010

In the metereological study performed in the PhD thesis of Hernandéz-Ceballo, 2011 at the *El Arenosillo* station, it has been found that the predominant synoptic situation, when air masses come from the Atlantic Ocean, is represented by an important advection from the West to the South-East. This advection is mainly influenced by the North Atlantic (Subtropical) High/Anticyclone, a large subtropical semi-permanent centre of high atmospheric pressure found near the Azores in the Atlantic Ocean. In the upper part of Figure 8.5 and Figure 8.6 the Weather charts at 500 hPa levels by the WetterZentrale, are shown for the studied episode. Usually in summer, as well as during this episode, the central pressure lies around 1025 mbar (hPa) and moves North towards the Iberian Peninsula, forcing advection of air to the South of the Iberian Peninsula (PhD thesis Hernandez-Ceballo, 2011).

Figures 8.5 and 8.6 show the back-trajectory analysis for this episode. It can be seen how the air masses come from the Atlantic Ocean and reach the *El Arenosillo* station passing over the South of Portugal. Air masses coming form the Ocean are well mixed and poor in radon, as it decays along its route from North America to the Iberian Peninsula, and this coul. This fact could help to explain the really low concentration observed in this episode.

The low atmospheric radon concentration measured at the *El Arenosillo* station may be due to a contribution from the area of South of Portugal. Indeed the back trajectories present air masses moving quickly over this area and they could take up the low radon exhaled from South Portugal. However, this phenomenon cannot be studied in dettail with the HYSPLIT4 using low spatial resolution metereological files such as GDAS data. The back trajectories at different levels seem to be quite similar and this could confirm the well mixed condition of air masses and explain the similar radon concentration observed at 10 m and at 100 m heights which cannot be simulated but could be included in the well-mixed conditions.

During this episode there is no evidence of a well-defined diurnal radon cycle and, actually, back trajectories do not show any difference during the day and nighttime analysis. Nevertheless, the day 8th June 2010 shows a higher radon concentration at both levels than during the other days. This difference could be explained by looking at back-trajectory results of Figure 8.5. It is seen how air masses pass over a large part of the North of Portugal which presents, as reported in the European Radon Flux in Figure **??** a ^{222}Rn flux of about 70-90 Bq m^{-2} h^{-1}. Furthermore, Figure 8.5 shows that the air masses remain over the North of Portugal for about 12 hours. This does not happen during others episode days where air masses quickly pass over this soil area. Finally, the back trajectory in Figure 8.5 shows that the vertical wind component is below 500 m height. All these previous observations could mean that air masses passing slowly over the North of Portugal and at a low level could be able to uptake and transport the radon exhaled from the land surface of the North of Portugal.

8.3.2 Episode II: August 2010

From the study carried out by Hernandéz-Ceballo, 2011 it have been observed the conditions, which allow air masses to come from Mediterranean areas, are usually linked to two synoptic situations (PhD thesis Hernandéz-Ceballo, 2011). One of these conditions is presented in Figure 8.7 for the selected episode. The presence of an anticyclone over the English Channel reached central Europe together with the existence of a low isobaric gradient in the whole Mediterranean area which helped the development East-West flows.

The back trajectories in Figure 8.7 show how air masses reaching the *El Arenosillo* station not only pass over the Bethics System, as can be seen from surface measurement of meteorological parameters, but air patterns also include the Pyrenees Mountain region. There is an uncoupling between atmospheric layers, started below 1000 m and layers above 3000 m heights. On the other hand, the back-trajectory patterns calculated during nocturnal and diurnal time do not show any significant difference for this episode. This means that the relative difference observed in the atmospheric radon concentration at 10 m during the nocturnal accumulation period and diurnal mixing period could be explained by the height of the nocturnal boundary layer. This cannot be investigated by back-trajectory analysis because a high spatial and temporal resolution is required.

8.3.3 Episode III: March 2010

The synoptic situation of air masses coming from the South of the Iberian Peninsula has usually been observed to be related with a central low pressure system to the southwest of the Peninsula (PhD thesis Hernandéz-Ceballo, 2011). Figure 8.8 represents the weather chart and the back-trajectories for the episode of March 2010. The weather chart shows a 1020 mbar pressure system centre and separated isobaric lines, which indicates low synoptic forcing. This low forcing allows the development of mesoscale phenomena. Looking at back-trajectory results for this period, it seems to be clear that there is a suspension of atmospheric air masses over the Atlas Mountain and a well mixed air condition at different levels. Furthermore, during the maximum radon concentration episode, shown in the central part of Figure 8.8 the back-trajectories at the lowest levels are below 500 m height. Finally, according to a recent study of the area of the Atlas Mountains there seems to be a high radon flux of about 150 Bq m^{-2} h^{-1} (Omori et al, 2009).

This could lead to the air masses remaining over the Atlas Mountains and uptaking the ^{222}Rn gas exhaled from the surface and transporting it over 300 km to the *El Arenosillo* station. This could be possibile due to the radon half life of 3.8 days which enables it able to travel for two days with a wind speed of 4 m s^{-1}, as observed at the *El Arenosillo* station and reported in Figure 8.3. Furthermore, the differences between the back-trajectory simulations during periods of maxima and minima in the observed radon concentration show that in the noctural period, which represents the maximum radon concentration measured at the *El Arenosillo* station, the back trajectories at the lowest level of 300 m are quite different from the others, which could be due to a very shallow nocturnal boundary layer thus making possible grater radon accumulation.

8.3.4 Episode IV: November 2009

The synoptic situation related to advection of air masses coming from the North are as always due to two main situations: the existence of a low pressure system over the United Kingdom and the presence of the high pressure system of the Azores, as it is presented in the upper part of Figure 8.9. The back-trajectory analysis in Figure 8.9 clearly shows the air mass pathway from the North but is not able to clarify the difference in radon concentration observed during the night time and the day time because of the low spatial/temporal resolution of the GDAS-HYSPLIT4 model. This process, which has been identified as one of the more frequent in the Guadalquivir Valley, as explained in the previous chapter, and needs to be studied in depth with a high spatial resolution meteorological model such as WRF, introduced in Chapter 1, as an input for the transport model HYSPLIT4.

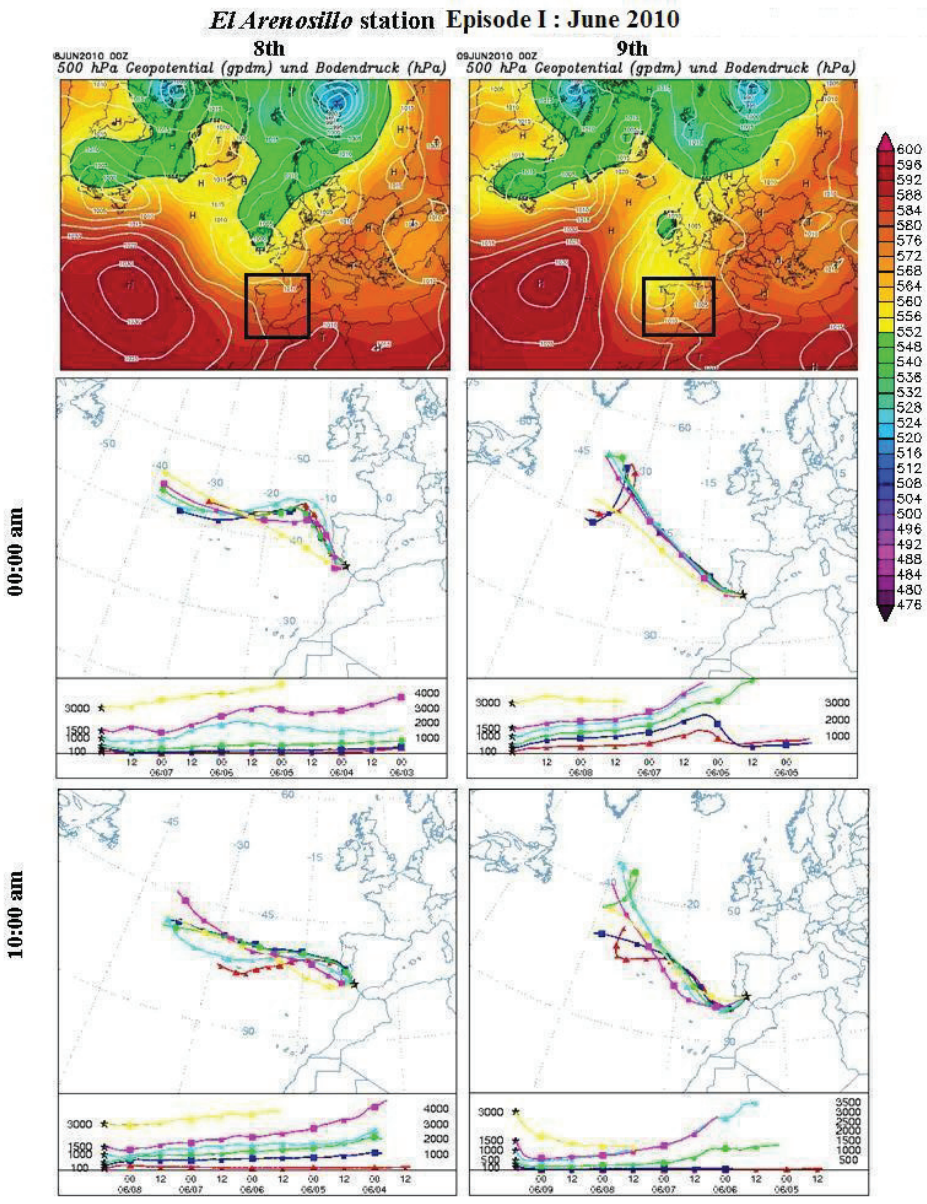

Figure 8.5: Back-trajectory analysis of air masses reaching the *El Arenosillo* station at 00:00 am and at 10:00 am on 8^{th} and 9^{th} of June 2010. Weather charts at 500 hPa levels by WetterZentrale are also shown.

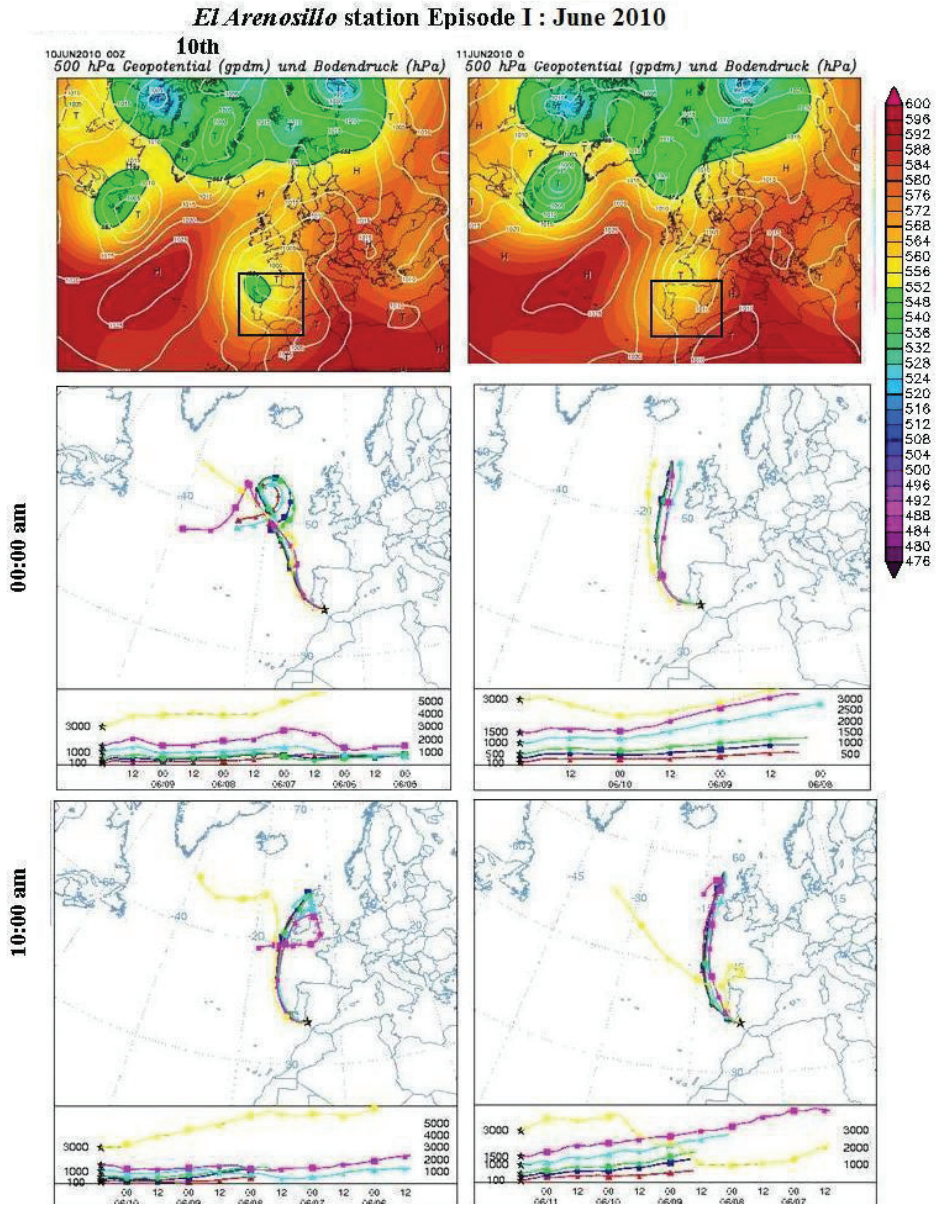

Figure 8.6: Back-trajectory analysis of air masses reaching the *El Arenosillo* station at 00:00 am and at 10:00 am on 10^{th} and 11^{th} of June 2010. Weather charts at 500 hPa levels by WetterZentrale are also shown.

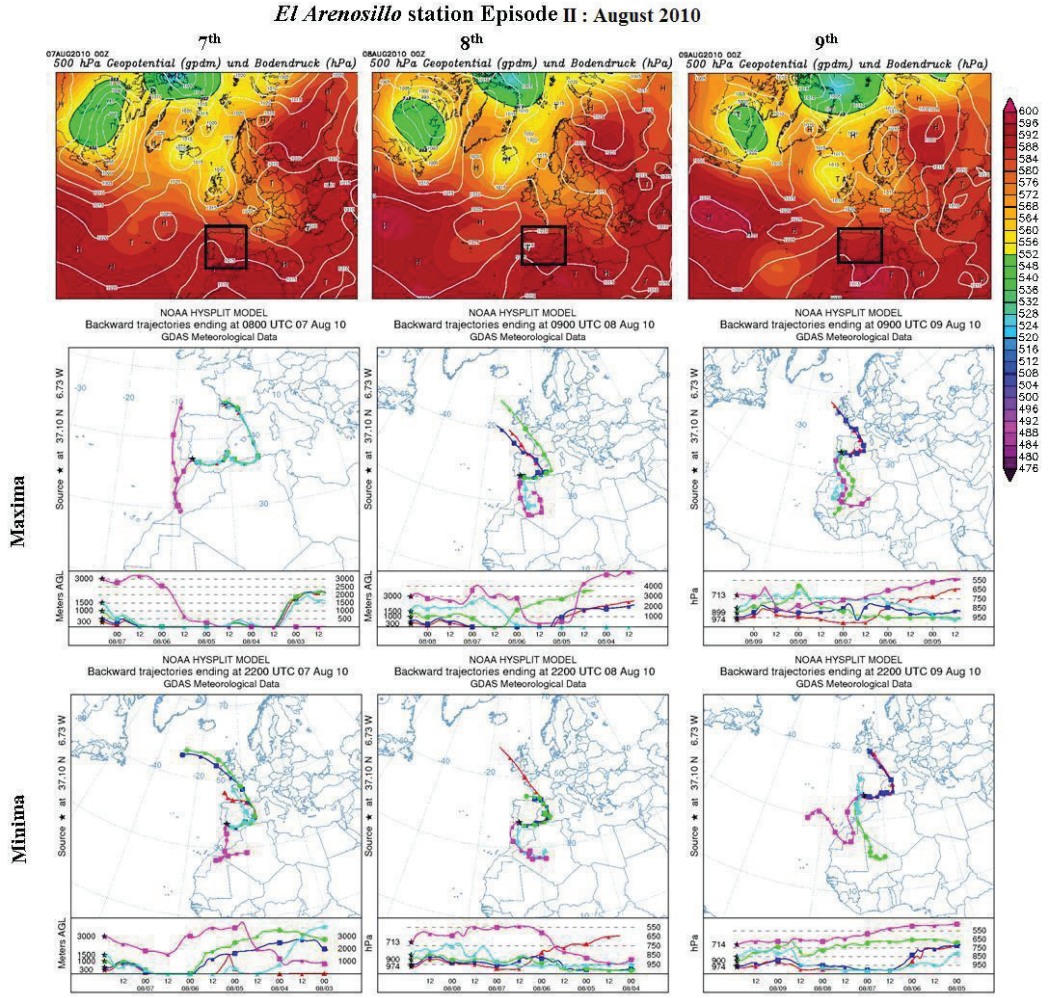

Figure 8.7: Back-trajectory analysis of air masses reaching the *El Arenosillo* station at nocturnal/diurnal time, corresponding with maxima/minima observed ^{222}Rn concentration, on 7^{th}, 8^{th} and 9^{th} of August 2010. Weather charts at 500 hPa levels by WetterZentrale are also shown.

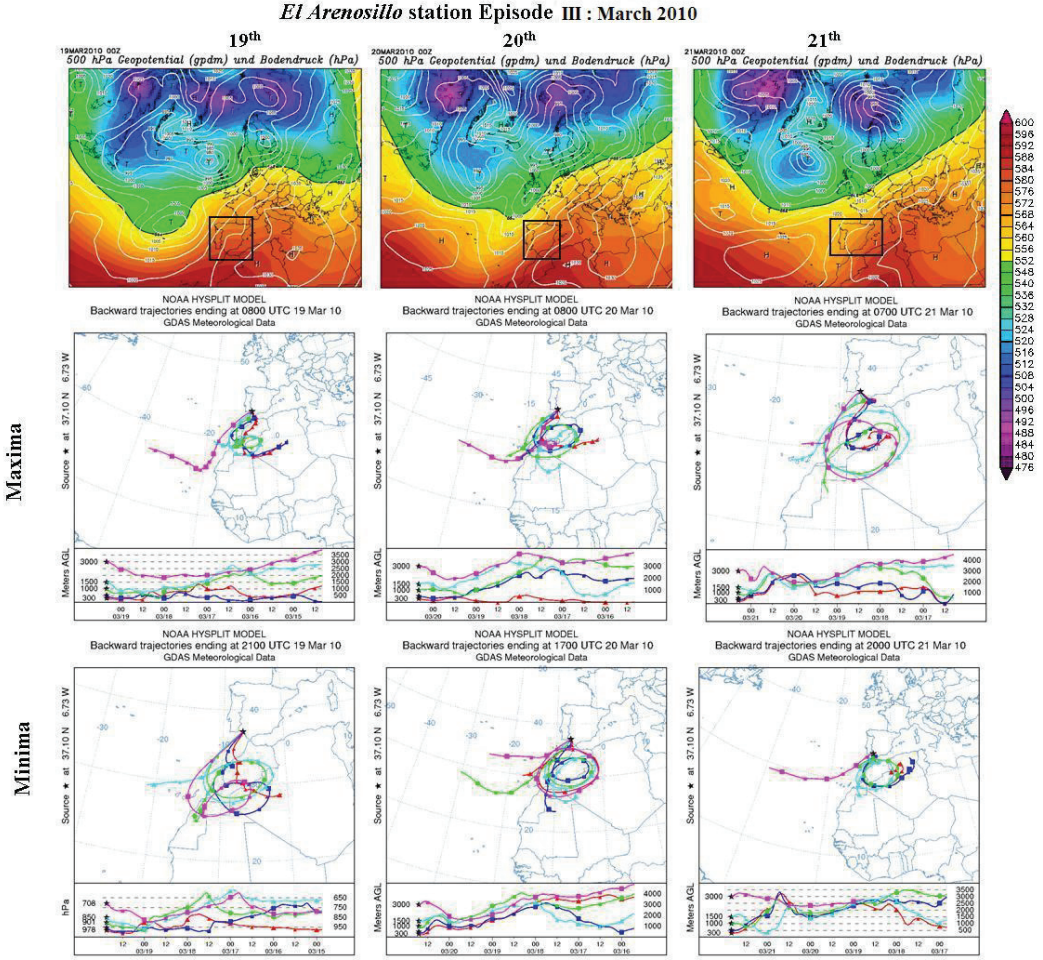

Figure 8.8: Back-trajectory analysis of air masses reaching the *El Arenosillo* station at nocturnal/diurnal time, corresponding with maxima/minima observed ^{222}Rn concentrations, on 19^{th}, 20^{th} and 21^{th} of March 2010. Weather charts at 500 hPa levels by WetterZentrale are also shown.

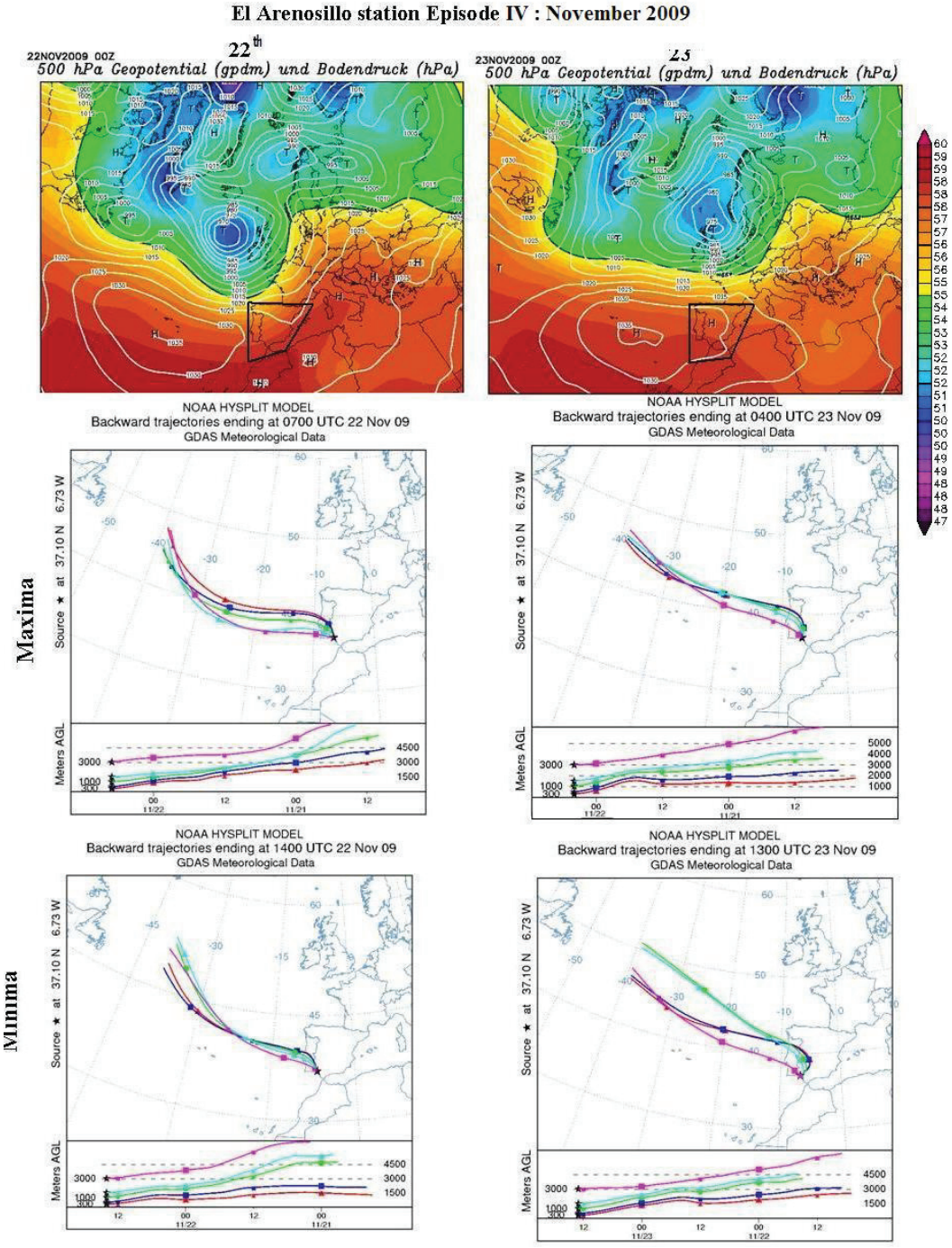

Figure 8.9: Back-trajectory analysis of air masses reaching the *El Arenosillo* station at nocturnal/diurnal time, corresponding with maxima/minima observed ^{222}Rn concentrations, on 22^{th} and 23^{th} of November 2009. Weather charts at 500 hPa levels by WetterZentrale are also shown.

8.4 Specific Conclusions

The experimental analysis of atmospheric radon behaviour at the *El Arenosillo* station performed in the previous Chapter 7 has pointed out the existence of specific radon-poor and radon-rich regions where the air masses generally come from. This chapter describes a back-trajectory analysis done using the transport model HYSPLIT4 with GDAS files as metereological input for four of these radon episodes in order to confirm the fact that air masses come from specific sectors and to show the poor/rich radon concentrations transported and measured at the *El Arenosillo* station. The back-trajectories for each radon episode have been runned during nocturnal/diurnal periods corresponding with maxima/minima atmospheric radon observations. Furthermore, weather charts by the WetterZentrale were compared with the back-trajectories for each day in order to better understand the origin of radon-poor and radon-rich air masses and to confirm specific regions as radon source regions.

The back-trajectories calculated by the HYSPLIT model with GDAS input files are quite useful for understanding generic synoptic situations at the *El Arenosillo* station which enable the radon to travel from remote areas to the *El Arenosillo* station. However, the low spatial/temporal resolution of the metereological input for the HYSPLIT4 model does not allow the study of local phenomena related to sea breezes, local radon contribution and nocturnal radon accumulation in a lower layer of the atmosphere (Pearson and Moses, 1966; Kataoka et al, 2001; PhD thesis Arnold, 2009; PhD thesis López-Coto, 2011). Indeed, the nocturnal radon accumulation in a shallow stable low layer of the atmosphere was observed during the experimental radon concentration analysis performed in the previous chapter due to the difference between the high radon concentration measured at 10 m height against the lower radon concentration measured at 100 m height. This is probably due to the residual radon stored in the higher atmospheric layer during the nocturnal inversion. This phenomenon has not been explained by back-trajectory analysis and needs to be simulated and explained by high resolution models in the near future.

Finally, the use of the HYSPLIT4 model to carry out a back-trajectories analysis with a metereological files, with a spatial resolution of 111 km and 23 vertical levels, has been usufull in order to confirm some specific radon source regions previously observed by experimental atmospheric radon concentration analysis. Furthermore, the origin of air masses, their velocity and the difference between back-trajectories run at different heights levels provide informations about the possibility of air masses reaching the *El Arenosillo* station to take up radon gas exhaled from remote sources and to tranport it to the INTA station. Anyway, the use of back-trajectory analysis for understanding synoptic air masses movement is hampered by its low resolution which does not allow for studying local atmospheric movements or understanding the vertical radon gas gradient observed by experimental analysis at 10 m and at 100 m heights.

Part IV

Conclusion

Chapter 9

Conclusion

9.1 Specific Conclusions

9.1.1 EIC ^{222}Rn flux monitors

The EIC radon flux monitors selected to perform the characterization of the *El Arenosillo* station were previously calibrated and their response was studied by different laboratory experiments on soil samples and an exhalation bed. Furthermore, they were compared with other direct and indirect radon flux methods in measurement campaigns. The laboratory experiments show that these monitors are not influenced by extreme environmental conditions of temperature and humidity. The measurement results are perfectly reproducible and reliable. Indeed, the radon flux results measured on the exhalation bed of phosphogypsum soil by RT-EIC radon flux monitors with configuration HST located directly on the soil surface and with configuration SST, located inside a sealed glass bottle show reproducible results and a good agreement which confirms the reliability of RT-EIC HST radon flux monitors. Furthermore, the EIC radon monitor response for the determination of radon flux directly from soil were compared with other direct and indirects radon flux methods during an inter-comparison campaign carried out at four selected Spanish sites in summer 2008 under dry climate conditions for the eastern Spain. The geological characteristics of the chosen sites allowed a wide range of radon flux values ranging from 40 Bq m^{-2} h^{-1} to 100 Bq m^{-2} h^{-1} to be observed. Direct methods to determine radon flux, including both continuous and integrated systems, showed a good agreement with a coefficient of variation between 10 % and 23 %. Indirect methods based on the measurement of terrestrial gamma dose rate, or ^{226}Ra soil activity, and their empirical correlation with radon flux, were also used for the EIC monitors evaluation response. The results show that these indirect methods give radon flux values within 20 % and 40 % respectively of the directly measured radon flux by EIC monitors when the ^{226}Ra activity and the terrestrial γ dose-rate measurements are accurately measured. This results was

observed both for ^{226}Ra activity obtained by MARNA map terrestrial dose data, or by direct measurement at the INTE and UHU laboratories on soil samples, and for terrestrial dose rate measured by RS-112 and by LB-1236 monitors at each campaign site. However, it was found that the terrestrial γ dose-rate values from the Automatic Spanish Surveillance network (REA) and those obtained by GammaTRACER lead to an overestimation of radon flux.

9.1.2 In situ ^{222}Rn flux measurement in soil

Radon flux is usually measured under the hypothesis that the Darcy law contribution, which takes into account the pressure difference between the air in the interstices of the pores material and the volume air where the radon is accumulated, can be neglected. In this case the only contribution to the radon accumulation inside the volume is because of the radon concentration gradient between the pore material and the air of the accumulation volume. Neverthless, laboratory experiments carried out on soil samples sealed in an accumulation volume and on an exhalation bed, where the monitor is not sealed because it is located on the ground surface, show that this hypothesis is not always true due to the air change between the accumulation volume and the free external air. However for the first 4-5 hours the linear increase of radon accumulation is still true. This result has been confirmed by hourly radon concentration measurements performed by DOSEman continuous radon monitors on phosphogypsum soil samples of different sizes and on an exhalation bed of the same material. The radon accumulation inside the volume shows an initial linear slope during the first 6-7 hours and is the same for both methods and allows the same radon flux value to be obtained. However, the influence of the environmental parameters on the radon flux is still an open research point. In the future the effect of the presence of a pressure gradient needs to be better investigated in order to properly measure the radon flux in situ in soil without any risk of underestimating it.

9.1.3 El Arenosillo station characterization

Direct radon flux measurements at the *El Arenosillo* tower show a low radon exhalation from soil with an average of 5.3 $\pm$ 1.8 Bq m^{-2} h^{-1}. This result is in agreement with indirect radon flux methods for the same area obtained in the PhD thesis of Arnold, 2009 which used the Szagvary equation together with terrestrial gamma dose data obtained by the MARNA map. However, experimental radon flux results obtained at the *El Arenosillo* tower are definitively lower than values of 50 Bq m^{-2} h^{-1} obtained by the European radon flux map (Szagvary et al, 2009). Radon flux results during dry and wet periods do not show significant differences due to the high permeability of sand which allows the water to quickly leave the soil pores (Nazaroff and Nero, 1988).

Atmospheric ^{222}Rn concentration behaviour was characterized at the *El Arenosillo* station. The work was done on a 100 m meteorological tower where two ARMON radon monitors for continuous gas concentration measurement were previously calibrated in the INTE-UPC radon chamber and then installed. The influence of local wind speed and direction on radon concentrations observed at 10 m and a 100 m, at the *El Arenosillo* station, were studied and an analysis of seasonal behaviour and diurnal cycle was done for one year.

The 100-m-high tower provides an opportunity to carry out a qualitative analysis of possible distant radon contribution sources using hourly radon concentrations at 10 m and at 100 m with the wind conditions at the *El Arenosillo* station. Indeed, this analysis has pointed out several possible sources of high radon flux close to the *El Arenosillo* station in the Sierra Morena range. A remote eventual source has also been found in the Moroccan area. Furthermore, the significant contribution of the Guadalquivir Valley as a channel of air masses coming from inland regions with high radon flux has also been studied. A significant difference was observed for average radon concentration at both heights when wind flows from the N-NE quadrant, which includes the Sierra Morena, the Guadalquivir Valley and the Bethics systems, also with high speeds. This could prove the existence of an important advected contribution at the lower level during the nocturnal hours along the southwest-northeast Guadalquivir depression axis and could help to explain these previous cases. The average hourly measured concentrations of radon gas obtained over a year at the 10 and 100 m heights at the El Arenosillo station were 3.51 Bq m^{-3} and 2.61 Bq m^{-3}, respectively. At 10 m, the standard deviations for the hourly, daily, weekly, and monthly data amounted to 2.87 Bq m^{-3} (N=3382), 2.35 Bq m^{-3} (N=169), 1.69 Bq m^{-3} (N=34), and 1.10 Bq m^{-3} (N=10), respectively. For 100 m, these standard deviations were 2.02 Bq m^{-3} (N=3684), 1.47 Bq m^{-3} (N=164), Bq m^{-3} (N=35) and 0.53 Bq m^{-3} (N=10), respectively. During the autumn season the geometric mean of radon concentration data at 10 m is 4.48 Bq m^{-3} with a standard deviation of 2.03 Bq m^{-3}. The geometric mean of radon concentration data at 100 m is 2.93 with 1.98 Bq m^{-3}. In the winter season the geometric mean of radon concentration data at 10 m is 3.82 Bq m^{-3} with a standard deviation of 2.34. At 100 m the geometric mean is and 3.06 Bq m^{-3} with 1.72. These radon concentrations are not as high as would be expected for winter and could be explained by the high frequency of radon-poor air masses coming from the Atlantic Ocean and from South Portugal during this season. The spring season shows a geometric mean of radon concentration data at 10 m of 3.60 Bq m^{-3} with a standard deviation equal to 2.18. The geometric mean at 100 m is 2.05 Bq m^{-3} with 2.20. These average radon concentrations indicate good atmospheric layer separation during this season. Finally, during the summer season the geometric mean of radon concentration data at 10 m is 2.64 Bq m^{-3} with a standard deviation of 1.86. At 100 m height, the geometric mean is 2.41 Bq m^{-3} with standard deviation of 1.88. These values indicate really good statistics for this season and a strong mixing layer, as was expected for an unstable summer.

The experimental analysis of atmospheric radon behaviour at the *El Arenosillo* station has pointed out the existence of specific radon-rich and radon-poor regions where the

air masses usually originate. A back-trajectory analysis was performed by the transport model HYSPLIT4 and using the GDAS files as metereological input for four of these radon episodes in order to confirm the air masses origin from specific sectors and to examine the poor/rich radon concentrations transported and measured at the *El Arenosillo* station. The back-trajectories for each radon episode were run for nocturnal/diurnal periods corresponding to maxima/minima atmospheric radon observations. Furthermore, weather charts by the WetterZentrale were compared with the back-trajectories for each day in order to better understand the synoptic situation developed in each episode, the origin of radon-rich and radon-poor air masses and to confirm whether specific regions were radon source regions.

The back-trajectories calculated by the HYSPLIT model with GDAS input files are quite useful for understanding generic synoptic situations at *El Arenosillo* station which enables the radon to travel from remote area to the *El Arenosillo* station. However, the low spatial/temporal resolution of the metereological input for the HYSPLIT4 model does not make it possible to study local phenomena related to sea breezes, local radon contribution and nocturnal radon accumulation in a lower layers of atmosphere. Indeed, the nocturnal radon accumulation in a shallow stable low layer of the atmosphere was observed during the experimental radon concentration analysis performed in the previous chapter due to the difference between the high radon concentration measured at 10 m height against the lower radon concentration measured at 100 m height. IThis is probabily due to the residual radon stored in the higher atmospheric layers during the nocturnal inversion. This phenomenon was not widely explained by back-trajectory analysis and needs to be simulated and explained by high resolution models in the near future.

Finally, the use of the HYSPLIT4 model to carry out a back-trajectory analysis with a metereological files, with a spatial resolution of 111 km and 23 vertical levels, was usufull in order to confirm some specific radon source regions previously observed by experimental atmospheric radon concentration analysis. Furthermore, the origin of air masses, their velocity and the difference between back-trajectories run at different height levels provide several information about the possibility of air masses reaching *El Arenosillo* station after having taken up radon gas exhaled from remote sources and tranporting it to the INTA station. Anyway, the usey of back-trajectory analyses for understanding synoptic air masses movement is hampered by its low resolution which does not allow for studying local atmospheric movements and understanding the vertical radon gas gradient observed by experimental analysis at 10 m and at 100 m heights.

9.1.4 Huleva phosphogypsum pile

^{222}Rn flux was measured at the Huelva phosphogypsum pile by integrated EIC monitors during two campaigns under wet and dry conditions. Furthermore, the phosphogypsum material collected at the Huelva pile was studied by laboratory experiment with different integrated and continuous ^{222}Rn flux monitors. The rests of the ^{222}Rn flux observed from

this phosphogypsum soil by different monitors and methods were in agreement between them and always quite low, with an average value of 33.5 ± 5.6 Bq m^{-2} h^{-1}, which is really low if it is compared with material ^{226}Ra activity concentration of 550 Bq kg^{-1}. These results obtained by EIC electret monitors, with configuration HST and SST and applied on phosphogypsum soil samples of different volume, on phosphogyspum exhalation bed and on direct in situ phosphogypsum pile were also confirmed by hourly radon concentrations measurements performed by a DOSEman monitor, which shows a slope during the first 5 hours in the radon concentration accumulation of sealed soil sample and on the exhalation bed which leads to a radon flux of 39.2 ± 8.4 Bq m^{-2} h^{-1}. These results could be explained by the low diffusion coefficient of radon gas in the phosphogypsum which has been discussed alsewhere (Nazaroff and Nero, 1988). Furthermore, the radon exhalation rate, which represents the bequerel exhaled per hour from the material, seems to increase when the soil sample dimension increase from 44 g to 248 g (Morawska and Phillips, 1980). Nevertheless, the 288 g soil sample shows the same exhalation rate observed from the exhalation bed, with a values of 0.6 Bq h^{-1}, which confirms that not all the radon emanated in the pore material will reach the soil-air interface and then exhaled to the free air.

^{222}Rn flux results at the phosphogypsum pile show low values which means that the PG is not a high radon flux source to be used for inverse modelling applications, which include the reconstruction of the source term by use of atmospheric transport models in backward mode. On the other hand, this low radon exhalation indicates that the whole *El Arenosillo* station is a low local radon area where studies of air masses origin can be done. In spite of the high activity of ^{226}Ra measured in the phopshogypsum soil, the laboratory experiments and the direct *in situ* measurements of radon flux showed that the high humidity content of this material does not allow the radon to be exhaled from the surface. Furthermore the phosphogypsum material does not exhale high radon concentration even when it is completely dry because of a very small radon diffusion coefficient in this material. Indeed, the radon flux measurement at the phosphogypsum pile was carried out in dry and wet periods and results show a significant difference between the two seasons. Nevertheless, the phosphogypsum soil was always really wet to the touch. Lopéz-Coto comments that this is due to the high rain season of year 2010 which meant that the phosphogypsum could not get completely dry (PhD thesis López-Coto, 2011). In addition, the atmospheric radon concentration measured at the *El Arenosillo* station does not show any significant increase when the wind comes from the S-SW sector which includes the area of the Huelva phosphogypsum pile.

In any case, experimental radon flux results found out at the Huelva phosphogypsum pile during this study are not in agreement with past studies by Dueñas et al, 2007 and by Abril et al, 2009. These studies, which were carried out using charcoal canisters method, found out extremely high radon flux values at the Huelva phosphogypsum pile with extreme great dispersion between 100-1000 Bq m^{-2} h^{-1}. This discrepancy is presently under study and will be published in a future paper. On the other hand, the indirect radon flux maps of Europe and of Spain regions offer useful informations in order to

evaluate the possible radon source contribution reaching the *El Arenosillo* station, but these methods, in special zone such as the phosphogypsum pile of Huelva, have not been shown to be completely reliable. Indeed, indirect radon flux maps need to take into account the possible environmental conditions and the geological material parameters which can influence radon exhalation.

9.1.5 ^{222}Rn flux models

Different indirect radon flux methods have been used and compared with direct methods in this work. They offer usefull information on a regional and global scale to point out several *hot spot* areas, with high radon flux. However, these models are not yet able to properly quantify either the radon flux variation due to different environmental conditions such as rain episodes or to quantify the radon flux variation due to an increase of the pressure gradient because of the presence of cracks in the studied soil. Although recent models have started to include the geological soil parameters and the metereological information, more improvements have to be added which can include high quality direct radon flux measurements.

9.2 General Conclusion and Future Research

This thesis work has been carried out in order to install and characterize a new atmospheric radon station in the South of Spain on a 100-m-high tower of the *El Arenosillo* station. This station, the only one in the South of Europe, is able to offer to the scientific community high quality data of atmospheric radon concentration at 10 m and at 100 m height with a time resolution of 1 h. Furthermore, the local radon flux contribution in this area is really low, of 5.3 ± 1.8 Bq m^{-2} h^{-1} which means that the atmospheric radon concentrations data will not have any strong noisy radon background and can be used in order to estimate remote radon sources.

The need for a new radon flux model has been identified. It has to be able to take into account the radon flux variation due to geological soil parameters, to metereological environmental conditions and to possible anomalies in the soil such as cracks which significantly can influence the radon flux behaviour. Furthermore, high quality and continuous radon flux measurements have to be implemented and used for models validation. Direct radon flux measurements have to be carried out in order to better understand the influence of the pressure gradient between the accumulation volume air and the free air which seems to strongly reduce the radon flux. This effect has to be better investigated in order to properly measure the radon flux in situ in soil without any risk of underestimating it. Furthermore, together with atmospheric radon concentrations measurement on a tower, the radon concentrations at really high altitude in the atmosphere should be measured by

aircraft measurement campaigns. This could offer useful information on radon transport and origin of air masses for applications in atmospheric models validation.

Future work will be carried out at *El Arenosillo* station with WRF-FLEXPART and with WRF-HYSPLIT models to investigate atmospheric process on high spatial resolution in depth.

Bibliography

Abril, J. M. García-Tenorio, R. and Manjón, G. 2009. Extensive radioactive characterization of a phosphogypsum stack in SW Spain: ^{226}Ra, ^{238}U, ^{210}Po concentrations and ^{222}Rn exhalation rate. J. of Hazardous Mat. 164, 790-797.

Andrew, J.N. Wood, D.F. 1972. Mechanism of radon relase in rock matrices and entry in groundwater. Trans. Inst. Min. Met. 81, 197-209.

Arnold, D. Vargas, A. and Ortega, X., 2009. Analysis of outdoor radon progeny concentration masured at the Spanish radioactive aerosol automatic monitoring network. Appl. Radiat. Isot. 67, 833-838.

Arnold, D. 2009. Study of the atmospheric radon concentration dynamics at the Spanish radiological surveillance stations and its application to air mass movements. Doctoral Thesis, Technical University of Catalonia, Barcelona.

Arnold, D. Vargas, A. Vermeulen, A.T. et al., 2010. Analysis of radon origin by backward atmospheric transport modelling. Atmos. Environ. 44, 494-502.

Bates, T.S., Huebert, B.J., Gras, J.L., Griffiths, F.B., Durkee, P.A., 1998. International Global Atmospheric Chemistry (IGAC) Project First Aerosol Characterization Experiment (ACE 1): overview. J. Geophys. Reas. 103 (D13), 16297-16318.

Beck, H. L. and Gogolak C. V., 1979. Time dependent calculation of the vertical distribution of 222Rn and its decay products in the atmosphere, J. Geophys. Reas., 84, 3139-3148.

Biraud, S. Ciais, P. Ramonet, M et al., 2000. European greenhouse gas emissions estimated from continuous atmospheric measurements and radon 222 at Mace Head, Ireland. J. Geophys. Reas. 105, No. 1, 1351-1366.

Bochicchio, F., 2008. The radon issue: Considerations on regulatory approaches and exposure valuations on the basis of recent epidemiological results. Appl. Radiat. Isot. 66, 1561-1566.

Bolívar, J. P. Gárcia-Tenorio, R. and Gárcia-Leon, M., 1996. Radioactive Impact of some Phosphogypsum Piles in Soils and Salt Marshes Evaluated by γ-Ray Spectrometry. Appl. Radiat. Isot. 47, No. 9-10, 1069-1075.

Bolívar, J. P. Gárcia-Tenorio, R. Mas, J. L. et al., 2002. Radioactive impact in

sediments from an estuarine system affected by industrial wastes releases. Environ. Interntl. 27, 639-645.

Bossus, D.A.W.,1984. Emanating power and specific surface area. Radiat. Prot. Dos. 7, 73- 76.

Butterweck,G. Reineking,A. Kesten, J, et al. 1994.The use of the natural radioactive noble gases radon and thoron as tracers for the study of turbulent exchange in the atmospheric boundary layer-case study in and above a wheat field. Atmos. Environ. 28, 12, 1963-1969.

Cecchi, L. Torrigiani Malaspina, T. Albertini, R. et al. 2007. The contribution of long-distance tranport to the presence of Ambrosia pollen in central northern Italy. Aerobiologia 23, 145-151.

Chambers, S. Zahorowski, W. Matsumoto, et al., Seasonal variability of radon-derived fetch regions for Sado Island, Japan, based on 3 years of observations: 2002-2004. Atmos. Environ. 43, 271-279.

Chan, S.W. Lee, C.W. Tsui. 2010 K.C. Atmospheric radon in Hong Kong. J. Environ. Radioact. 101, 494-503.

Chevillard, A. Ciais, P. Heimann, M. et al., 2002. Transport of ^{222}Rn using the regional model REMO: a detailed comparison with measurement over Europe, Tellus B 54, 850-871.

Cohen, L., Barr, S., Krablin, R. et al.,1972. Steady-state vertical turbulent diffusion of radon. J. Geophys. Reas. 77, 2654-2668.

Colle, R., Underweger, M.P., Hodge, P.A. et al., 1995. An international intercomparison of marine atmospheric radon 222 measurements in Bermuda. J. Geophys. Reas. 100, 16617-16638.

Conen, F. and Robertson, L.B., 2002. Latitudinal distribution of ^{222}Rn flux from continents. Tellus. 54B, 127-133.

Consejo Seguridad Nuclear, 2011. Estudio y Evaluación del impacto radiológico producido por las actividades de diversas industrias no nucleares del sur de Espanã. Industrias de ácido fosfórico. Colección Informes Técnicos 29.2011.

Considine, D. B. Bergmann, D. J. and Liu, H., 2005. Sensitivity of Global Modeling Initiative chemistry and transport model simulations of radon-222 and lead-210 to input metereological data. Atmos. Chem. Phys. 5, 3389-3406.

Countess, R.J., 1976. Rn-222 flux measurement with a charcoal canister. Health Phys., 31, 455-456.

Crawford, J. Zahorowski, W. et Cohen D.D., 2009. A new metric space incorporating radon-222 for generation of back trajectory clusters in atmospheric pollution studies. Atmos. Environ. 43, 371-381.

Cuculeanu, V. Lupu, A. 1996. Effects of vegetation-induced turbulence on radon

diffusion in the atmosphere. Environ. Internatl. 22, 161-170.

Currie, L.A., 1968. Limits for qualitative detection and quantitative determination: application to radiochemistry. Analytical Chem. 40, 586-593.

Damkjaer, A. and Korsbech, U. 1985. Measurement of the amanation of radon-222 from Danish soils. Science Tot. Environ. 45, 343-350.

De Martino, S. and Sabbarese, C., 1997. A Method for Emanation Coefficient Measurement of 222Rn and 220Rn from Soils. Phys. Chem. Earth 22, 1-2, 19-23.

De Martino, S. Sabbarese, C. and Monetti, G. 1998. Radon Emanation and Exhalation Rates from Soils Measured with an Electrostatic Collector, Appl. Radiat. Isot. 49, 4, 407-413.

Draxler, R.R., and G.D. Hess, 1998. An overview of the HYSPLIT4 modeling system of trajectories, dispersion, and deposition. Aust. Meteor. Mag. 47, 295-308.

Draxler, R.R. Stunder, B. Rolph, G. Taylor, A. HYSPLIT4 Users Guide, via NOAA.ARL Silver Spring, MD: NOAA Air Resources Laboratory; 2009.

Dueñas, C. Liger, E. Canéte, S. et al., 2007. Exhalation of ^{222}Rn from phosphogypsum piles located at Southwest of Spain. J. Environ. Radioact. 95, 63-74.

Esposito, A.M. 2000. La raccolta elettrostatica dei discendenti del radon: un approccio numerico. Master thesis, Universita degli studi di Napoli Federico II, Naples.

Font, LL., Baixeras, C. and Moreno, V. 2008. Indoor radon levels in underground working places of Catalonia, Spain. Rad. Meas. 43, 467-470.

Fontan, J., Guedalia, D., Druilhet, A. et al., 1979. Une methode de mesure de la stabilite verticale de l'atmosphere pres du sol, Bound.-Layer Meteorol., 17, 3-14.

Fremman, H.D. and Hartley, J.N., 1986. Measurement technology for radon in the soil. Indoor Radon SP-54, 167-181.

Galmarini, S., 2006. One year of 222Rn concentration in the atmospheric surface layer, Atmos. Chem. Phys. 6, 2865-2887.

GAW, 2007. WMO Global Atmosphere Watch (GAW) Strategic Plan: 2008-2015.GAW Report No. 172.

Grossi, C. Vargas, A. Camacho, A. et al., 2011. Inter-comparison of different direct and indirect methods to determine radon flux from soil. Radiat. Meas. 46-1, 112-118.

Grossi, C., 2007. Measurement of thoron progeny for assessing radiation doses from inhalation. University College London, London.

Grossi, C. 2006. Misure continue di radon per lo studio di processi geofisici. Master thesis in Physics, Universitá degli studi di Napoli Federico II, Naples.

Guedalia, D., Allet, C., Fontan J., 1974. Vertical exchange measurements in the lower troposphere using ThB (212Pb) and radon (222Rn), J. Appl. Meteorol. 13, 27-39.

Guimond, R. J. and Hardin, J. M., 1989. Radioactivity released from phosphate-containing fertilizers and from gypsum. Rad. Phys. Chem. 34, 309-315.

Hawkins, L.N. Russell, L.M. Covert, D.S. et al., 2010. Carboxylic acids, sulfates and organosulfates in processed continental organic aerosol over the southeast Pacific Ocean during VOCALs-REx 2008. J. Geophys. Reas. 115, D13201.

Hernández-Ceballos, M.A., Adame, J.A., Bolívar, J.P. et al. 2011. The climatology of air masses in south western Europe from 1997 to 2007. Submitted to Dynam. of Atmos. and Oceans.

Hopke P.H., 1989. Use of electrostatic collection of ^{218}Po for measuring ^{222}Rn, Health Phys. 57, 1 (July), 39-42.

Hutter, A.R., and Knutson, E.O., 1998. An international inter-comparison of soil gas radon and radon exhalation measurements. Health Phys., 74 (1), 108-114.

Iida, T., Ikebe, Y., Suzuki, K., Ueno, K., Wang, Z., Jin, Y., 1996. Continuous measurements of outdoor radon concentrations at various locations in east Asia. Environ. Internatl. 22 (Suppl. 1), 139-147.

Ikebe, Y., 1970. Variation of radon and thoron concentrations in relation to the wind speed, J. Meteorol. Soc. Jpn., 48, 461-467.

ISO, International Organization for Standardization, 1997. X and gamma reference radiation for calibration dosemeters and dose rate and for determining their response as a function of photon energy; calibrationof area and personal dosemeters of their response as a function of energy and angle of incidence. ISO 4037-3.

Jacobi, W. Andre, K., 1963. The vertical distribution of radon 222, radon 220 and their decay products in atmosphere. J. Geophys. Reas. 68, 3700-3813.

Kalnay,E. 2003. Atmospheric Modeling, Data Assimilation and Predictability. Cambridge University Press, Cambridge.

Kaplan, I., 1963. Nuclear physics II. Addison-Wesley, Japan.

Kataoka, T., Yunoki, E., Shimizu, M. et al., 2001. A study of the atmospheric boundary layer using raon and air pollutants as tracers, Bound.-Layer Meteorol., 101, 131-155.

Keller, G. Folkerts, K.H. and Muth, H., 1982. Method for the determination of 222Rn radon and 220Rn Thoron, exhalation rates using alpha spectrometry. Radiat. Prot. Dosim. 3,2, 83-89.

Keller, G. and Schutz, M.,1988. Radon exhalation from the soil. Radiat. Prot. Dosim. 24 (4), 43-46.

Kotrappa,P. Dempsey, J.C. and Stieff, L.R., 1993. Recent advances in electret ion chamber technology for radiation measurements. Radiat. Prot. Dosim. 47, 4, 461-464.

Kotrappa,P. and Stieff, L.R. 1994. Applicaton of NIST ^{222}Rn emanation standards for calibrating ^{222}Rn monitors. Radiat. Prot. Dosim. 55, 211-218.

Kotrappa, P. Steck, D.J., 2009. Radon flux monitor for in situ measurement of granite and concrete surfaces, Radon Symposium, American Association of Radon Scientists and Technologists, 20-23 Septembre, Missouri.

Kotrappa, P. Stieff, L.R. Volkovitsky, P., 2004. Radon monitor calibration using nist radon emanation standards: steady flow method. Radiat. Prot. Dosim. 113 (1), 70-74.

Kritz, M. A., Le Roulley, J.C. Danielsen, E. F., 1990. The China Clipper: fast advective transport of radon-rich air from the Asian boundary layer to the upper troposphere near California. Tellus 42B, 46-61.

Lambert, G., Polian, G., Taupin, D., 1970. Existence of periodicity in radon concentrations in large scale circulation at lower altitude between 40 and 70vS. J. Geophys. Res. 75, 2341-2345.

Lehmann, B.E., Ihly, B., Salzmann, S. et al., 2003. An automatic static chamber for continuous ^{222}Rn and ^{222}Rn flux measurements from soil. Radiat. Meas. 38, 43-50.

Levin, I. Born, M. Cuntz, M. et al., 2002. Observations of atmospheric variability and soil exhalation rate of radon-222 at a Russian forest site. Tellus 54B, 462-475.

L*ó*pez-Coto, I. 2011. Variabilidad especial y temporal de fuentes y concentraciones de rad*ó*n en la baja atm*ó*sfera. Doctoral Thesis, Huelva University, Huelva.

Lupu, A. and Cuculeanu, V., 2001. Code for calculating the vertical distribution of radon isotopes and their progeny in the atmosphere. Computer Phys. Comm. 141, 149-162.

Mahata, R.H. Bradleyb, D. A. Amina, Y. M. et al., 2001. The effect of humidity on the accuracy of measurement of an electret radon dosimeter. Rad. Phyis. Chem. 61, 489-490.

Mahowald, N. M. Rasch, P. J. Eaton, B. E. et al., 1997. Transport of ^{222}Rn to the remote troposphere using the model of atmospheric transport and chemistry and assimmilated winds from ECMWF and the National Center of Environmental Prediction NCAR. J. Geophys Res. 102, 28139-28151.

Mahou, E.S. Fernandez Amigot, J.A. Garcia Pomar, D. 2005. Proyecto MARNA. IV Workshop Radiacion ambiental y medio ambiente. Suances 4-8 July 2005.

Martinéz-Aguirre, A. and Gárcia-Leon, M. and Ivanovich, H.,1994. Identification and effects of anthropogenic emissions of U and Th on the composition of sediments in a river/estuarine system in southern Spain. J. Environ. Radioact. 23, 231-248.

Morawska, L., 1989.Two ways of ^{222}Rn determining the emanation coefficient. Health. Phys. 57, 481-483.

Morawska, L. Phillips, C.R., 1980. Determination of the radon surface emanation rate from laboratory emanation data. Sci. of The Total Environ. 106, 253-262.

Moreno, V. Baixéras, C. Amgarou, K. et al., 2011. Estudio de la instrumentacion de medida de radon en condiciones ambientales extremas. II Congreso Conjunto

SEFM-SEPR. 10-13 May, 2011. Seville, Spain.

Moses, H. Lucus, Jr. H. F. Zerbe, G. A., 1963. The Effect of Meteorological Variables upon Radon concentration three feet above the ground, J. Air Pollut. Control. Assoc., 13, 12-19.

Nazaroff, W and Nero, A.V., 1988.Radon and its decay products in indoor air.John Wiley and Sons, New York.

Omori, Y. Tohbo, I. Nagahama, H. et al., 2009. Variation of atmospheric radon concentration with bimodal seasonality. Rad. Meas. 44, 1045-1050.

Ortega, X. Amor Duch, Ma. Vargas, A. et al., 2008. Dose assessment at a phosphate industry landfill using solid state detectors, Rad. Meas. 43, 664-667.

Pearson, J. E. Moses H., 1966. Atmospheric Rn-222 concentration variation with height and time, J. Appl. Meteorol. 5, 175-181.

Peréz-Lopéz, R. Miguel Nieto, J. López-Coto, I. et al., 2010. Dynamics of contaminants in phosphogypsum of the fertilizer industry of Huelva (SW Spain): From phosphate rock ore to the environment. App. Geochem. 25, 705-715.

Piesch, E. and Burgkhardt, B., 1983. A review of environmental monitoring using solid state dosemeters, and guidelines for technical procedures. Radiat. Prot. Dosim. 5, 79-94.

Pörstendorfer, J., 1994. Proprieties and behaviour of radon and thoron and their decay products in air. J. Aerosol. Sci. 25, 219-263.

Quindós Poncela, L.S. Fernández, P.L. Gómez Arozamena, J. et al., 2004. Natural gamma radiation map (MARNA) and indoor radon levels in Spain. Environ. Internatl. 29, 1091-1096.

Rash, P. J. et al., 2000. A comparison of scavenging and deposition processes in global models: results from the WCRP Cambridge Workshop of 1995. Tellus 52B, 1025-1056.

Roca, V. De Felice, P. and al. 2004. The influence of environmental parameters in electrostatic cell radon monitor responce. Appl. Radiat. Isot. 61, 243-247.

Ronca-Battista, M. and Gray, D., 1988. The influence of changing exposure conditions on measurement of radon concentration with charcoal absorption technique. Radiat. Prot. Dosim. 24, 361-365.

Sáez-Vergara, J.C. Romero Gutiérrez, A.M. and Rodríguez Jiménez, R., 2002. Resumen de las medidas comparadas en las estaciones de REVIRA. Acuerdo Especifico CIEMAT-CSN 97/187 sobre Optimización de la calidad en la explotación de la red REVIRA, Madrid.

San José, R. Stohl, A. Karatzas, K. et al., 2005. A modeling study of an extraordinary night time ozone episode over Madrid domain. Environ. Mod. Softw. 20, 587-593.

Schery,S. D. and Huang, S., 2004. An Estimate of the Global Distribution of ^{222}Rn

Emissions from the Ocean, Geophys. Res. Let. 31, L19104.

Seibert, P. Kromp Kolb H., Kasper, A. et al., 1998. Transport of polluted boundary layer air from the Po valley to high alpine sites. Atmos. Environ. 32, 23, 3953-3965.

Seibert P. and Frank A.,2004. Source-receptor matrix calculation with a Lagrangian particle dispersion model in backward mode. Atmos. Chem. Phys. 4, 51-63.

Sorimachi, A. Takahashi, H. and Tokonami, S., 2009. Influence of the presence of humidity, ambient aerosols and thoron on the detection responses of electret radon monitors. Rad Meas. 44, 111-115.

Stach, A. Smith, M. Skjoth, C. et al., 2007. Examining ambrosia pollen episodes at Poznan (Poland) using back-trajectories analysis. Intern. J. of Biomet. 51, 275-286.

Stohl, A., Huntrieser, H. Richter, A. et al., 2003. Rapid intercontinental air pollution transport associated with a meteorological bomb. Atmos. Chem. Phys. 3, 969-985.

Stohl, A., 1996. Trajectory statistics - a new method to establish source-receptor relationships of air pollutants and its application to the transport of particulate sulfate in Europe. Atmos. Environ. 30, 579-587.

Stranden, E. 1984. Radon exhalation: Moisture and Temperature dependence, Health Phys. 47, 3, 480-484.

Stull, R. B., 1988. An Introduction to boundary layer meteorology. Kluwer Academics Publisher. London.

Szagvary, T. Conen, F. Stohlker, U. et al., 2007. Mapping terrestrial gamma dose rate in Europe based on routine monitoring data. Radiat. Meas. 42, 1561-1572.

Szagvary, T. Conen, F. Ciais, P., 2009. European ^{222}Rn inventory for applied atmospheric studies. Atmos. Environ. 43, 1536-1539.

Szagvary, T. Leuenberger, M.C. and Conen, F., 2007. Predicting terrestrial ^{222}Rn flux using gamma dose rate as a proxy. Atmos. Chem. Phys. 7, 2789-2795.

Taguchi, S. Iida, T. and Moriizumi, J., 2002. Evaluation of the atmospheric transport model NIRE-CTM-96 by using measured radon-222 concentrations. Tellus B 54, 250-268.

Taylor, J.A., Lucas, H. F., 1966. Atmospheric Radon Monitor. Argonne National Laboratory Report ANL-7220.

Oufni, L., 2003. Determination of the radon diffusion coefficient and radon exhalation rate in Moroccan quaternary samples using the SSNTD technique, J. Radioanalyt. Nucl. Chem. 256, 3, 581-586.

UNSCEAR, 2000. Sources and Effects of Ionizing radiation. Report to the General Assembly, with scientific annexes. United Nations. New York.

Ussler III, W., Chanton, J.P., Kelley, C.A., et al., 1994. Radon222 tracing of soil and forest canopy trace gas exchange in an open canopy boreal forest. J. Geophys. Res. 99,

1953-1963.

Vargas, A. Ortega, X. and Martin Matarranza, J.L., 2004. Traceability of radon-222 activity concentration in the radon chamber at the technical university of Catalonia (Spain). Nuclear Instruments & Methods Phys. Res. A 256, 501-509.

Vargas, A. and Ortega, X., 2006. Influence of environmental changes on integrating radon detectors: results of an intercomparison exercise. Radiat. Prot. Dosim. 123, 4, 529-536.

Vinuesa, J.F. Basu, S. Galmarini, S., 2007. The diurnal evolution of 222Rn and its progeny in the atmospheric boundary layer during the Wangara experiment. Atmos. Chem. Phys., 7, 5003-5019.

Vinuesa, J.F. Galmarini, S., 2007. Characterization of the ^{222}Rn family turbulent transport in the convective atmospheric boundary layer. Atmos. Chem. Phys. 7, 697-712.

Whittlestone, S. Robinson, E. and Ryan, S., 1992. Radon at the Mauna Loa Observatory; Transport from distant continents. Atmos. Environ. 26A, 2, 251- 260.

Whittlestone S., Zahorowski W., 1995. The Cape Grim huge radon detector. In Baseline Atmospheric Program (Australia) 1992, 26-30.

Wilkening M. H., 1970. ^{222}Radon concentrations in the convective patterns of a mountain environment, J. Geophys. Res. 75, 1733-1740.

Wissman, F. Rupp, A. Stohlker, U., 2007. Characterization of dose rate instruments for environmental radiation monitoring. Zeitschrift Kerntechnik 72(4), 193-198.

WMO, 2004. 1st International IAEA/WMO Technical Meeting on sources and measurements of natural radionuclides applied to climate and air quality studies. Technical report No 155, World Meteorological Organization Global Atmosphere Watch.

WMO, 2009. 2st International IAEA/WMO Technical Meeting on sources and measurements of radon and radon progeny applied to climate and air quality studies. Technical report of World Meteorological Organization Global Atmosphere Watch, in press.

Yumimoto, K. and Itsushi, U., 2006. Adjoint inverse modeling of CO emissions over Easternn Asia using four-dimensional variational data assimilation. Atmos. Environ. 40, 6836-6845.

Zahorowski, W. Chambers, S.D. Henderson-Sellers A., 2004. Ground based ^{222}Rn observations and their applications to atmospheric studies. J. Environ. Radioact. 76, 3-33.

Zanetti, P. 1990. Air Pollution Modelling, Theories, Computational Methods and Available Software, Van Nostrand Reinhold, New York.